TAMPEREEN TEKNILLINEN YLIOPISTO
TAMPERE UNIVERSITY OF TECHNOLOGY

Kristo Mela

Mixed Variable Formulations for Truss Topology Optimization

Julkaisu 1134 • Publication 1134

Tampere 2013

Tampereen teknillinen yliopisto. Julkaisu 1134
Tampere University of Technology. Publication 1134

Kristo Mela

Mixed Variable Formulations for Truss Topology Optimization

Thesis for the degree of Doctor of Science in Technology to be presented with due permission for public examination and criticism in Konetalo Building, Auditorium K1702, at Tampere University of Technology, on the 20th of June 2013, at 12 noon.

Tampereen teknillinen yliopisto - Tampere University of Technology
Tampere 2013

ISBN 978-952-15-3076-0 (printed)
ISBN 978-952-15-3116-3 (PDF)
ISSN 1459-2045

Abstract

A study on formulating truss topology optimization problems using continuous and binary variables is presented. The ground structure approach, where members and nodes are allowed to vanish from an initial dense truss, is adopted. Member cross-sections are chosen from a discrete set of alternatives. The binary variables are used to determine the existence of members and nodes as well as the selection of a profile for the truss members. Normal forces of the members and nodal displacements are chosen as continuous variables. The equations of structural analysis are written as constraints of the optimization problem. Further constraints ensure that the truss is able to carry the loads and is kinematically stable. Member strength and buckling constraints are formulated according to the design rules of Eurocode 3.

The aim of the optimization problems considered is to find economical truss designs. The weight of the truss serves as the default criterion as it can be easily evaluated and it is related to the total cost. However, it is well-known that the actual minimum cost design can differ from the minimum weight truss. Therefore, a feature-based cost function is also devised for tubular plane trusses for cost optimization. For design situations, where the cost data is not available, a multicriterion optimization problem where weight is minimized simultaneously with the number of truss members, nodes and profiles used in the design, is formulated and Pareto optimal solutions are generated.

The proposed formulations lead to mixed-integer linear optimization problems. State-of-the-art software is employed to solve a set of benchmark problems that verify the formulations and demonstrate the effect of different constraints. Optimum topologies for Euler buckling and Eurocode 3 buckling constraints are compared. Topology optimization of a roof truss is presented as a case study. The conflict of weight and cost is studied in conjuction with the roof truss.

Preface

This study was conducted from the beginning of 2009 to the last days of 2012. From the rather vague topic "topology optimization with stress constraints", the subject was first narrowed down to trusses and later specified to truss topology optimization with discrete cross-sections using mixed variable formulations.

Nothing grows in the void, and I'm grateful for having so many people from different backgrounds helping me along the way. Lecturer Risto Silvennoinen (Department of Mathematics, TUT) deserves thanks for igniting the spark for optimization. Emeritus Professor Juhani Koski transformed that spark into flame by introducing me to the realm of structural optimization and engineering mechanics. His deep knowledge on structural optimization and our myriad discussions have prepared me to become an independent researcher, and I feel privileged for the opportunity to conduct this research under his supervision.

After Professor Koski retired, Professor Arto Lehtovaara (Department of Engineering Design, TUT) took over as my supervisor. Even though our research fields did not coincide, he provided sound advice for preparing the manuscript throughout. Our regular meetings and his devotion helped me to keep the work organized and in schedule.

In late 2010, the thesis got an unexpected thrust that gave the research wonderful momentum and a new and interesting direction. I got acquainted with Professor Markku Heinisuo (Department of Structural Engineering, TUT), who introduced me to the Eurocodes and other aspects of practicing structural engineer. In addition to providing supporting funding for my research, his open-mindedness, firm belief in the potential of structural optimization, and his valuable practice-oriented advice encouraged me to venture deeper into the field of structural design. His help was so remarkable that eventually he became my other supervisor, which I am grateful for.

In autumn 2011, I decided it was necessary to seek outside help in order to hasten things. I contacted Senior Scientist Mathias Stolpe (Technical University of Denmark (DTU), DTU Wind Energy), whose earlier work on mixed variable formulations had inspired me. During my two short stays at DTU that he hosted, I was able to achieve the main results of the thesis. Mathias' unconditional help and guidance, as if I was one of his PhD Students, was astounding and a sign of a true scientist. I am greatly indebted to his efforts in aiding me by sharing his experiences and thoughts.

The main funding of the research was provided by the National Graduate Program of Engineering Mechanics. I would like to thank the leader of the program, Professor Jukka Tuhkuri (Department of Applied Mechanics, Aalto University), for this unique opportunity to do basic research and to meet other graduate students from other Finnish universities.

I have been fortunate to have the endless support from my friends and family. I am forever grateful to my parents Sinikka and Kari for their encouragement, and to my brothers, Jaakko and Mikko, for listening to my rants over the years.

My warmest thanks go to Snowchange Cooperative for showing me other ways of being in the world and reminding me that not all knowledge is in the books.

Finally, I express my gratitude for my dear wife Jenni, the architect of my heart, who never ceased to believe and understand.

Table of Contents

Nomenclature

Abbreviations

DM	Decision maker	(page 86)
LP	Linear programming	(page 4)
MILP	Mixed-integer linear programming	(page 8)
MINLP	Mixed-integer nonlinear programming	(page 8)
NAND	Nested analysis and design	(page 22)
NLP	Nonlinear programming	(page 4)
RHS	Rectangular hollow section	(page 14)
SAND	Simultaneous analysis and design	(page 5)
SHS	Square hollow section	(page 14)
SOS	Special ordered set	(page 75)

Cost function

C_B	Blasting cost of a truss [€]	(page 41)
c_{CA}	Welding consumables cost [€/min]	(page 44)
c_{CP}	Painting consumables cost [€/min]	(page 46)
c_{CS}	Cost of sawing consumables [€/min]	(page 42)
c_{EnA}	Welding energy cost [€/min]	(page 44)
c_{EnS}	Cost of sawing energy [€/min]	(page 42)

c_{EqA}	Welding equipment cost [€/min]	(page 44)
c_{SeA}	Welding real-estate maintenance cost [€/min]	(page 44)
c_{SeP}	Painting real-estate maintenance cost [€/min]	(page 46)
c_{ReA}	Welding real-estate investment cost [€/min]	(page 44)
c_{ReP}	Painting real-estate investment cost [€/min]	(page 46)
c_{LA}	Welding labor cost [€/min]	(page 44)
c_{LP}	Painting labor cost [€/min]	(page 46)
C_M	Material cost of a truss [€]	(page 41)
C_P	Painting cost of a truss [€]	(page 46)
C_S	Sawing cost of a truss [€]	(page 42)
C_A	Welding cost of a truss [€]	(page 44)
A_p	Total painted area of a truss [mm^2]	(page 46)
T_{NS}	Non-productive sawing time [min]	(page 42)
T_{PA}	Productive assembling time [min]	(page 44)
T_{PP}	Productive painting time [min]	(page 46)
T_{PS}	Productive sawing time [min]	(page 42)
T_{Ta}	Tack welding time [min]	(page 44)
T_{We}	Welding time [min]	(page 44)
L_{fw}	Weld length [mm]	(page 45)
A_h	Horizontal (solid) part of the sawn cross-section [mm^2]	(page 42)
A_t	Cross-sectional area of a sawn profile [mm^2]	(page 43)
$c_{M,i}$	Unit cost of a tubular profile [€/kg]	(page 41)
F_{sp}	Thickness-dependent saw blade durability parameter	(page 43)
F_s	Saw blade durability parameter	(page 43)
p_{SB}	Price of the saw blade [€]	(page 43)
Q	Sawing efficiency [mm^2/min]	(page 42)
S	Vertical feeding speed of saw blade [mm/min]	(page 42)
S_m	Material factor for sawing	(page 42)
S_t	Durability of the saw blade [mm^2]	(page 43)

Sets

$\mathcal{A}$	Set of available cross-sectional areas	(page 23)
$\mathcal{J}_c$	Interior nodes of chain c	(page 33)
$\mathcal{E}_c$	Indices of members of chain c	(page 33)
$\mathcal{M}_c(s)$	Members of chain c connected to node s	(page 33)
$\mathcal{V}_c$	Indices of nodes of chain c	(page 33)
$\mathcal{E}_c^o(s)$	Members of chain c overlapping the node v_s	(page 35)
$\mathcal{N}_c(s)$	Members not belonging to chain c connected to node s	(page 33)
$\mathcal{E}_c(s)$	Members of chain c partially or fully belonging to the line segment defined by consecutive nodes v_s and v_{s+1}	(page 33)
$\mathcal{C}$	Set of chains	(page 33)
$\mathcal{G}$	Group of members that must have identical profiles	(page 37)
$\mathcal{I}$	Set of available moment of inertias	(page 23)
$\mathcal{L}$	Loading conditions	(page 23)
$\mathcal{N}_L$	Set of loaded nodes	(page 26)
$\mathcal{M}$	Ground structure members	(page 23)
$\mathcal{M}_\ell$	Set of members connected to node ℓ	(page 26)
$\mathcal{D}_\ell$	Global degrees of freedom of node ℓ	(page 36)
$\mathcal{N}$	Ground structure nodes	(page 23)
$\mathcal{P}$	Available profiles	(page 23)
$\mathcal{N}_S$	Set of supported nodes	(page 26)

Mechanics

α	Imperfection factor	(page 18)
$\hat{\mathbf{B}}$	Extended statics matrix of a truss	(page 28)
χ	Reduction factor for buckling	(page 17)
ε_i^k	Axial strain of member i in loading condition k	(page 15)
f_y	Yield strength	(page 16)
$\mathbf{B}$	Statics matrix of a truss	(page 15)
$\mathbf{Q}$	Matrix containing equivalent nodal forces of a line load.	(page 29)
$N_{\mathrm{b,Rd}}$	Design buckling resistance of a compression member	(page 17)
N_{cr}	Elastic critical force for Euler buckling	(page 18)

$N_{\mathrm{c,Rd}}$	Design resistance to normal force for uniform compression	(page 17)
N_{Ed}	Design normal force	(page 17)
$N_{\mathrm{t,Rd}}$	Design value of the resistance to tension forces	(page 17)
$\tilde{p}_{j\ell}$	Auxiliary load for degree of freedom j of node ℓ	(page 36)
$\tilde{p}_j$	Auxiliary load for degree of freedom j	(page 36)
γ_{M0}	Partial safety factor for resistance of cross-sections	(page 17)
γ_{M1}	Partial safety factor for resistance of members to buckling	(page 17)
$\bar{\lambda}$	Non-dimensional slenderness	(page 18)
σ_i^k	Normal stress of member i in loading condition k	(page 15)
$\mathbf{b}_i$	Column i of the statics matrix	(page 15)
$\mathbf{N}^k$	Vector of member force in loading condition k	(page 15)
$\tilde{\mathbf{N}}$	Member forces in the auxiliary loading condition.	(page 36)
$\mathbf{p}^k$	Global load vector of loading condition k	(page 15)
$\mathbf{q}$	Vector of equivalent nodal forces.	(page 29)
E_i	Young's modulus of member i	(page 15)
L_i	Length of member i	(page 15)
L_n	Buckling length of a truss member	(page 18)
N_i^k	Normal force of member i in loading condition k	(page 15)
q_i	Equivalent nodal force due to line loading to degree of freedom i	(page 28)
q_{ij}	Equivalent nodal force due to line loading to degree of freedom i related to member j	(page 28)
V	Material volume of the truss	(page 38)
W	Weight of the truss	(page 38)
W_i	Weight of member i [kg]	(page 41)

Numbers

N_B	Number of binary variables	(page 72)
N_C	Number of continuous variables	(page 72)
n_d	Number of nodal degrees of freedom	(page 15)
n_E	Number of ground structure members	(page 15)
N_c	Number of connections	(page 26)
n_L	Number of loading conditions	(page 15)

N_y	Number of members	(page 26)
N_p	Number of member profiles	(page 39)
N_R	Number of support reactions	(page 26)
n_S	Number of available profiles	(page 24)
R_s	Number of support reactions at supported node s	(page 26)

Profile characteristics

$\hat{A}$	An available cross-sectional area	(page 23)
$\hat{A}_{u,j}$	Outer surface area of profile j per unit length [mm^2/mm]	(page 46)
c	Side length of the hollow part of a rectangular section	(page 16)
H	Side length of a rectangular section	(page 16)
$\hat{I}$	An available moment of inertia	(page 23)
t	Wall thickness of a hollow section	(page 16)
A_i	Cross-sectional area of a truss member	(page 15)
I	Moment of inertia	(page 18)
I_i	Moment of inertia of truss member i	(page 24)
N_i^k	Normal force of member i in loading condition k	(page 25)

Variables

α_j	Binary auxiliary variable for profile counting	(page 39)
$\hat{\mathbf{N}}$	Extended member force vector in loading condition k	(page 28)
$\mathbf{N}_i^k$	Vector of force variables of member i in loading condition k	(page 27)
$\mathbf{u}^k$	Global nodal displacements in loading condition k	(page 15)
N_{ij}^k	Force of member i if profile j is chosen in loading condition k	(page 25)
w_j	Variable for selecting a profile for a group of members	(page 37)
z_ℓ	Nodal variable (binary)	(page 25)
y_{ij}	Binary variables for profile selection	(page 23)
y_i	Binary variables for member existence	(page 24)

CHAPTER 1

Introduction

The question begs the answer –
can you forgive me somehow?
Tom Waits

1.1 Background

Structural design is a task that requires expertise in structural mechanics, engineering ingenuity, and creative collaboration with other disciplines involved in the design process. In truss design, the goal is to find an economical structure which is able to carry the given loads and which can be manufactured by available technologies. This goal is often pursued by trial and error, where the designer gradually modifies an initial structure. While this design methodology can be efficient in simple and to the designer familiar cases, it can be very time-consuming for more complex situations, especially if an entirely new conceptual design is desired. For such instances, a more systematic approach should be considered.

Structural optimization is a research field which provides an efficient tool for creating a synthesis of design, fabrication and economy of structures. By formulating the design task at hand as an optimization problem, economical solutions can be found systematically by numerical optimization algorithms. This approach has at least the following benefits over the traditional design methodology:

- Any design aspect or quantity that can be expressed mathematically can be taken into account. Thus, complex structural systems, where dependencies of different quantities are difficult for the designer to quantify, can be considered.

- The solution is not entirely dependent on the experience of the designer. This means that new economical solutions that are beyond the intuition of the designer can be found. Obviously, the designer is still needed for a meaningful problem formulation and interpretation of the results.
- The time needed to find economical designs is reduced.

Trusses are especially suitable for optimization, since their analysis is simple (if they are considered as pin-jointed structures with loads at the nodes), and they possess a great deal of mathematical structure that can be exploited in the solution process. Trusses are also frequently used in practical applications, for example, in civil and aerospace engineering.

Truss optimization problems are generally divided into three categories. Before introducing them, a remark on the terminology is in place. In the literature, the terms layout, configuration, topology, geometry, and shape of the truss are commonly used. In this thesis, these terms are defined as follows.

The *layout* of the truss means the number of nodes and members, the location of the nodes, and the connectivity of the members. The *topology* of the truss consists of the member connectivity, which includes the number of nodes as well. However, topology does not contain information about nodal position. The *geometry* of the truss means the node locations for fixed topology. The terms *configuration* and *shape* are equivalent to *layout* and *geometry*, respectively, but they are not used in this thesis.

The simplest truss optimization problem is *sizing optimization* (Fig. 1.1a), where the optimum cross-sections of truss members are to be determined for a fixed layout. This problem can be extended in two directions, both leading to substantially more complicated formulations.

In *geometry optimization* (Fig. 1.1b), the optimum locations of selected joints are to be determined in addition to member cross-sections. The topology of the truss remains fixed during optimization. Introducing nodal coordinates as design variables greatly increases the nonlinearity of the optimization problem, making the numerical solution substantially more difficult.

The other extension of sizing optimization is *topology optimization* (Fig. 1.1c). As suggested by the name, the goal is to determine the optimum topology for given loads, supports, and material properties. Even though the topology of the truss does not include information about the location of the nodes, the optimum topology depends strongly on where the nodes are placed. Thus, determining the optimum topology automatically includes finding the optimum node positions as well as member cross-sections. Consequently, by optimizing the topology, the *optimum layout* is also found. In this thesis, only problems of topology optimization are considered.

Topology optimization can be understood as an extension of sizing optimization, if the so-called *ground structure approach* (Dorn, Gomory & Greenberg 1964) is adopted. In the ground structure approach, an initial truss, called the *ground structure*, with an excessive number of members and joints is employed. During optimization the joint locations are fixed, but members (and joints) are allowed to vanish. This procedure can then be viewed as sizing optimization with zero cross-section allowed. However, removing members from the ground structure leads to serious theoretical and numerical

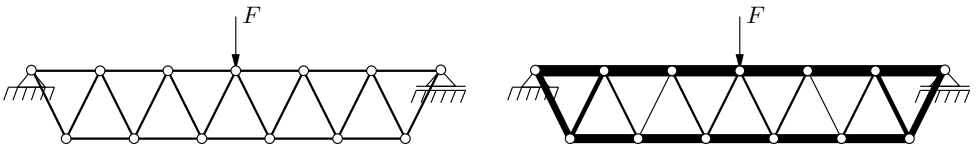

(a) Sizing optimization.

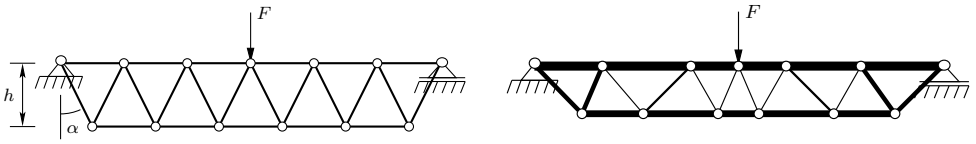

(b) Geometry optimization.

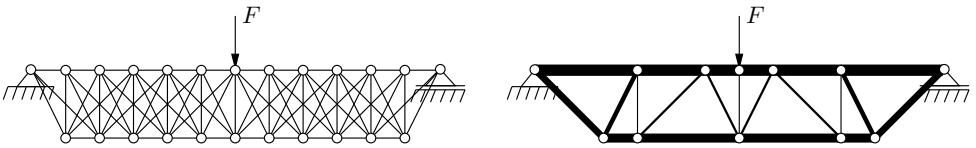

(c) Topology optimization.

Figure 1.1: Truss optimization problem types.

difficulties that make topology optimization the most difficult optimization problem in truss optimization.

Topology optimization can also be performed on more general structures that are modelled using continuum mechanics. The goal is, roughly speaking, to determine the optimal number, location and shape of the holes and outer boundary of the structure. This approach differs from truss topology optimization substantially, even though there are some similar issues as well. Topology optimization of continuum structures is not considered in this thesis. For an overview of the topic, see (Eschenauer & Olhoff 2001) and (Bendsøe & Sigmund 2003).

The work of the designer is regulated by law and a series of design codes. For example, the Eurocodes provide mandatory rules for designing structures in the European Union. Therefore, in order to make the results of optimization applicable, the requirements of the respective design codes should be included in the problem formulation. Any requirement that is excluded from optimization must be checked separately for the solution. If some requirements are violated, the solution of optimization must be modified appropriately.

On the other hand, if optimization is applied to find a conceptual design, or a draft of the design is needed quickly, simplified problem formulations that are easier to solve can be employed. In such instances, it is acknowledged that the result of optimization has to be modified, but optimization provides a good starting point for more refined design. This approach is often the only possibility to apply optimization in practice, as taking into account all the necessary requirements would lead to an optimization problem that is intractable by current solution methods. By pertinent research on structural optimization, the gap between the structural designer and the researcher

can be gradually narrowed. This is especially the case for truss topology optimization, which holds a great potential in producing new conceptual designs.

1.2 Literature Review

Extensive research on truss topology optimization has been carried out since the latter part of the 20th century, especially since the 1980s. Starting from the simplest problem formulations, the theoretical pitfalls lurking within the subject as well as some properties of optimum topologies have been uncovered. Further research has extended the problem formulations, and methods for circumventing the theoretical difficulties have been proposed.

Elsewhere, structural optimization under design codes has been studied. This research rarely considers truss topology optimization, but provides valuable insight for extending the conventional formulations of topology optimization to include the design codes.

In order to proceed with the research, the results and achievements of the research community need to be understood.

1.2.1 General Theoretical Results

The earliest problem that has been considered in the literature is the minimization of weight of the truss with constraints on member strength. The cross-sectional areas of the ground structure members and their normal forces are taken as the continuous design variables. If the kinematic compatibility conditions are neglected, the weight minimization problem can consequently be written as a *linear programming (LP)* problem (Dorn et al. 1964). For a thorough review of this formulation and its properties, see Kirsch (1989) and Rozvany, Bendsøe & Kirsch (1995).

Under a single loading condition, the minimum weight topology is statically determinate (Sved 1954, Barta 1957, Dorn et al. 1964, Fleron 1964). As a statically determinate structure satisfies the compatibility conditions automatically, the actual minimum weight design for stress constraints can be found by the LP formulation. However, under multiple loading conditions, the minimum weight truss is typically statically indeterminate. In this case, the LP formulation is unable to find the optimum solution, providing only a lower bound for the minimum weight.

If statically determinate optimum topology cannot be guaranteed, the kinematic compatibility conditions must be included in the problem formulation. For continuous cross-sections, this leads to a *nonlinear programming (NLP)* formulation (Cheng & Guo 1997, Guo, Cheng & Yamazaki 2001, Stolpe 2004), which imposes both theoretical and numerical issues. The theoretical difficulties are solely due to vanishing members.

The first observation that needs attention is the occurrence of singular and local optima (Kirsch 1990, Kirsch 1993). The feasible set usually contains degenerate parts with dimension smaller than the dimension of the feasible set. These parts correspond to designs, where members have been eliminated from the ground structure. The global

optimum may lie in such a degenerate part. Unfortunately, gradient-based solution methods that are commonly used, are unable to find solutions in these parts. This is due to the fact that the constraint qualification of the Karush-Kuhn-Tucker conditions does not hold in the degenerate regions. Local optima appear as a consequence of the nonconvexity of the problem.

The essential problem with vanishing members is that the structural model is not altered during the optimization. In the finite element setting, that is frequently employed, this means that the structure includes members with zero cross-sectional area, which can lead to a singular stiffness matrix. Bruns (2006) identifies two cases, where the singularity may appear: the removal of members may lead to an isolated node or an isolated element. Both of these cases lead to singular stiffness matrix, which causes the numerical optimization procedure to halt.

The singularity of the stiffness matrix can be circumvented by imposing a small positive lower bound on member areas. At the solution, members having this lower bound area are removed from the design, effectively rounding the member areas to zero. However, this approach may fail to find the global optimum, as explained by Cheng & Guo (1997).

Another approach for treating the singularity of the stiffness matrix is to formulate the optimization problem according to the principle of *simultaneous analysis and design (SAND)*, where the nodal displacements are taken as variables in the optimization and the stiffness equation is considered as a set of equality constraints (Sankaranarayanan, Haftka & Kapania 1994). Such a formulation requires special solution methods. Consequently, the theoretical issues with vanishing members are transferred to computational matters which can be approached by developing numerical optimization algorithms.

Even if the structure that remains after vanishing members are removed would have a non-singular stiffness matrix, the vanishing members cause severe problems to the optimization. Arguably the most serious issue appears with constraints that depend on the stress of the members.

It was observed by Sved & Ginos (1968) that the computational value of the stress of a vanishing member may be non-zero which may lead to erroneous results, when gradient-based optimization methods are applied. Cheng & Jiang (1992) investigated this issue further and showed that the stress is a discontinuous function of the member area at zero. They also showed that for small values of the cross-sectional area, the stress in a member can be too high, but as the member is removed, the resulting structure can be feasible. This observation provides another obstacle for gradient-based solution methods.

To avoid the problems associated with stress constraints and singular optima, several approaches have been proposed. Cheng & Jiang (1992) suggest multiplying the stress constraint function by a so-called *quality function*, which has the following properties: it is continuous, zero at zero cross-section and positive for positive cross-sectional areas. This modification removes the discontinuity issue. However, the feasible set still includes degenerate parts.

In order to allow numerical optimization methods to find solutions in these parts, Cheng & Guo (1997) introduced a so-called ϵ*-relaxation technique*, where the stress

constraint $g(\mathbf{x}) \leq 0$ is replaced by $g(\mathbf{x}) \leq \epsilon$, with $\epsilon > 0$, and a lower bound ϵ^2 is issued on member areas. An iterative procedure is obtained, where the problem is solved for a given ϵ that is made ever smaller until a satisfactory numerical accuracy has been reached. However, Stolpe & Svanberg (2001) have shown that the trajectory of the global optima of the relaxed problems can be discontinuous. Therefore, this strategy might fail to find the global optimum.

Rozvany (1992) has proposed the so-called *smooth envelope functions*, see also (Rozvany 1996), to handle the singularity of the stress constraints. In this approach, the allowable stress is replaced by a smooth function that removes the singularity issue. The ϵ-relaxation method can be seen as a special case of such an envelope function (Rozvany 2001). Smooth envelope functions suffer from the same discontinuity of the trajectory of the global optima as the ϵ-relaxation approach.

Introducing member buckling constraints poses new difficulties. A first observation is that singular and local optima are also present, when member buckling is included (Guo et al. 2001). The feasible set is even disjoint. An ϵ-relaxation technique with a modified buckling constraint can be employed to make the feasible set connected and to remove the singularities (Guo et al. 2001).

Arguably the main issue with buckling constraints is the *jump in the buckling length*. It is quite common that the optimum truss includes a chain of successive members having the same orientation and cross-sectional area. Such chains possess unstable nodes. One approach for obtaining a stable structure is to remove these nodes to merge the members of the chain into a single, longer member. The buckling length of this resulting longer member is greater than the buckling lengths of the individual chain members, resulting in decrease in the buckling strength, which leads to unsafe design. As shown by Zhou (1996), the optimum topology is very sensitive to this phenomenon.

Rozvany (1996) suggests the addition of system stability constraints and imperfections to the ground structure as a solution to the difficulties associated with node cancellation. The idea is to introduce appropriate nodal displacements that need to be supported by the structure. However, even if these approaches produce more stable solutions, they may still give the incorrect optimum topology.

Achtziger (1999*a*) discusses buckling constraints for circular and square sections, and without compatibility conditions. Through a careful definition of *chains* (consecutive members laying on a line), a constraint for *topological buckling* is introduced. In this constraint, the node cancellation is taken into account by defining the *active buckling length*. However, as Achtziger points out, this problem formulation may not have an optimal solution. This is due to the discontinuity of the active buckling length, which leads to non-closed feasible set. This phenomenon can be circumvented by adding the so-called *slenderness condition* (a positive lower bound on member areas for members present in the topology). The numerical treatment is alleviated by noticing that all members in a chain have the same axial force. Then, the complicated buckling constraint needs to be introduced for only one member of that chain, while for the others, a simple side-constraint for the member area is sufficient.

In the second part of the paper, Achtziger (1999*b*) proposes a numerical solution method for minimum weight problem with buckling constraints. The conditional

buckling constraints are transformed into regular constraints by an approximation parameter, and the resulting problem is solved by a sequential linear programming method. The numerical example show that including topological stability leads to a different topology than the "simple" buckling constraints.

To tackle the problem of unstable topologies that often appear with buckling constraints, Guo, Cheng & Olhoff (2005) apply the fact that an unstable truss has a zero critical load factor. By adding a positive lower bound for the critical load factor, unstable solutions are avoided. Determining the critical load factor requires the solution of the generalized eigenvalue problem of linear stability theory.

1.2.2 Discrete Cross-Sections and Design Codes

As a first step towards actual design situations, the assumption that the member areas are continuous is altered such that only a finite set of predefined discrete values for cross-sectional areas is available. This change in problem formulation leads to a *discrete optimization* problem. The main implication is that the solution methods of continuous optimization become inapplicable, and different approaches are needed. Surveys of methods for discrete structural optimization are provided by Arora, Huang & Hsieh (1994), Thanedar & Vanderplaats (1995) and Arora (2002). Textbooks on discrete and mixed variable optimization include those by Floudas (1995) (nonlinear problems) and Nemhauser & Wolsey (1999) (linear problems).

To further take into account the needs of the structural designer, design code requirements can be included in the optimization problem as constraints. Galante (1996), Dominguez, Stiharu & Sedaghati (2006), and Balling, Briggs & Gillman (2006) include member buckling and cross-sections according to the AISC design code. Erbatur, Hasançebi, Tütüncü & Kılıç (2000) optimize trusses according to the Turkish code, Pedersen & Nielsen (2003) formulate sizing and geometry optimization according to the Danish code, and Shea & Smith (2006) incorporate the Swiss code for transmission tower optimization. In most cases, the structures are analyzed as pin-jointed trusses with loads at the nodes, such that bending, shear, and torsion of the members are not included.

In Europe, the Eurocodes have become the unified design codes in the European Union. Farkas & Jármai (1997, Chapter 11) include constraints on member buckling and joint strength for optimization of tubular trusses according to Eurocode. Similar formulations, where joint strength and eccentricity are taken into account, can be found in (Farkas & Jármai 2003, Farkas & Jármai 2008). Jalkanen (2007) formulates tubular truss optimization problems, where bending and torsion of the members are included, as well as joint strength. Šilih, Premrov & Kravanja (2005) optimize timber trusses according to Eurocode 5.

In most cases, where design codes are incorporated in the optimization problem, only sizing and geometry optimization is considered. A rare study on truss topology optimization under Eurocode constraints is presented by Šilih & Kravanja (2008), but the details of the formulation are not given.

1.2.3 Mixed Variable Formulations

It was noted earlier, that the theoretical issues related to the vanishing members can be circumvented by employing the SAND formulation. However, as reported by Sankaranarayanan et al. (1994), convergence to the solution, where member areas actually become zero is slow. To gain better control over the topology of the truss during optimization, binary variables can be introduced to indicate the existence of members and nodes. In the case of discrete member profiles, binary variables can also be used for profile selection.

Ghattas & Grossmann (1991) and Grossmann, Voudouris & Ghattas (1992) seem to be the first to propose this approach for truss topology optimization. As in the SAND formulation, the equations of structural analysis are included as constraints in the optimization problem. However, in contrast to Sankaranarayanan et al. (1994), the equations of mechanics are written for each element separately. If the member areas are continuous, the problem becomes nonlinear. Interestingly, a *mixed-integer linear optimization (MILP)* problem formulation is obtained in the case of discrete member areas. Member profiles are selected by binary variables, whereas member forces, stresses and elongations as well as nodal displacements are chosen as continuous state variables.

A general framework for mixed variable formulations in structural optimization is presented by Kravanja, Kravanja & Bedenik (1998). However, no explicit formulations for trusses are presented.

Bollapragada, Ghattas & Hooker (2001) propose a formulation for discrete sizing and topology optimization, where the selection of the member profile is stated as a logical disjunction. Then, a logic-based branch and bound algorithm is proposed, where a *quasi-relaxation* problem that is formulated as an LP problem is solved sequentially. Lower bounds are obtained by the solutions of the quasi-relaxation problem, and upper bounds are obtained, if the binary variables take integer values at the solution. Branching is performed with respect to member area variables, and also the so-called *logic cuts* can be employed. The benefit of the logic-based approach is the fact that the quasi-relaxation problem is substantially smaller than the MILP formulation of the truss optimization problem.

As mentioned above, in the case of continuous member areas, the mixed variable formulation leads to a *mixed-integer nonlinear programming (MINLP)* problem, which is nonconvex (Stolpe 2004, Ohsaki & Katoh 2005). The nonlinearities appear as bilinear terms in equality constraints. If Euler buckling is included, univariate concave terms in inequality constraints appear as well. A nonlinear *branch-and-bound* algorithm can be applied to find the global optimum of truss topology optimization problems. However, these problems are very difficult to solve to global optimum.

Recently, the MILP formulation resulting for discrete member areas has been studied and extended (Faustino, Júdice, Ribeiro & Neves 2006, Rasmussen & Stolpe 2008, Kanno & Guo 2010). Even though well-established software exists for these formulations, and there are less difficulties in finding the global optimum than in the continuous (nonlinear) case, only relatively small problems have been solved in the literature. This indicates a need for further development of this approach.

The binary variables that indicate member and node existence can be employed to express topological properties of the truss in the form of linear constraints. Ohsaki & Katoh (2005) formulate constraints for the minimum and maximum number of members that can be connected to an existing node. A different set of constraints disallow members from intersecting each other. Rasmussen & Stolpe (2008) present inequality constraints that explicitly ensure that the structure is statically feasible.

A serious drawback of the conventional formulations of topology optimization is that the optimum structure may be kinematically unstable (Dorn et al. 1964, Kirsch 1989). This means that the structure is in equilibrium with respect to the given loads, but it is unstable with respect to variations of the loads. This problem is present both in the LP and in the NLP formulations since the optimum solution of the two formulations are equal, if the optimum topology is statically determinate. This issue is commonly handled by introducing small auxiliary loads at predefined nodes (Ben-Tal & Nemirovski 1997, Rasmussen & Stolpe 2008). The problem with this approach is that it is very difficult to know *a priori*, which nodes will be present in the optimal topology. As all loaded nodes will be included in the optimum structure, adding auxiliary loads to nodes that are not needed in the optimal topology will distort the solution.

The problem of kinematic instability can be treated in the mixed variable framework in an elegant manner. Faustino et al. (2006) write the necessary condition for kinematic stability of the truss (Grubler's criterion) as a linear constraint with respect to the binary variables. To further enforce kinematic stability, a new loading condition is added to the problem, where each degree of freedom is given a small load that is applied, if the corresponding node is present. The truss is then required to be in equilibrium with respect to these loads. A similar approach is proposed by Kanno & Guo (2010).

1.2.4 Discussion

The main observation from the literature review is that truss topology optimization problems with continuous member areas possesses properties that makes their solution very difficult. If the nested approach is adopted, singularity phenomena related to vanishing members and problems with buckling constraints pose serious difficulties, as well as the issue of kinematic stability. The mixed variable formulations circumvent these problems, but face the issues of global optimization of MINLP problems. Presently, in the mixed variable framework, only relatively small problems can be solved to global optimality.

If the member profiles are chosen from a predefined discrete set, the nested approach has to deal with the same difficulties as in the continuous case. Furthermore, gradient-based solution methods become unavailable, and also deterministic methods of discrete optimization are difficult to apply, since analytical expressions of the constraint functions are not available. Heuristic methods, such as genetic algorithms, can be applied to solve discrete topology optimization problems, but they require a huge number of structural analyses, and are limited in the size of problems they can solve. In the discrete setting, the mixed variable formulation of the SAND approach leads to a MILP

problem that does not suffer from the singularity issues or other theoretical problems of topology optimization.

Even though truss topology optimization has been studied for decades, there is still an obvious demand for further research. For the general development, the issues with buckling length and kinematic stability lack a satisfying solution. In order to make topology optimization more directly applicable for structural designers, the requirements of the design codes should be introduced in the problem formulation where possible. The present work is a study of truss topology optimization with regard to these questions.

1.3 Scope and Aims of the Thesis

The main focus of the thesis is the mixed variable approach for truss topology optimization with discrete member cross-sections. This approach was chosen due to following reasons:

- the formulation is not susceptible to singularities and other theoretical issues caused by vanishing members;
- if the solution algorithm finds an optimum solution, it is guaranteed to be the global optimum;
- topological constraints can be expressed efficiently by binary variables.

The first goal is to unify the mixed variable formulations presented in the literature. Then, the formulations are extended such that member buckling and kinematic stability of the truss are treated properly. Furthermore, requirements of Eurocode 3 are incorporated in the problem. In this thesis, member strength, stability, and stiffness are considered, and the structure is analyzed as a pin-jointed truss. Thus, joint strength and the effects of bending and torsion are not included in the study. This restriction clearly implies that the solution provided by optimization is not necessarily applicable to the structural designer as such, but might need further modifications to satisfy the requirements that were not included in the problem formulations.

In truss optimization, typically the weight of the truss is minimized, and it serves as the default objective function in this thesis as well. However, often the most interesting objective function is the cost of the structure. In this study, the cost function of Haapio (2012) is modified for tubular plane trusses and taken as an objective function. For situations, where actual cost data is not available, other quantities that affect the cost are chosen as objective functions. These include the number of members, the number of joints, and the number of profiles appearing in the truss. As none of these criteria are likely to yield a solution that is close to the minimum cost design, multicriterion formulations are proposed, where the three criteria and the weight are minimized simultaneously. Consequently, a set of Pareto optimal solutions, which represent mathematically better designs than the other feasible solutions, is generated.

A further interesting issue is the relationship between the minimum cost and minimum weight structures. This matter is investigated by a multicriterion problem formulation,

where cost and mass of the truss are minimized simultaneously. By this formulation, quantitative information about the conflict of cost and mass is obtained in the context of topology optimization.

The various formulations presented in this study serve to answer the following research questions:

Q1. What possibilities does the mixed variable approach offer for solving the present open issues of truss topology optimization and for taking into account the needs of the structural designer?

Q2. Is the mixed variable approach a suitable tool for cost optimization? If the details of a cost function are not available, what other possibilities are there to find economical solutions?

The second major goal of the thesis is to investigate the capability of modern algorithms to solve the optimization problems of the proposed formulation in practical design situations. In this study, commercial state-of-the-art software is employed for solving the mixed variable problems. This part of the thesis will give guidelines about the cases that are presently solvable. The research question related to the numerical solution process is:

Q3. What is the quality of the solutions that can be obtained in given time, when the mixed variable formulations are applied to practical design situations?

The quality of the solution means, roughly speaking, how far the obtained solution is from the global optimum or its conservative approximation. Such information is readily available with the method applied in this thesis.

1.4 Main Contribution

The study contains several results. In the following, the most significant contributions are briefly discussed.

Unification of mixed variable formulations Each of the few papers dealing with mixed variable formulations for truss topology optimization emphasizes different aspects. In this thesis, the ideas presented in the literature are brought together and unified under the same problem formulation.

Extensions of basic formulations Typically, the weight of the truss is minimized subject to strength (stress) constraints. In the present study, this basic formulation is extended to include member buckling constraints. Both Euler buckling and buckling according to Eurocode 3 are considered. The issue of the jump in buckling length phenomenon is resolved by introducing *chains* to the ground structure. Chains are also used to ensure kinematic stability of the solution and to treat line loading properly.

Multicriterion formulations Economy of a design is generally not determined only by its weight. Other factors affecting the economy of the truss are identified and written as criteria that are optimized simultaneously with the weight. The Pareto optimal solutions of the resulting multicriterion problem can be further evaluated for cost and manufacturing purposes.

Computational studies The proposed formulations are verified by benchmark problems, most of them devised for the purposes of the thesis. The problem data and the results are given in detail so they can be used for testing the performance of future algorithms. The applicability of the formulations to practical design situations is explored by a case study considering the optimization of a roof truss.

CHAPTER 2

Design of Tubular Trusses

A common mistake that people make when trying to design something completely foolproof is to underestimate the ingenuity of complete fools.

Douglas Adams

2.1 Introduction

In structural design a great number of decisions must be made, ranging from the choice of structure type and materials to the fine details of the connections. It is commonly accepted, that the decisions made at the conceptual design phase have the strongest influence on the economy and performance of the structure. In truss design, this means that the layout of the truss is the key element for achieving an economical structure. In this thesis, the scope of design is limited to determining the optimum layout (topology) of the truss. Finer details, such as joint design, are not considered.

A design procedure that is commonly described in the literature (Trahair & Bradford 1988, Haapio 2012) can be stated for trusses as follows. Based on the loads and the span or other geometric data of the truss, the designer chooses the initial layout and member sections. Then, structural analysis is performed and the design rules are checked. If some rules are violated or if the designer thinks that the solution can be improved, the member sections are modified. This iterative process of structural analysis and design modification is repeated until the solution satisfies the design rules

and is economical enough. Finally, the details of the truss are designed such that the truss can be manufactured.

The above design process can be partly automated by the means of structural optimization. The level of automation depends on which of the three problem types presented in Chapter 1 is chosen. Sizing optimization automates the loop of structural analysis and verification of the design rules. Geometry and topology optimization relieve the designer from fixing the layout of the truss, thus providing more flexibility. Of the three problem types, topology optimization gives the most freedom to the designer, since only the ground structure needs to be determined in the beginning.

For choosing the member cross-section alternatives, many kinds of profiles are available. Every commercially available profile has its benefits and drawbacks in terms of mechanical behaviour and applications. As an economical design is most often sought, choosing a favourable cross-section type is crucial. In this thesis, the profiles chosen for the truss members are *square hollow sections (SHS)* or *rectangular hollow sections (RHS)* made of steel. However, the formulations presented are also applicable (with modifications) for other cross-section shapes and materials. In this chapter, the analysis and design of tubular trusses is considered as related to the thesis. Both the structural analysis model and the design code requirements are essential for formulating the optimization problems, as they provide the constraints which ensure the applicability of the solution.

In truss design, selecting the appropriate shape and size of the member profiles has a great impact on the economy of the structure. Tubular cross-sections have become very popular due to their excellent mechanical properties which enable economical designs. Presently, tubular trusses can be found in constructions such as roofs of public and industrial buildings and arenas, bridges, transmission towers, and cranes.

Compared to their weight, hollow sections have high torsional and bending stiffness, and they are well-suited for compression members. Hollow sections are also less susceptible to lateral and torsional buckling. Also, the outer surface of a closed shape is relatively small which, together with the lack of sharp corners, reduces the cost of fire and corrosion protection.

A more detailed discussion about the benefits and applications of structural hollow sections can be found in (Wardenier, Packer, Zhao & van der Vegte 2010) and (Jalkanen 2007).

In the European Union, the Eurocodes provide a series of rules that a steel truss has to satisfy in any construction (EN 1993–1–1 2005). The rules concern the strength, stability, durability, serviceability and fire safety. In this work, the constraints of the optimization problem concerning member strength and buckling are derived from Eurocode 3 (EN 1993–1–1 2005). In the following, truss design according to Eurocode 3 as related to the present study is discussed.

2.2 Structural Analysis

According to the Eurocode, either elastic or plastic design methodology can be applied in truss design (EN 1993–1–1 2005, Clause 5). In this thesis, the structural analysis

is performed according to the theory of linear elasticity. The truss is modelled as a pin-jointed structure which is loaded at the nodes. Thus, the only stress resultant appearing in the members is the normal force.

The basis of structural analysis is the displacement method, which is also implemented in most finite element programs. However, in this thesis, the stiffness equation of the displacement method is disaggregated in order to avoid the singularity of the stiffness matrix, which is a common phenomenon in topology optimization as explained in Chapter 1.

In truss analysis, the three conditions that must be satisfied are: equilibrium of forces at the nodes, compatibility conditions, and force-displacement relations.

Suppose the truss is subjected to n_L loading conditions. The nodal equilibrium equations can be written as

$$\mathbf{B}\mathbf{N}^k = \mathbf{p}^k \quad \forall\, k = 1, 2, \ldots, n_L \tag{2.1}$$

where $\mathbf{B} \in \mathbb{R}^{n_d \times n_E}$ is the *statics matrix* of the structure, $\mathbf{N}^k$ is the vector of member forces and $\mathbf{p}^k \in \mathbb{R}^{n_d}$ is the load vector. The number of nodal degrees of freedom is n_d and the number of truss members is n_E.

The axial strain of member i in loading condition k is

$$\varepsilon_i^k = \frac{1}{L_i}\mathbf{b}_i^{\mathrm{T}}\mathbf{u}^k \tag{2.2}$$

where L_i is the length of the member, $\mathbf{b}_i \in \mathbb{R}^{n_d}$ is the i^{th} column of the statics matrix, and $\mathbf{u}^k \in \mathbb{R}^{n_d}$ is the vector of global nodal displacements in the k^{th} loading condition. Applying Hooke's law gives the member stress σ_i^k:

$$\sigma_i^k = E_i\varepsilon_i^k = \frac{E_i}{L_i}\mathbf{b}_i^{\mathrm{T}}\mathbf{u}^k \tag{2.3}$$

where E_i is the Young's modulus.

Finally, the normal force, N_i^k, is related to the displacements by the definition of normal stress, $\sigma_i^k = N_i^k/A_i$:

$$N_i^k = \frac{E_i A_i}{L_i}\mathbf{b}_i^{\mathrm{T}}\mathbf{u}^k \tag{2.4}$$

where A_i is the cross-sectional area of the member. Eqs. (2.1) and (2.4) constitute the equations of structural analysis that the truss must satisfy. Alternatively, Eq. (2.3) can be used along with the equation $N_i^k = \sigma_i^k A_i$ instead of Eq. (2.4). Eq. (2.4) includes the compatibility conditions and force-displacement relations.

2.3 Classification of Cross-Sections

Member cross-sections are divided into four classes according to the role of local buckling in limiting the resistance and rotation capacity of the section (EN 1993–1–1 2005, Clause 5.5). In this thesis, classes 1, 2 and 3 are considered. Cross-sections in class 1 can develop their plastic moment resistance with the rotation capacity as required by plastic analysis before local buckling, i.e. buckling of the cross-section walls, occurs.

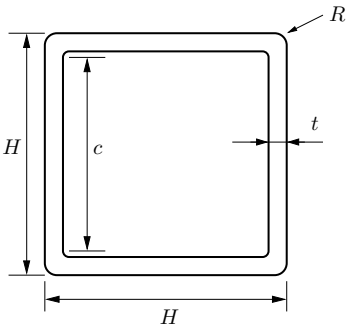

Figure 2.1: Square hollow section dimensions. The dimension R is the outer radius of the corner rounding. The length c is the side length of the hollow part, from which the inner radii have been subtracted.

Class 2 sections can also develop their plastic moment resistance, but the rotation capacity at the plastic hinge is limited by local buckling. For class 3 cross-sections, the yield strength can be reached, but local buckling occurs before the plastic moment resistance is attained.

The class of a cross-section is defined by its geometry and the type of loading the section is subjected to. For rectangular sections, the limiting inequality is

$$\frac{c}{t} \leq C\epsilon \tag{2.5}$$

where t is the wall thickness of the section, c is the length of the hollow part of the section where the inner radii of the roundings have been subtracted as shown in Fig. 2.1, C is a constant depending on the loading type and

$$\epsilon = \sqrt{\frac{235}{f_\mathrm{y}}} \tag{2.6}$$

where f_y is the yield strength of the material of the section. The value of C depends on whether the part of the cross section is subject to bending, compression or their combination. For example, rectangular compression members belong to class 3, if Eq. (2.5) is satisfied with $C = 43$.

The dimension c appearing in Eq. (2.5) can be computed by

$$c = H - 2R \tag{2.7}$$

where H is the side length of the section.

2.4 Resistance of Cross-Sections

Members under axial force N_{Ed} must satisfy the conditions (EN 1993–1–1 2005, Clauses 6.2.2 and 6.2.3)

$$\frac{N_{\mathrm{Ed}}}{N_{\mathrm{t,Rd}}} \leq 1.0 \quad \text{(tension)} \tag{2.8}$$

$$\frac{N_{\mathrm{Ed}}}{N_{\mathrm{c,Rd}}} \leq 1.0 \quad \text{(compression)} \tag{2.9}$$

where the *design resistance* is

$$N_{\mathrm{t,Rd}} = N_{\mathrm{c,Rd}} = A\frac{f_{\mathrm{y}}}{\gamma_{\mathrm{M0}}} \tag{2.10}$$

Here, A is the member area, f_{y} is the yield strength and γ_{M0} is the partial safety factor. In this thesis, the value $\gamma_{\mathrm{M0}} = 1.0$ given in (EN 1993–1–1 2005, clause 6.1(1)) is used as stated in the Finnish National Annex of the Eurocode (EC 3 NA 2005).

If the common sign convention is employed, where the normal force in compression is negative, Eqs. (2.8) and (2.9) can be combined to a form, which is suitable for optimization:

$$-A\frac{f_{\mathrm{y}}}{\gamma_{\mathrm{M0}}} \leq N_{\mathrm{Ed}} \leq A\frac{f_{\mathrm{y}}}{\gamma_{\mathrm{M0}}} \tag{2.11}$$

Eq. (2.11) is commonly used in truss topology optimization to express the strength (stress) constraints.

2.5 Buckling Resistance of Members

Stability is the predominant phenomenon that dictates the sizing of compression members. Typically in the literature on truss optimization, Euler buckling is considered. However, as shown by Farkas & Jármai (1997, Chapter 9), design according to Euler buckling might lead to unsafe designs, since the effects of initial crookedness and residual stresses are not taken into account. Therefore, the design rules of the Eurocode should be considered.

According to Eurocode 3, members in compression must satisfy the condition (EN 1993–1–1 2005, Clause 6.3.1)

$$\frac{N_{\mathrm{Ed}}}{N_{\mathrm{b,Rd}}} \leq 1 \tag{2.12}$$

where the buckling resistance

$$N_{\mathrm{b,Rd}} = \frac{\chi A f_{\mathrm{y}}}{\gamma_{\mathrm{M1}}} \tag{2.13}$$

and χ is the reduction factor. Its value is determined from the *non-dimensional slenderness*, $\bar{\lambda}$, by

$$\chi = \frac{1}{\Phi + \sqrt{\Phi^2 - \bar{\lambda}^2}}, \quad \text{but } \chi \leq 1.0 \tag{2.14}$$

where

$$\Phi = 0.5\left[1 + \alpha(\bar{\lambda} - 0.2) + \bar{\lambda}^2\right] \tag{2.15}$$

and

$$\bar{\lambda} = \sqrt{\frac{Af_y}{N_{cr}}} \tag{2.16}$$

Here, N_{cr} is the elastic critical force according to Euler buckling:

$$N_{cr} = \pi^2 \frac{EI}{L_n^2} \tag{2.17}$$

In the above, I is the moment of inertia of the cross-section with respect to the major principal axis, and L_n is the buckling length of the member.

The *imperfection factor*, α, in Eq. (2.15) depends on the cross-section. For cold formed rectangular sections, $\alpha = 0.49$ (EN 1993–1–1 2005, Tables 6.1 and 6.2).

Employing the same sign convention as above, the buckling constraint can be expressed as

$$N_{Ed} \geq -\frac{\chi A f_y}{\gamma_{M1}} \tag{2.18}$$

According to the Finnish National Annex (EC 3 NA 2005), the value $\gamma_{M1} = 1.0$ stated in (EN 1993–1–1 2005, clause 6.1(1)) is used.

2.6 Other Design Aspects

The requirements for member strength and buckling constitute the primary constraints of the optimization problems presented later in the thesis. The Eurocode contains further rules to guarantee the safety of the structure. These rules are not included in the optimization problems of this thesis. In the following, a short discussion on some of the design aspects that have been neglected, is presented.

2.6.1 Design of Joints

In general, joint behaviour should be considered early in the design process (Wardenier et al. 2010). In tubular trusses, mostly welded joints are used. In (EN 1993–1–8 2005), design rules for joint strength are given. Each joint type has its own design rules, which correspond to the different failure modes of the joint. The design rules are given in terms of the normal forces of the bracing members, and the weld sizes are then determined as multiples of member wall thickness.

In order to apply the joint design rules, the details of the geometry of the joint must be known. If the center lines of the connecting braces do not intersect at the center line of the chord, an eccentricity appears at the node, which leads to a bending moment to the chord. This eccentricity must be taken into account for the compression chord, and also in the joint design, if the eccentricity is greater than given bounds.

The greatest challenge for incorporating the joint strength rules in topology optimization is the fact that the design rules depend on the type of the joint, which is

determined by the number of members joining at a node. In topology optimization, the number of members present at a node is not fixed but may vary. Thus, the design rule to apply also varies during optimization. If a dense ground structure is employed, keeping track of the members at a node and enforcing the correct design rule becomes very tedious.

Consequently, the joint strength is not considered in this thesis. A possible approach for including joint strength in the optimization is to proceed in two phases. First, the optimum topology is determined without joint strength constraints. Then, the joints of the design obtained from topology optimization are checked. If any joint fails to satisfy the design rules, a sizing optimization is performed for the fixed topology and with joint strength constraints.

2.6.2 Chords as Continuous Beams

In the structural model of the truss that is employed in this thesis, only axial force of members is present and the effects of bending and torsion are neglected. This model is justified in many cases. However, there are also situations, where bending and torsion need to be considered. For example, if transversal loads are applied elsewhere than at the nodes or if the eccentricity of the nodes is too large, the resulting bending moments need to be taken into account. Also, in roof trusses, the chords are manufactured as long members, extending over the nodes at which the braces are connected. Consequently, transversal loads cause bending moment in the chords. In such cases, it is recommended to consider the chords as continuous beams to which the braces are connected by pin joints (EN 1993–1–8 2005, Clause 5.1.5) and (Wardenier et al. 2010, pp. 68). This requires a frame analysis of the structure, which is considerably more involved than the analysis of trusses. As the scope of the thesis is specifically limited to trusses, treating the structures as frames is left for future studies.

2.7 Discussion

In the literature on truss topology optimization, the design codes are scarcely included in the problem formulations. One reason for this could be that most rules other than the strength constraints are mathematically difficult to handle in the optimization. For example, the expressions for computing the reduction factor for member buckling, Eqs. (2.14)–(2.17), are rather involved, Eq. (2.14) being non-differentiable at $\bar{\lambda} = 0.2$. The joint design rules are also very difficult mathematically: expressions of some factors depend on whether the member is in tension or in compression, and the design rules depend on the type of the joint which may vary at the node during topology optimization.

The mixed variable formulations studied in this thesis allow to incorporate some of the design rules of the Eurocode in the optimization problem. For example, member buckling reduces to a linear constraint in the employed formulations. This thesis provides a starting point for further studies for including the different rules of the Eurocodes and possibly other design codes in truss topology optimization.

CHAPTER 3

Mixed Variable Formulations for Discrete Sections

Mathematicians are like Frenchmen: whatever you say to them they translate into their own language, and forthwith it is something entirely different.

GOETHE

3.1 Introduction

In this chapter, truss topology optimization problems are formulated. The main assumption is that the member cross-sections are chosen from a predefined set of discrete alternatives. This corresponds to common design situations, where the designer must choose the profiles from commercially available catalogue provided by the manufacturer.

The formulation of optimization problems consists of three main components: *variables*, *objective function*, and *constraints*. The variables are the quantities that can be altered in order to improve the objective function which is either minimized or maximized. The variables can be categorized to *design variables*, which constitute the actual design, and *state variables*, which determine the state of the design. Common choices for design variables are the cross-sectional areas of the truss members, whereas the member forces and nodal displacements are often chosen as state variables.

An optimization problem is written in standard form as

$$\begin{aligned} \min_{\mathbf{x}} \quad & f(\mathbf{x}) \\ \text{subject to} \quad & g_i(\mathbf{x}) \leq 0 \quad i = 1, 2, \ldots, q \\ & h_j(\mathbf{x}) = 0 \quad j = 1, 2, \ldots, p \end{aligned} \tag{3.1}$$

where $\mathbf{x}$ is the vector of design variables, f is the objective function, and g_i and h_j are the inequality and equality constraint functions, respectively. Problem Eq. (3.1) can be written more compactly as

$$\min_{\mathbf{x} \in \Omega} f(\mathbf{x}) \tag{3.2}$$

where

$$\Omega = \{\, \mathbf{x} \,|\, g_i(\mathbf{x}) \leq 0,\, h_j(\mathbf{x}) \leq 0,\, \forall i = 1, 2, \ldots, q,\, j = 1, 2, \ldots, p \,\} \tag{3.3}$$

is the *feasible set*. The points of the feasible set are called *feasible designs*.

There are several approaches for formulating structural optimization problems. The prevailing philosophies are the *nested analysis and design* (NAND), and the *simultaneous analysis and design* (SAND) approach (Arora & Wang 2005).

In NAND formulations, the optimization variables are solely the design variables, and all the responses, such as displacements, stresses, and internal forces are treated as implicit functions of the design variables. Each time these implicit functions need to be evaluated, a structural analysis is performed for given design variable values. Furthermore, by the means of sensitivity analysis, the gradients of the responses can be computed.

If the optimization problem is formulated according to the SAND approach, the state variables are included as optimization variables, and the equations of structural analysis are treated as equality constraints. Consequently, no structural analysis is performed during optimization, but the constraints guarantee that the optimum design satisfies the equations of mechanics.

The two approaches have been compared by Arora & Wang (2005). The main advantages of the NAND approach are that fewer variables and constraints are included in the optimization problem and that the equilibrium equations are satisfied at each iteration. On the other hand, solving the equilibrium equations at each iteration and performing sensitivity analysis can be very time-consuming. Furthermore, as the responses are known only implicitly as functions of the design variables, the mathematical properties of these functions cannot be fully utilized in optimization.

The SAND approach does not suffer from the disadvantages of the NAND approach. As the equations of structural analysis are now included as equality constraints, neither a separate structural analysis nor sensitivity analysis needs to be performed. Furthermore, in some instances, certain constraints become linear in the variables. As the analytical expressions of structural analysis are available, their mathematical properties can be exploited in the solution process. On the other hand, the number of optimization variables and constraints becomes large in the SAND approach. Thus, large-scale optimization algorithms must be used for most problems in the SAND formulation. Another disadvantage of the SAND approach is that the intermediate

solutions might not satisfy the equilibrium equations. Consequently, only at the end of the optimization, a usable design is guaranteed.

For further discussion on the different formulation approaches in structural optimization, see (Arora & Wang 2005).

An instance of the SAND approach for truss topology optimization is presented and studied in this thesis. By introducing binary variables for member and node existence and by considering the normal forces and nodal displacements as state variables, the topology optimization problem can be stated as a mixed-integer linear optimization problem. According to the SAND philosophy, the equations of structural analysis are treated as equality constraints. The stiffness equation is disaggregated as presented in Chapter 2. Consequently, the singularity issues and discontinuities induced by vanishing members are avoided.

3.2 Variables

The optimization variables are both continuous and binary. The continuous variables, which are also the state variables, are the member normal forces and nodal displacements. The design variables are binary and they are used to determine the existence of members and nodes as well as the actual profile selection for members present in the truss.

The following index sets are defined to facilitate notation. The set of members of the ground structure is denoted $\mathcal{M} = \{1, 2, \ldots, n_E\}$. The set of ground structure nodes is $\mathcal{N} = \{1, 2, \ldots, n_N\}$. The set of loading conditions is $\mathcal{L} = \{1, 2, \ldots, n_L\}$, and the set of available profiles is $\mathcal{P} = \{1, 2, \ldots, n_S\}$.

3.2.1 Profile Selection

Suppose the member profiles are to be chosen from a set of n_S alternatives, which have been ordered in increasing cross-sectional area. Denote the sets of available member areas and moment of inertias, respectively, by

$$\mathcal{A} = \{\hat{A}_1, \hat{A}_2, \ldots, \hat{A}_{n_S}\} \tag{3.4}$$

$$\mathcal{I} = \{\hat{I}_1, \hat{I}_2, \ldots, \hat{I}_{n_S}\} \tag{3.5}$$

Here, $\hat{A}_j < \hat{A}_{j+1}$ for all j, but $\hat{I}_j > \hat{I}_{j+1}$ is possible.

A profile is chosen for each member by binary variables, y_{ij}, defined by (Rasmussen & Stolpe 2008)

$$y_{ij} = \begin{cases} 1 & \text{if profile } j \text{ is chosen for member } i \\ 0 & \text{otherwise} \end{cases} \qquad i \in \mathcal{M},\ j \in \mathcal{P} \tag{3.6}$$

A constraint enforcing a unique profile to member i is

$$\sum_{j=1}^{n_S} y_{ij} \leq 1 \tag{3.7}$$

If the left-hand side of Eq. (3.7) is zero, member i is not included in the truss. Another possibility is to include variables y_{i0} for explicitly stating that the member is removed. Then, the constraint Eq. (3.7) is replaced by

$$\sum_{j=0}^{n_S} y_{ij} = 1 \tag{3.8}$$

The variables y_{i0} can be interpreted either as *slack variables* for the inequality constraint Eq. (3.7), or variables for selecting a profile with zero cross-sectional area.

The cross-sectional properties of member i are expressed by

$$A_i = \sum_{j=1}^{n_S} \hat{A}_j y_{ij} \tag{3.9}$$

$$I_i = \sum_{j=1}^{n_S} \hat{I}_j y_{ij} \tag{3.10}$$

More generally, let X any cross-sectional property to be selected from a set of available values, $\hat{X}_j$, $j \in \mathcal{P}$. This property for member i is determined by

$$X_i = \sum_{j=1}^{n_S} \hat{X}_j y_{ij} \tag{3.11}$$

A separate binary variable, y_i, can be assigned for each member to control the existence of the member. This variable takes the value 1 if member i is included in the truss and 0 otherwise, and it is related to the profile selection variables by

$$y_i = \sum_{j=1}^{n_S} y_{ij} \tag{3.12}$$

This constraint replaces Eq. (3.7). Note that if the variables y_i are included, the variables y_{i0} become redundant and should be excluded from the problem formulation. Further implications of the variables y_i to the solution process are discussed later.

The binary variables can be compiled in a vector form by

$$\mathbf{y} = \{y_{11}\ y_{12}\ \dots\ y_{1,n_S}\ \dots\ y_{n_E,1}\ y_{n_E,2}\ \dots\ y_{n_E,n_S}\} \tag{3.13}$$

$$\mathbf{Y} = \{y_1\ y_2\ \dots\ y_{n_E}\} \tag{3.14}$$

$$\mathbf{y}_0 = \{y_{10}\ y_{20}\ \dots\ y_{n_E,0}\} \tag{3.15}$$

3.2.2 Member Forces

The member forces are taken as state variables in the optimization. Here, the developments of Rasmussen & Stolpe (2008) are followed. For the purposes of the proposed problem formulation, it is beneficial to define a separate member force variable for each available profile and each loading condition k:

$$N_{ij}^k = \frac{E_i}{L_i} \hat{A}_j \mathbf{b}_i^{\mathrm{T}} \mathbf{u}^k y_{ij} \quad \forall\, i \in \mathcal{M},\, j \in \mathcal{P},\, k \in \mathcal{L} \tag{3.16}$$

In the above, Eq. (2.4) is employed. The member forces are obtained as the sum of the N_{ij}^k variables:

$$N_i^k = \sum_{j=1}^{n_S} N_{ij}^k \tag{3.17}$$

A force variable is defined for each available profile for every member in the ground structure for all loading conditions. Consequently, the number of force variables increases rapidly, if the ground structure is made denser and if several loading conditions are considered.

Note that

$$N_{ij}^k = \begin{cases} \dfrac{E_i}{L_i}\hat{A}_j \mathbf{b}_i^{\mathrm{T}} \mathbf{u}^k & \text{if } y_{ij} = 1 \\ 0 & \text{otherwise} \end{cases} \tag{3.18}$$

Suppose each nodal displacement u_r is bounded by $\underline{u}_r$ and $\overline{u}_r$. Then the following lower and upper bounds can be derived for the force variables N_{ij}^k:

$$\underline{N}_{ij}^k = \min_{\underline{\mathbf{u}} \le \mathbf{u}^k \le \overline{\mathbf{u}}} \left\{ \frac{E_i}{L_i}\hat{A}_j \mathbf{b}_i^{\mathrm{T}} \mathbf{u}^k \right\} = \frac{E_i \hat{A}_j}{L_i} \left(\sum_{r:b_{ir}>0} b_{ir}\underline{u}_r + \sum_{r:b_{ir}<0} b_{ir}\overline{u}_r \right) \tag{3.19}$$

$$\overline{N}_{ij}^k = \max_{\underline{\mathbf{u}} \le \mathbf{u}^k \le \overline{\mathbf{u}}} \left\{ \frac{E_i}{L_i}\hat{A}_j \mathbf{b}_i^{\mathrm{T}} \mathbf{u}^k \right\} = \frac{E_i \hat{A}_j}{L_i} \left(\sum_{r:b_{ir}>0} b_{ir}\overline{u}_r + \sum_{r:b_{ir}<0} b_{ir}\underline{u}_r \right) \tag{3.20}$$

where b_{ir} are the components of the vector $\mathbf{b}_i$.

The crucial step that allows a linear problem formulation is the transformation of the equality constraint Eq. (3.16) into a set of the linear inequalities:

$$\underline{N}_{ij}^k y_{ij} \le N_{ij}^k \le \overline{N}_{ij}^k y_{ij} \tag{3.21}$$

$$(1 - y_{ij})\underline{N}_{ij}^k \le \frac{E_i}{L_i}\hat{A}_j \mathbf{b}_i^{\mathrm{T}} \mathbf{u}^k - N_{ij}^k \le (1 - y_{ij})\overline{N}_{ij}^k \tag{3.22}$$

It is easy to verify that if $y_{ij} = 0$, Eq. (3.21) implies $N_{ij}^k = 0$ and if $y_{ij} = 1$, Eq. (3.22) implies $N_{ij}^k = \frac{E_i}{L_i}\hat{A}_j \mathbf{b}_i^{\mathrm{T}} \mathbf{u}^k$.

3.2.3 Nodal Variables

Binary variables can also be related to the nodes of the truss. Each node of the ground structure is given a binary variable, z_ℓ, $\ell \in \mathcal{N}$. These variables provide flexibility for modeling topological properties of the truss. Also, they allow to deal with the number of members connected to each node as well as kinematic stability of the truss.

The variable z_ℓ controls the displacements of the corresponding node by

$$\underline{\mathbf{u}}_\ell z_\ell \le \mathbf{u}_\ell^k \le \overline{\mathbf{u}}_\ell z_\ell \quad \forall\, \ell \in \mathcal{N},\, k \in \mathcal{L} \tag{3.23}$$

where $\mathbf{u}_\ell^k$ is the vector of displacements of node ℓ in loading condition k. Note that the above constraints need to be included only for unsupported degrees of freedom.

Let $\mathcal{M}_\ell \subseteq \mathcal{M}$ the members connected to node ℓ. The following constraints relate these members with the node (Faustino et al. 2006):

$$\sum_{i\in\mathcal{M}_\ell} y_i = \sum_{i\in\mathcal{M}_\ell}\sum_{j=1}^{n_S} y_{ij} \le |\mathcal{M}_\ell| z_\ell \quad \forall\, \ell \in \mathcal{N} \tag{3.24}$$

$$\sum_{i\in\mathcal{M}_\ell} y_i = \sum_{i\in\mathcal{M}_\ell}\sum_{j=1}^{n_S} y_{ij} \ge \underline{C}_\ell z_\ell \quad \forall\, \ell \in \mathcal{N} \tag{3.25}$$

The first constraint makes all the members connected to node ℓ vanish, if $z_\ell = 0$. The latter constraint guarantees that if a node is present, there are at least $\underline{C}_\ell$ members connected to it. For free nodes, $\underline{C}_\ell = 2$ (plane trusses), and for supported nodes, $\underline{C}_\ell = 1$. Note that Faustino et al. (2006) use $\underline{C}_\ell = 1$ for all nodes.

In mixed variable problems, it is beneficial to find a formulation that has as tight a relaxation as possible (see Chapter 4). Eq. (3.24) can be replaced by a set of constraints

$$y_i = \sum_{j=1}^{n_S} y_{ij} \le z_\ell \quad \forall\, \ell \in \mathcal{N},\, i \in \mathcal{M}_\ell \tag{3.26}$$

If an upper bound, say $\overline{C}_\ell$, for the number of members connected to node ℓ is desired, the constant $|\mathcal{M}_\ell|$ appearing on the right-hand side of Eq. (3.24) can be replaced by $\overline{C}_\ell$. For example, Ohsaki & Katoh (2005) use this limit to ensure the manufacturability of joints by disallowing too many members to connect to any node. The appropriate value of $\overline{C}_\ell$ depends on the design situation and joint technology. The node is related with a set of constraints as in Eq. (3.26) along with a constraint of the form Eq. (3.24).

The binary variables can be employed to state the necessary condition of kinematic stability of the truss as a linear constraint. If the truss is kinematically stable, then the number of nodes, N_c, the number of members, N_y, and the number of support reactions, N_R, satisfy the inequality

$$N_y + N_R \ge 2N_c \tag{3.27}$$

The condition Eq. (3.27) can be written in terms of the design variables as

$$\sum_{i=1}^{n_E} y_i + \sum_{s\in\mathcal{N}_S} R_s z_s \ge 2\sum_{\ell=1}^{n} z_\ell \tag{3.28}$$

$$\Rightarrow \quad \sum_{i=1}^{n_E}\sum_{j=1}^{n_S} y_{ij} + \sum_{s\in\mathcal{N}_S} R_s z_s \ge 2\sum_{\ell=1}^{n} z_\ell \tag{3.29}$$

where $\mathcal{N}_S \subseteq \mathcal{N}$ is the set of supported nodes and R_s is the number of support reactions at the supported node s.

Further constraints for nodal variables can be derived as follows. First, let $\mathcal{N}_L \subseteq \mathcal{N}$ be the set of loaded nodes. These nodes must be present in the structure, so $z_\ell = 1$, for all $\ell \in \mathcal{N}_L$. Second, a truss needs at least two supporting nodes. The following inequality constraint enforces this condition:

$$\sum_{\ell\in\mathcal{N}_S} z_\ell \ge 2 \tag{3.30}$$

3.3 Constraints

In the previous section, a set of constraints was related to each variable type. In this section, constraints ensuring the strength and stability of the truss are presented.

As noted in Section 2.2, the equations of structural analysis are treated as constraints in the optimization problem. The force-displacement relations and compatibility conditions are included in the definition of the force variables, Eq. (3.18), and in the resulting linear inequality constraints Eqs. (3.21) and (3.22). It remains to include the nodal equilibrium equations as equality constraints.

3.3.1 Nodal Equilibrium

The structural analysis of trusses is based on the assumption that all loads are located at the nodes. Therefore, usually only point loads are considered in the truss optimization literature. In some applications, such as roof trusses, the structure can be subjected to a distributed load. This load can be transmitted to the nodes of the truss by additional structural elements. In the structural model, the distributed load is then replaced by equivalent nodal loads. If the number of nodes under the distributed load is fixed, then this procedure is simple. In topology optimization, the number of nodes subjected to the distributed load is not known in advance. Therefore, to appropriately include distributed loads in the problem formulation, special modeling techniques must be employed. Here, the binary variables y_i controlling the existence of the members are invaluable.

General Equations

As already presented in Eq. (2.1), the equilibrium of forces at the nodes leads to the following equality constraint:

$$\mathbf{B}\mathbf{N}^k = \mathbf{p}^k \quad \forall\, k \in \mathcal{L} \tag{3.31}$$

Recall from Section 2.2 that $\mathbf{B} \in \mathbb{R}^{n_d \times n_E}$, $\mathbf{N}^k \in \mathbb{R}^{n_E}$ and $\mathbf{p}^k \in \mathbb{R}^{n_d}$. Denote by $\mathbf{N}_i^k$ the vector

$$\mathbf{N}_i^k = \{N_{i1}^k \; N_{i2}^k \; \dots N_{in_S}^k\} \in \mathbb{R}^{n_S} \tag{3.32}$$

of force variables of member i in loading condition k. The left-hand side of Eq. (3.31) can then be written as

$$\mathbf{B}\mathbf{N}^k = \mathbf{B}\begin{bmatrix} \sum_{j=1}^{n_S} N_{1j}^k \\ \sum_{j=1}^{n_S} N_{2j}^k \\ \vdots \\ \sum_{j=1}^{n_S} N_{n_E,j}^k \end{bmatrix} = \underbrace{\mathbf{B}\begin{bmatrix} \mathbf{1}^{\mathrm{T}} & \mathbf{0}^{\mathrm{T}} & \mathbf{0}^{\mathrm{T}} & \cdots & \mathbf{0}^{\mathrm{T}} \\ \mathbf{0}^{\mathrm{T}} & \mathbf{1}^{\mathrm{T}} & \mathbf{0}^{\mathrm{T}} & \cdots & \mathbf{0}^{\mathrm{T}} \\ \vdots & \vdots & \vdots & \vdots & \vdots \\ \mathbf{0}^{\mathrm{T}} & \mathbf{0}^{\mathrm{T}} & \cdots & \cdots & \mathbf{1}^{\mathrm{T}} \end{bmatrix}}_{\mathbf{C}} \underbrace{\begin{bmatrix} \mathbf{N}_1^k \\ \mathbf{N}_2^k \\ \vdots \\ \mathbf{N}_{n_E}^k \end{bmatrix}}_{\hat{\mathbf{N}}^k} \tag{3.33}$$

where $\mathbf{1} \in \mathbb{R}^{n_S}$ is a vector of ones and $\mathbf{0} \in \mathbb{R}^{n_S}$ is a vector of zeros. Thus, $\mathbf{C} \in \mathbb{R}^{n_E \times (n_E \cdot n_S)}$ and $\hat{\mathbf{N}}^k \in \mathbb{R}^{n_E \cdot n_S}$. The product $\mathbf{BC}$ leads to

$$\hat{\mathbf{B}} = \left[\begin{array}{cccc:c:cccc:c:c:cccc} \mathbf{b}_1 & \mathbf{b}_1 & \cdots & \mathbf{b}_1 & \vdots & \mathbf{b}_2 & \mathbf{b}_2 & \cdots & \mathbf{b}_2 & \vdots & \cdots & \vdots & \mathbf{b}_{n_E} & \mathbf{b}_{n_E} & \cdots & \mathbf{b}_{n_E} \end{array} \right] \tag{3.34}$$

The matrix $\hat{\mathbf{B}} \in \mathbb{R}^{n_d \times (n_E \cdot n_S)}$ consists of n_E blocks, where the each column of $\mathbf{B}$ is repeated n_S times. Thus, the nodal equilibrium in loading condition k is

$$\hat{\mathbf{B}}\hat{\mathbf{N}}^k = \mathbf{p}^k \tag{3.35}$$

The number of nodal equilibrium equations is $n_L \cdot n_d$.

Line Loading

Suppose the truss is subjected to a line loading. For simplicity, it is assumed that the distribution of the load is uniform and it is either in the global x or y direction.

Usually a line load is converted to equivalent nodal loadings to the nodes of all members subjected to the load. In topology optimization, however, the number of nodes and members subjected to the load is not fixed. As all the loaded nodes must be present in the optimum structure, increasing the number of nodes in the ground structure will increase the number of loaded nodes, which leads to more members in the optimum topology.

For example, consider the rectangular design domain subject to line load q depicted in Fig. 3.1a. Two possible ground structures are shown in Fig. 3.1b and Fig. 3.1c, with the line load converted to equivalent nodal loads. Note that the moments at the nodes caused by the line load are neglected. In both cases, the optimum topology must contain all the nodes of the upper boundary, i.e. all nodes subjected to the line load.

By using the binary variables, y_i or y_{ij}, the above problem can be circumvented. For the part of the ground structure under the line load, members between *all* nodes of the ground structure are introduced. Some of these members will be overlapping. Additional constraints disallow overlapping members from the optimum structure, as described in Section 3.3.3 below. In Fig. 3.2a, three elements are subjected to the line load. To allow the intermediate nodes between elements 1 and 2 and elements 2 and 3 to vanish, elements 4, 5, and 6 are added, as shown in Fig. 3.2b. Each element 1–6 is subjected to the line load separately.

For the global degree of freedom i, the equivalent nodal force due to the line load can be expressed as

$$q_i = \sum_{j \in \mathcal{M}_{\ell(i)}} q_{ij} y_j = \sum_{j \in \mathcal{M}_{\ell(i)}} q_{ij} \sum_{\ell=1}^{n_S} y_{j\ell} = \sum_{j \in \mathcal{M}_{\ell(i)}} \sum_{\ell=1}^{n_S} q_{ij} y_{j\ell} \tag{3.36}$$

where $\mathcal{M}_{\ell(i)}$ is the set of members connected to the node ℓ corresponding to the i^{th} degree of freedom, and q_{ij} are the equivalent nodal loads of these members. The load vector due to the line load is then

$$\mathbf{q} = \mathbf{Q}\mathbf{y}, \quad \mathbf{Q} \in \mathbb{R}^{n_d \times n_E} \tag{3.37}$$

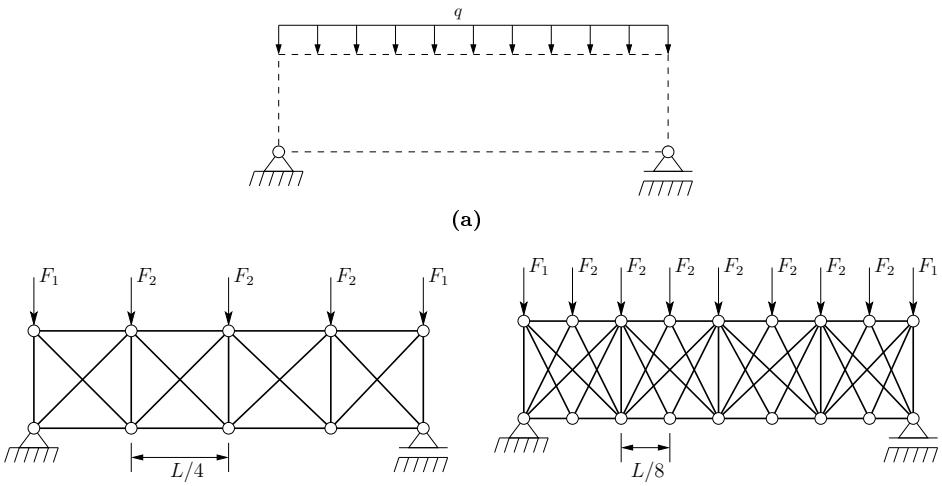

(a)

(b) $F_1 = \frac{qL}{8}$, $F_2 = \frac{qL}{4}$.

(c) $F_1 = \frac{qL}{16}$, $F_2 = \frac{qL}{8}$.

Figure 3.1: Two ground structures subject to line loading. In both cases, the force F_1 is half of force F_2.

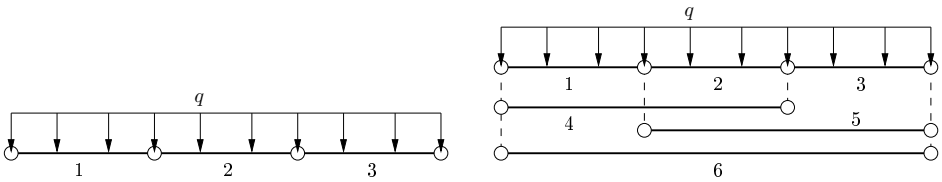

(a) (b)

Figure 3.2: Overlapping elements are created along the line load. Each element is subjected to the line load.

The equilibrium equations become

$$\mathbf{B}\mathbf{N}^k = \mathbf{p}^k + \mathbf{q}^k \quad \Rightarrow \quad \mathbf{B}\mathbf{N}^k - \mathbf{Q}^k\mathbf{y} = \mathbf{p}^k \tag{3.38}$$

The elements of the matrix $\mathbf{Q}$ are derived as follows. Suppose that the member j related to degree of freedom i is in angle of α_j with the x-axis, as in Fig. 3.3a. If the line load is in y-direction, then the equivalent nodal load related to the degree of freedom i is

$$q_{ij} = \frac{1}{2} q L_j \cos\alpha_j \quad (y\text{-directional load}) \tag{3.39}$$

Similarly, if the load is in the x-direction, the equivalent nodal load becomes

$$q_{ij} = \frac{1}{2} q L_j \sin\alpha_j \quad (x\text{-directional load}) \tag{3.40}$$

A constraint stating that the sum of the equivalent nodal loads equals the resultant of the line load is added to ensure that the total line load is actually carried by the

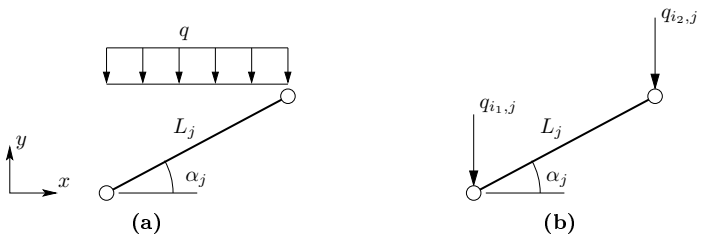

Figure 3.3: Equivalent nodal loads of a member subject to a vertical line load.

truss:

$$\sum_{i\in\mathcal{U}_x} q_i = F_x - R_x \quad \Rightarrow \quad \sum_{i\in\mathcal{U}_x}\sum_{\ell=1}^{n_S} q_{ij}y_{j\ell} = F_x - R_x = qL_y - R_x \tag{3.41}$$

$$\sum_{i\in\mathcal{U}_y} q_i = F_y - R_y \quad \Rightarrow \quad \sum_{i\in\mathcal{U}_y}\sum_{\ell=1}^{n_S} q_{ij}y_{j\ell} = F_y - R_y = qL_x - R_y \tag{3.42}$$

where $\mathcal{U}_x$ and $\mathcal{U}_y$ are the global x- and y-directional degrees of freedom, respectively, related to the nodes of the line load, F_x and F_y are the resultants in x and y directions, R_x and R_y are the equivalent loads at supported degrees of freedom, and L_x and L_y are the dimensions of the load in the global x and y directions, respectively.

3.3.2 Strength Constraints

The basis for member strength constraints is Eq. (2.11). Denote by $\overline{\sigma}$ and $\underline{\sigma}$ the upper and lower bounds for member stress, respectively. A general form of the strength constraint is

$$-\underline{\sigma}A_i \le N_i^k \le \overline{\sigma}A_i \quad \forall\, i \in \mathcal{M},\, k \in \mathcal{L} \tag{3.43}$$

which resembles Eq. (2.11) closely. In Eq. (2.11), $\overline{\sigma} = \underline{\sigma} = f_{\mathrm{y}}/\gamma_{\mathrm{M0}}$.

Substituting Eq. (3.9) and Eq. (3.17) into Eq. (3.43) gives

$$-\underline{\sigma}\sum_{j=1}^{n_S}\hat{A}_j y_{ij} \le \sum_{j=1}^{n_S} N_{ij}^k \le \overline{\sigma}\sum_{j=1}^{n_S}\hat{A}_j y_{ij} \quad \forall\, i \in \mathcal{M},\, k \in \mathcal{L} \tag{3.44}$$

Since only one of the y_{ij} can be non-zero for each i, these constraints can be replaced by a set of constraints for each force variable:

$$-\underline{\sigma}\hat{A}_j y_{ij} \le N_{ij}^k \le \overline{\sigma}\hat{A}_j y_{ij} \quad \forall\, i \in \mathcal{M},\, j \in \mathcal{P},\, k \in \mathcal{L} \tag{3.45}$$

Eq. (3.45) can be combined with Eq. (3.21) to yield

$$\max\{\underline{N}_{ij}^k, -\underline{\sigma}\hat{A}_j\}y_{ij} \le N_{ij}^k \le \min\{\overline{N}_{ij}^k, \overline{\sigma}\hat{A}_j\}y_{ij} \quad \forall\, i \in \mathcal{M},\, j \in \mathcal{P},\, k \in \mathcal{L} \tag{3.46}$$

Thus, adding strength constraints does not increase the number of constraints of the problem.

3.3.3 Stability Constraints

Euler Buckling

Member buckling according to Euler buckling can be incorporated in optimization by adding the constraints

$$N_i^k \geq -\pi^2 \frac{E_i I_i}{L_{ni}^2} \quad \forall\, i \in \mathcal{M},\, k \in \mathcal{L} \tag{3.47}$$

where the right-hand side is the critical load for member i. Typically in trusses, the buckling length, L_n, equals the length of the member.

Eq. (3.47) can be expressed in terms of the design variables by substituting Eq. (3.10) and Eq. (3.17):

$$\sum_{j=1}^{n_S} N_{ij}^k \geq -\pi^2 \frac{E_i \hat{I}_j}{L_{ni}^2} \sum_{j=1}^{n_S} y_{ij} \quad \forall\, i \in \mathcal{M},\, k \in \mathcal{L} \tag{3.48}$$

Again, as only a single y_{ij} can be non-zero for each i, these constraints can be replaced by constraints written for each force variable N_{ij}^k:

$$N_{ij}^k \geq -\pi^2 \frac{E_i \hat{I}_j}{L_{ni}^2} y_{ij} \quad \forall\, i \in \mathcal{M},\, j \in \mathcal{P},\, k \in \mathcal{L} \tag{3.49}$$

The buckling constraints can be combined with Eq. (3.46) to give, for all $i \in \mathcal{M}$, $j \in \mathcal{P}$, $k \in \mathcal{L}$

$$\max\left\{\underline{N}_{ij}^k, -\underline{\sigma}\hat{A}_j, -\pi^2 \frac{E_i \hat{I}_j}{L_{ni}^2}\right\} y_{ij} \leq N_{ij}^k \leq \min\{\overline{N}_{ij}^k, \overline{\sigma}\hat{A}_j\} y_{ij} \tag{3.50}$$

Therefore, including Euler buckling in the problem formulation does not increase the number of constraints.

Buckling According to Eurocode 3

The design rule for buckling in Eurocode 3 can be expressed as an inequality constraint on the member forces as in Eq. (2.18):

$$N_i^k \geq -\chi(A_i, I_i) A_i \frac{f_{\mathrm{y}}}{\gamma_{\mathrm{M1}}} \quad \forall\, i \in \mathcal{M},\, k \in \mathcal{L} \tag{3.51}$$

where

$$\chi(A, I) = \frac{1}{\Phi(A, I) + \sqrt{\Phi(A, I)^2 - \bar{\lambda}(A, I)^2}}, \quad \text{but } \chi \leq 1.0 \tag{3.52}$$

is the reduction factor, and

$$\Phi(A, I) = 0.5\left[1 + \alpha(\bar{\lambda}(A, I) - 0.2) + \bar{\lambda}(A, I)^2\right] \tag{3.53}$$

with

$$\bar{\lambda}(A, I) = \sqrt{\frac{Af_{\mathrm{y}}}{N_{\mathrm{cr}}}} = \sqrt{\frac{AL_n^2 f_{\mathrm{y}}}{\pi^2 EI}} = \frac{L_n}{\pi}\sqrt{\frac{Af_{\mathrm{y}}}{EI}} \tag{3.54}$$

As above, the simplest way of incorporating the buckling constraint is to include the following constraint for all force variables:

$$N_{ij}^k \geq -\chi(\hat{A}_j, \hat{I}_j) f_{\mathrm{y}} \hat{A}_j y_{ij} \quad \forall\, i \in \mathcal{M},\, j \in \mathcal{P},\, k \in \mathcal{L} \tag{3.55}$$

Now if section j is not chosen for member i, i.e. $y_{ij} = 0$, then the right-hand side is 0. On the other hand, by Eq. (3.18), also $N_{ij}^k = 0$, so the buckling constraint is satisfied for non-existing sections. Furthermore, if $y_{ij} = 1$ for some j, then Eq. (3.55) must be satisfied by the corresponding profile. If this happens, then Eq. (3.51) is also satisfied, since $y_{i\ell} = 0$, for all $\ell \neq j$.

As in the previous cases, the force variable constraints can be combined to a single set of linear constraints for all $i \in \mathcal{M}$, $j \in \mathcal{P}$, $k \in \mathcal{L}$:

$$\max\left\{\underline{N}_{ij}^k, -\underline{\sigma}\hat{A}_j, -\chi(\hat{A}_j, \hat{I}_j) f_{\mathrm{y}} \hat{A}_j\right\} y_{ij} \leq N_{ij}^k \leq \min\{\overline{N}_{ij}^k, \overline{\sigma}\hat{A}_j\} y_{ij} \tag{3.56}$$

Chains

Frequently in truss topology optimization, the optimum design contains consecutive members sharing a node that is not supported in directions other than the direction of the members. A common solution to this is to remove the unstable node from the optimum truss and combine the members sharing that node to a single member. This post-processing method works for members in tension, but for compression members, a difficulty with buckling constraints arises. The buckling length of the unified member is the sum of buckling lengths of the members sharing the unstable nodes. Thus, the buckling load of this longer member is significantly smaller than the buckling load of the individual shorter members. As buckling constraints are predominantly active for compression members, it is to be expected that the cross-section of the shorter members does not satisfy the buckling constraint of the longer member. Therefore, simply removing the unstable nodes and combining the members sharing those nodes to longer members, is not a valid solution for compression members.

To avoid this difficulty with unstable nodes and the resulting jump in the buckling length, additional members are included in the ground structure, as shown in Fig. 3.4. First, so-called *chains* are identified in the ground structure. A chain is a set of consecutive members such that each pair of members shares one common node and they have the same orientation. Next, a member is added between each pair of nodes of every chain. These new members overlap some of the original members of a chain. Strength and buckling constraints are written for the new members. Finally, additional constraints are included to disallow members from overlapping in the optimum solution.

In the following, the above approach and the corresponding constraints are presented. The mathematical notation is rather involved.

A ground structure member e_i, $i \in \mathcal{M}$, can be identified with its nodes as $e_i = \{v_{i_1}, v_{i_2}\}$, $v_{i_1}, v_{i_2} \in \mathcal{N}$. A *chain* is a sequence of $K \geq 2$ pair-wise distinct members,

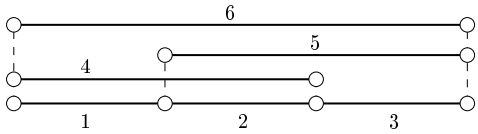

Figure 3.4: Idea of chains. Members 1, 2, and 3 form the basis of the chain. The overlapping members 4, 5, and 6 are added to the ground structure to handle the jump in buckling length phenomenon.

denoted by $c = (e_{i_1}, \ldots, e_{i_K})$, such that each member shares a node with another member, i.e. for all $k = 1, 2, \ldots, K$, there exists an ℓ such that $e_{i_k} \cap e_{i_\ell} \neq \emptyset$. Furthermore, each chain member is parallel to every other member of the chain. This definition of a chain is similar to the one proposed by Achtziger (1999*a*), except that in the present definition, overlapping of chain members is allowed. The set of chains is denoted by $\mathcal{C}$. For each chain $c \in \mathcal{C}$, the sets of members and nodes are denoted by $\mathcal{E}_c$ and $\mathcal{V}_c$, respectively.

Every chain has two nodes that are connected to only one chain member. The set of *interior nodes* of chain c, denoted by $\mathcal{J}_c$, is obtained by removing these two nodes from $\mathcal{V}_c$. Then, denote by $\mathcal{M}_c(s)$ the set of members of the chain connected to the interior node $v_s \in \mathcal{J}_c$. Similarly, $\mathcal{N}_c(s)$ is the set of members of the ground structure connected to v_s but not belonging to the chain. Mathematically, these two sets can be expressed as

$$\mathcal{M}_c(s) = \{i \mid i \in \mathcal{E}_c \text{ and } e_i \cap \{v_s\} \neq \emptyset, v_s \in \mathcal{J}_c\} \tag{3.57}$$

$$\mathcal{N}_c(s) = \{i \mid i \notin \mathcal{E}_c \text{ and } e_i \cap \{v_s\} \neq \emptyset, v_s \in \mathcal{J}_c\} \tag{3.58}$$

The main purpose of chains is to prevent unstable nodes from appearing in the optimum solution. Furthermore, as buckling constraints are written for every chain member, the correct buckling length is automatically employed. A set of constraints is needed to guarantee that only kinematically stable topologies appear in the solutions.

Firstly, the overlapping of the members of the chain must be prevented. This condition is expressed by the constraint

$$\sum_{i \in \mathcal{E}_c(s)} y_i \leq 1 \quad \forall\, v_s \in \mathcal{V}_c \tag{3.59}$$

$$\Rightarrow \quad \sum_{i \in \mathcal{E}_c(s)} \sum_{j=1}^{n_S} y_{ij} \leq 1 \quad \forall\, v_s \in \mathcal{V}_c \tag{3.60}$$

where $\mathcal{E}_c(s) \subseteq \mathcal{E}_c$ is the set of chain members partly or fully belonging to the line segment between the nodes v_s and v_{s+1}. A constraint of Eq. (3.59) is included for each line segment between two consecutive nodes of every chain.

Consider the truss shown in Fig. 3.5. The nodes 1, 2, 3, and 4 lie on the line defined by the members 1, 2, and 3. The complete chain includes also the additional members 4, 5, and 6, that is, members 1–6 constitute the chain. Members 7–12 have to be

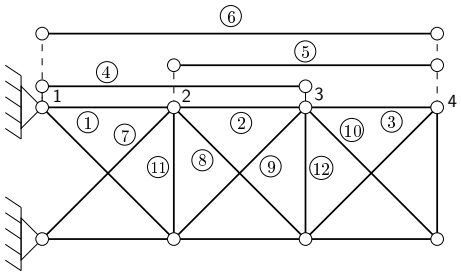

Figure 3.5: Example of a chain.

included in the chain constraints. Note that members connected to nodes 1 and 4 that do not belong to the chain need not be considered.

In this case, the overlapping constraints are

$$y_1 + y_4 + y_6 \leq 1 \tag{3.61}$$
$$y_2 + y_4 + y_5 + y_6 \leq 1 \tag{3.62}$$
$$y_3 + y_5 + y_6 \leq 1 \tag{3.63}$$

Secondly, if all ground structure members connected to an interior node but not belonging to a chain vanish, then the chain members connected to that node must also vanish. This eliminates the possibility of unstable nodes that are supported only in the direction of the chain. A constraint for this condition is

$$\sum_{i \in \mathcal{M}_c(s)} y_i \leq |\mathcal{M}_c(s)| \sum_{r \in \mathcal{N}_c(s)} y_r \quad \forall\, v_s \in \mathcal{J}_c \tag{3.64}$$

$$\Rightarrow \quad \sum_{i \in \mathcal{M}_c(s)} \sum_{j=1}^{n_S} y_{ij} \leq |\mathcal{M}_c(s)| \sum_{r \in \mathcal{N}_c(s)} \sum_{j=1}^{n_S} y_{rj} \quad \forall\, v_s \in \mathcal{J}_c \tag{3.65}$$

where $|\mathcal{M}_c(s)|$ is the number of members of the chain connected to the node v_s.

Now if any $y_r = 1$, $r \in \mathcal{N}_c(s)$, which means that a member not belonging to the chain but connected to the node is present in the design, then any member of the chain connected to node v_s is allowed to be present. On the other hand, if all $y_r = 0$, $r \in \mathcal{N}_c(s)$, then also all chain members connected to that node must vanish.

The constraint Eq. (3.64) can be modified to yield tighter relaxations (see Chapter 4) by replacing it with the following set of constraints:

$$y_i \leq \sum_{r \in \mathcal{N}_c(s)} y_r \quad \forall\, v_s \in \mathcal{J}_c,\, i \in \mathcal{M}_c(s) \tag{3.66}$$

For the chain in Fig. 3.5, constraint Eq. (3.64) for node 2 is

$$y_1 + y_2 + y_5 \leq 3(y_7 + y_8 + y_{11}) \tag{3.67}$$

Alternatively, Eq. (3.66) for node 2 is

$$y_1 \leq y_7 + y_8 + y_{11} \tag{3.68}$$
$$y_2 \leq y_7 + y_8 + y_{11} \tag{3.69}$$
$$y_5 \leq y_7 + y_8 + y_{11} \tag{3.70}$$

Finally, if any ground structure members not belonging to the chain are present at an interior node of the chain, members of the chain overlapping that node are not allowed. This condition eliminates situations, where nodes of the chain are supported by non-chain members only. This condition is included in the optimization problem by the following constraint:

$$\sum_{i \in \mathcal{E}_c^o(s)} y_i \leq |\mathcal{E}_c^o(s)|(1 - y_r) \quad \forall\, r \in \mathcal{N}_c(s),\, v_s \in \mathcal{J}_c \tag{3.71}$$

$$\Rightarrow \quad \sum_{i \in \mathcal{E}_c^o(s)} \sum_{j=1}^{n_S} y_{ij} \leq |\mathcal{E}_c^o(s)| \left(1 - \sum_{j=1}^{n_S} y_{rj} \right) \quad \forall\, r \in \mathcal{N}_c(s),\, v_s \in \mathcal{J}_c \tag{3.72}$$

In the above, $\mathcal{E}_c^o(s)$ is the set of chain members overlapping the node v_s.

Tighter relaxations are obtained, if Eq. (3.71) is replaced by the set of following constraints:

$$y_i \leq 1 - y_r \quad \forall\, r \in \mathcal{N}_c(s),\, s \in \mathcal{J}_c,\, i \in \mathcal{E}_c^o(s) \tag{3.73}$$

For the node 2 of the chain in Fig. 3.5, the constraint Eq. (3.71) becomes

$$y_4 + y_6 \leq 2(1 - y_7) \qquad y_4 + y_6 \leq 2(1 - y_8) \qquad y_4 + y_6 \leq 2(1 - y_{11}) \tag{3.74}$$

Alternatively, if Eq. (3.73) is employed, the constraints are

$$y_4 \leq 1 - y_7 \qquad y_4 \leq 1 - y_8 \qquad y_4 \leq 1 - y_{11} \tag{3.75}$$
$$y_6 \leq 1 - y_7 \qquad y_6 \leq 1 - y_8 \qquad y_6 \leq 1 - y_{11} \tag{3.76}$$

Kinematic Stability

A well-known result in truss topology optimization is that the optimum topology can be a mechanism that is in equilibrium with respect to the given loads but unstable for arbitrary load variations. This issue is commonly handled by introducing an additional loading condition with small loads at predefined nodes (Ben-Tal & Nemirovski 1997, Rasmussen & Stolpe 2008). The problem with this approach is that usually it is very difficult to know in advance which nodes will be present in the optimal topology. As all loaded nodes will be included in the resulting structure, adding auxiliary loads to nodes that are not needed in the optimal topology will distort the solution.

In this thesis, a different approach is adopted, that resembles closely the method presented by Faustino et al. (2006), and Kanno & Guo (2010). When the nodal binary variables are included in the problem formulation, they can be used also to control the existence of loads. Therefore, a convenient solution for finding stable topologies is

to include in the problem a separate loading condition, where small loads are applied at *all* nodes of the ground structure in every degree of freedom. If a node is removed from the ground structure, the corresponding auxiliary load also vanishes. A formal presentation of this idea is given below.

Denote by $\mathcal{D}_\ell$ the global degrees of freedom of node ℓ. Then, the auxiliary loads for this node are

$$\tilde{p}_j = \tilde{p}_{j\ell} z_\ell \quad j \in \mathcal{D}_\ell \tag{3.77}$$

where $\tilde{p}_{j\ell} > 0$ are predefined values for the loads. Essentially, any values can be given to the $\tilde{p}_{j\ell}$, but they should be small enough such that they do not affect the optimum selection of member profiles. In order to minimize the possibility that the structure is a mechanism but is in equilibrium with respect to the auxiliary loads, the resultant force of the load components at a node should not be parallel to any of the members connected to that node, and all $\tilde{p}_{j\ell}$ are chosen to be positive.

The auxiliary loads can be gathered to a load vector. This is denoted by

$$\tilde{\mathbf{p}} = \mathbf{P}\mathbf{z} \in \mathbb{R}^{n_d} \tag{3.78}$$

where $\mathbf{P} \in \mathbb{R}^{n_d \times n_N}$. The elements of $\mathbf{P}$ are $P_{ij} = \tilde{p}_{ij}$, when $i \in \mathcal{D}_j$ and $P_{ij} = 0$ otherwise. The nodal equilibrium is then expressed in matrix form as

$$\mathbf{B}\tilde{\mathbf{N}} = \tilde{\mathbf{p}} = \mathbf{P}\mathbf{z} \tag{3.79}$$

where $\tilde{\mathbf{N}}$ is the vector of auxiliary member forces.

The number of additional variables and constraints due to the stability conditions can be kept small by only considering nodal equilibrium and stress constraints and neglecting the compatibility conditions for the auxiliary loading condition. Then, a single force variable per member, n_d equality constraints, and $2n_E$ inequality constraints are sufficient to model the stability conditions. The inequality constraints are the member strength constraints, and they are expressed as

$$-\underline{\sigma}\sum_{j=1}^{n_S} \hat{A}_j y_{ij} \le \tilde{N}_i \le \overline{\sigma}\sum_{j=1}^{n_S} \hat{A}_j y_{ij} \quad \forall\, i \in \mathcal{M} \tag{3.80}$$

If member variables, y_i, are employed, the above constraint can be written as

$$-\underline{\sigma}\max_{j=1,2,\ldots,n_S}\{\hat{A}_j\} y_i \le \tilde{N}_i \le \overline{\sigma}\max_{j=1,2,\ldots,n_S}\{\hat{A}_j\} y_i \quad \forall\, i \in \mathcal{M} \tag{3.81}$$

Here, also min could be used instead of max. The justification for this expression is that as the auxiliary loads are small, the main role of the strength constraints is to ensure that the member forces of the vanishing members become zero and that the strength constraints never become active.

Remark The success of the presented scheme for preventing mechanisms from appearing in the optimal topologies depends on the choice of the auxiliary loads. It should be acknowledged that there is a chance – even if a very small chance – that the auxiliary loads are not able capable of detecting all possible mechanisms. One

possibility –although perhaps not very efficient– to deal with this remote chance, is to include in the problem formulation a constraint that excludes the topology of the mechanism appearing in the solution, and then solve the new problem.

Suppose $\tilde{\mathbf{y}} \in \mathbb{R}^{n_E}$ is the vector of binary variables that represent the topology of the solution of the original problem. Then the constraint

$$\sum_{i:\tilde{y}_i=1} (1 - y_i) + \sum_{i:\tilde{y}_i=0} y_i \geq 1 \tag{3.82}$$

forces the topology to change.

3.3.4 Member Grouping

It is sometimes necessary to force certain members to have equal profiles. In topology optimization, introducing this condition is not as straightforward as in sizing optimization, since a member belonging to a group may also vanish.

Suppose the members of the group $\mathcal{G} \subseteq \mathcal{M}$ appearing in the truss are to have an identical profile. This condition can be enforced by introducing binary variables $w_j \in \{0, 1\}$, $j \in \mathcal{P}$, with the following constraints:

$$\sum_{j=1}^{n_S} w_j \leq 1 \tag{3.83}$$

$$y_{ij} \leq w_j \quad \forall\, i \in \mathcal{G},\, j \in \mathcal{P} \tag{3.84}$$

$$\sum_{i \in \mathcal{G}} y_{ij} \geq w_j \quad \forall\, j \in \mathcal{P} \tag{3.85}$$

The first constraint ensures that at most one profile is selected, but the possibility that the whole group vanishes is allowed. The second constraint implies that if a profile is not chosen ($w_j = 0$), then the corresponding profile variables must be zero. Finally, the third constraint enforces the condition that if a profile is chosen ($w_j = 1$), then one of the profile variables must actually be equal to one. This eliminates the possibility that $w_j = 1$ and $y_{ij} = 0$ for all $i \in \mathcal{G}$.

3.4 Criteria

The primary aim of the problems treated in this study is to find economical solutions. This is reflected in the choice of the objective function. Commonly, the weight of the truss is minimized. On the other hand, it is well known that other factors contribute to the economy, or the cost of the design. For instance, Sarma & Adeli (2000*b*) present a series of cost factors for steel structures. The authors identify as the five most significant cost factors the cost of the sections, the number of different section types used in the structure, the weight of the sections, the number of connections, and the geographic location of the project site. They consider a multiobjective optimization problem, where the criteria are the cost of the sections, the weight of the sections, and number of section types.

The cost of the truss can also be minimized directly by devising a cost function that includes the different manufacturing stages. Jármai & Farkas (1999) and Pavlovčič, Krajnc & Beg (2004) have proposed such cost functions. Recently, Haapio (2012) has presented a feature-based costing method for steel structures. This approach is adopted in the present work for cost optimization of tubular trusses. A chronological review of cost optimization of steel structures is given in (Sarma & Adeli 2000*a*), and a thorough discussion of the topic can be found in (Adeli & Sarma 2006).

Cost optimization requires detailed cost data of the manufacturing process. If such data is not available, then quantities that affect the cost, such as the five cost factors mentioned above, can be optimized simultaneously without cost data. In the multicriterion environment, the solutions provide information on the trade-off between the factors that constitute the total cost of the structure. In this thesis, the number of members, nodes and section types are the three cost factors, that are minimized as separate criteria along with weight in the multicriterion problems. For each of these criteria, an explicit expression with respect to the design variables is given. The author has not found such expressions elsewhere in the literature.

To summarize, the following criteria are considered:

1. weight of the structure;
2. cost of the structure.
3. number of truss members;
4. number of connections;
5. number of section types;

In the following, explicit expressions for these criteria are presented.

3.4.1 Weight

The weight of the truss can be written in terms of the design variables as

$$W(\mathbf{x}) = \sum_{i=1}^{n_E} \rho_i L_i A_i = \sum_{i=1}^{n_E} \rho_i L_i \left(\sum_{j=1}^{n_S} \hat{A}_j y_{ij} \right) = \sum_{i=1}^{n_E} \sum_{j=1}^{n_S} \rho_i L_i \hat{A}_j y_{ij} \tag{3.86}$$

where ρ_i is the density of the material of member i. If all members are made of the same material, minimizing the weight is equivalent to minimizing the material volume of the truss. This can be written as

$$V(\mathbf{x}) = \sum_{i=1}^{n_E} L_i A_i = \sum_{i=1}^{n_E} L_i \left(\sum_{j=1}^{n_S} \hat{A}_j y_{ij} \right) = \sum_{i=1}^{n_E} \sum_{j=1}^{n_S} L_i \hat{A}_j y_{ij} \tag{3.87}$$

3.4.2 Number of Members

The number of members of the truss can be expressed simply as the sum of all binary variables y_i, or y_{ij}:

$$N_y(\mathbf{x}) = \sum_{i=1}^{n_E} y_i = \sum_{i=1}^{n_E} \sum_{j=1}^{n_S} y_{ij} \tag{3.88}$$

3.4.3 Number of Profiles

According to Sarma & Adeli (2000*b*), the number of profiles appearing in the truss should be kept to minimum in order to reduce the costs related to purchasing, storing and fabrication of members. The binary variables y_{ij} can be used to express the number of profiles conveniently.

Note that $\max_{i=1,2,\ldots,n_E} y_{ij} = 1$, if profile j is present in the truss, and zero otherwise. Then, the total number of different profiles in the truss is

$$N_p(\mathbf{y}) = \sum_{j=1}^{n_S} \max_{i=1,2,\ldots,n_E} y_{ij} \tag{3.89}$$

A frequently employed method for transforming the minimization of the max-function into a differentiable optimization problem is to introduce additional binary variables α_j as follows:

$$\begin{aligned} \min \quad & N_p = \sum_{j=1}^{n_S} \alpha_j \\ \text{subject to} \quad & y_{ij} \leq \alpha_j \quad \forall\, i \in \mathcal{M}, j \in \mathcal{P} \\ & \sum_{i=1}^{n_E} y_{ij} \geq \alpha_j \quad \forall\, j \in \mathcal{P} \\ & \alpha_j \in \{0,1\} \quad \forall\, j \in \mathcal{P} \end{aligned} \tag{3.90}$$

The latter constraint assures that, if $\alpha_j = 1$, at least one member in the truss has the profile j.

Thus, minimizing the number of profile requires n_S additional variables and $(n_E{+}1){\cdot}n_S$ constraints. The amount of constraints can be reduced by aggregating the additional constraints, which leads to the following formulation

$$\begin{aligned} \min \quad & N_p = \sum_{j} \alpha_j \\ \text{subject to} \quad & \sum_{i=1}^{n_E} y_{ij} \leq n_E \alpha_j \quad \forall\, j \in \mathcal{P} \\ & \sum_{i=1}^{n_E} y_{ij} \geq \alpha_j \quad \forall\, j \in \mathcal{P} \\ & \alpha_j \in \{0,1\} \quad \forall \in \mathcal{P} \end{aligned} \tag{3.91}$$

Remark It is worth mentioning that the solution of the problem where the number of profiles is minimized is in most cases not unique. For any truss satisfying the constraints of the problem, the number of profiles can be set to one by choosing for all members the largest profile appearing in the current configuration. If there are larger profiles available than the largest profile present in the truss, then by selecting any of these profiles for all members yields a solution with $N_p = 1$. As many of the structures with a single profile for all members can be highly uneconomical, minimizing the number of profiles is only reasonable in conjunction with mass minimization.

3.4.4 Number of Connections

When nodal variables are included in the optimization problem, a simple linear expression can be written for the number of connections:

$$N_c(\mathbf{x}) = \sum_{i=1}^{n_N} z_i \tag{3.92}$$

The purpose of minimizing the number of connections is to reduce the fabrication, erection, connection material, and labor costs of the truss (Sarma & Adeli 2000*b*).

Similarly to the number profiles, also the minimum number of connections can in general be obtained by more than one structure. Even if the optimum design is unique, it may be uneconomical from the point of view of material consumption and other fabrication aspects. Therefore, also this criterion is included in the problem formulation only when other criteria are considered as well.

3.4.5 Cost

Of the several cost functions found in the literature, the feature-based cost model proposed by Haapio (2012) is adopted in this thesis. The idea is to decompose the manufacturing process in so-called cost centers, and to write a cost function for each of them. The form of the cost function for every cost center is identical, and it includes the non-productive and productive times, the cost for labour, equipment, real estate, consumables, energy, and maintenance. For different cost centers, some of the terms in the generic cost function may be neglected.

Below, the cost function of Haapio is modified for tubular trusses and written in terms of the design variables. All the expressions and constants are taken from (Haapio 2012), unless otherwise stated. The cost factors that are considered in this thesis are material, blasting, sawing, assembling by welding, and painting cost. Further cost factors, such as grinding after sawing, can be added to the cost function by employing the method of Haapio (2012).

Material Cost

The material cost of tubular profiles is computed by

$$C_M = \sum_{i=1}^{n_E} W_i c_{M,i} \tag{3.93}$$

where W_i is the weight of the profile [kg] and $c_{M,i}$ is the unit cost of the profile [€/kg]. In this thesis, the unit cost $c_{M,i} = 0.8$ €/kg is used for hollow sections of grade S355. The material cost function can be written in terms of the profile variables y_{ij} as

$$C_M(\mathbf{x}) = \sum_{i=1}^{n_E} \sum_{j=1}^{n_S} c_{M,i} \rho_i L_i \hat{A}_j y_{ij} \tag{3.94}$$

Note that C_M is a linear function of the design variables y_{ij}.

Blasting Cost

The blasting cost of the members constitute of labour, equipment, real estate, maintenance, consumables and energy required by the blasting equipment. The blasting cost function is:

$$C_B(\mathbf{x}) = \sum_{i=1}^{n_E} 3.63 \cdot 10^{-4} L_i y_i = \sum_{i=1}^{n_E} \sum_{j=1}^{n_S} 3.63 \cdot 10^{-4} L_i y_{ij} \tag{3.95}$$

where L_i [mm] is the length of member i. The unit of the constant is €/mm.

Sawing Cost

Both ends of each member are sawn. Additionally, if a member is diagonally positioned in the truss, one or both of its ends must be bevelled. Here, it is assumed that the saw blade cuts through the profile vertically. This affects some of the expressions below as demonstrated in Fig. 3.6. On the left, a side view of a member with a RHS to be bevelled in angle θ is shown. The saw is able to create the bevelling only if the profile is turned on its longer side, as shown on the right in the figure, where the turned member is viewed from above. Thus, when applying the expressions below, the positioning of the profile must be considered. However, for square hollow sections that are mainly used in this thesis, the positioning is not important.

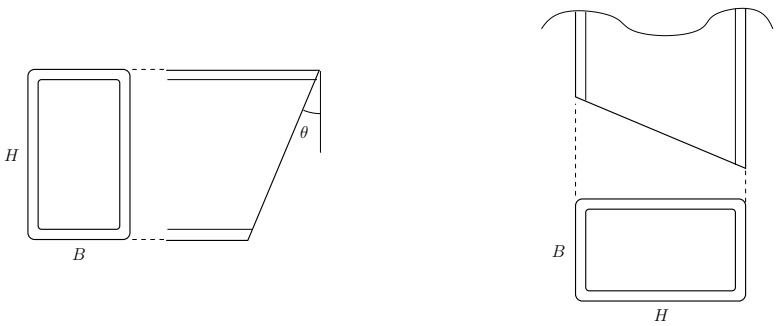

Figure 3.6: Bevelling a RHS. Left: side view of a member to be bevelled in θ angle. Right: the view from above as the profile is turned on its longer side such that the saw blade is able to create the bevelling.

The sawing cost is expressed as

$$C_S = c_S(T_{NS} + T_{PS}) + T_{PS}(c_{CS} + c_{EnS}) \tag{3.96}$$

where T_{NS} is the non-productive time, T_{PS} is the productive time, c_{CS} is the cost of sawing consumables, and $c_{EnS} = 0.02$€/min is the cost of energy used by the saw. $c_S = 1.2$€/min is a constant that includes the unit costs of labour, equipment, equipment maintenance, and real estate investment and maintenance.

The expression for the non-productive time is

$$T_{NS} = 4.5 + 1 \cdot \lceil 1 - \cos\theta_1 \rceil + 1 \cdot \lceil 1 - \cos\theta_2 \rceil + \frac{1}{20000} L \quad \text{[min]} \tag{3.97}$$

where $\lceil \cdot \rceil$ means the smallest integer greater than the argument, and θ_1 and θ_2 are the bevelling angles of the member ends. If $\theta_i = 0$, the end is not bevelled, and the term $\lceil 1 - \cos\theta_i \rceil = 0$. This indicates that the saw blade need not to be rotated to the bevelling angle, which saves time. For any other values of θ_i, the term $\lceil 1 - \cos\theta_i \rceil = 1$, and the time needed to rotate the saw blade is included in the non-productive time. Note that $0 \leq \theta_i < 90°$.

The expression for the productive time, T_{PS}, is

$$T_{PS} = \frac{h}{S \cdot S_m} + \frac{A_h}{Q} \quad \text{[min]} \tag{3.98}$$

where the first term corresponds to the part of the cross-section, where the thickness of the sawed material is comparable to the wall thickness, and the second term concerns the part where the sawed material is solid:

Here, h is the vertical dimension of the hollow part of the section. For SHS,

$$h = H - 2t \tag{3.99}$$

S is the vertical feeding speed that depends on the thickness of the sawed material. Values for S are given in Table 3.1. The material factor S_m depends on the material grade. For S355, $S_m = 0.9$.

The term A_h [mm^2] is the total area of horizontal parts of the profile. For SHS, this is

$$A_h \approx \frac{2Ht}{\cos\theta} \tag{3.100}$$

where $\theta \in [0, 90°)$ is the angle between the saw blade and the profile. (From this value, the areas corresponding to the roundings should be subtracted.)

Finally, Q [mm^2/min] is the sawing efficiency. For S355, $Q = 8800\,\text{mm}^2/\text{min}$.

The cost of sawing consumables, c_{CS}, includes only the wear of the blades. The expression for c_{CS} is

$$c_{CS} = \frac{A_t p_{SB}}{S_t \cdot T_{PS}} \tag{3.101}$$

Table 3.1: Feeding speed S of the saw and durability parameter F_{sp}.

Wall thickness [mm]	Feeding speed S [mm/min]	F_{sp}
–5	120	0.4
6–10	100	0.45
11–15	90	0.5
16–20	80	0.55
21–25	70	0.6
26–30	60	0.65
31–35	50	0.7
36–	40	0.8

where A_t is the cross-sectional area of the sawn profile, $p_{SB} = 100€$ is the price of the saw blade, and S_t is the overall durability of the blade. Its expression is

$$S_t = Q \cdot F_s \cdot F_{sp} \tag{3.102}$$

where S_t [mm^2] is the overall cross-sectional area a blade can saw before it has to be replaced, $F_s = 1350$ is a parameter that depends on the equipment type, and F_{sp} is a parameter depending on the thickness of the material. Its values are given in Table 3.1.

The area of the sawed cross-section depends on whether or not the end is bevelled. If the angle between the saw blade and the profile is θ, the total sawed area is

$$A_t = \frac{A}{\cos\theta} \tag{3.103}$$

Note that for each member the sawing of both ends must be considered.

The sawing cost function is

$$C_S(\mathbf{x}) = \sum_{i=1}^{n_E} \sum_{j=1}^{n_S} C_{S,ij} y_{ij} \tag{3.104}$$

where $C_{S,ij}$ is the sawing cost of profile j for member i.

Obtaining the values for $C_{S,ij}$ is not straightforward in general. Several cost factors, such as the productive time, depend on the sawing angle, which is not given *a priori* in many cases. Several ground structure members are connected to a given node, so for each member, several possible sawing angles exist. Furthermore, it is not always evident, if the end of a member should be bevelled. Consider the case where two members meeting in an angle other than 90° are to be joined. It might be sufficient to just bevel one of the members and leave the other unbevelled. Then, which one should be bevelled? Probably the one with smaller outer dimensions, since it can be welded to the side of the larger member. Stating this condition as a linear constraint without additional variables is not obvious.

Thus, in general, the sawing cost of profile j for member i depends on the other members and possibly on their profiles as well. Consequently, $C_{S,ij} = C_{S,ij}(y_s, y_{sr})$,

where y_s are member variables of the other members meeting at a joint and y_{sr} are their corresponding profile variables. Even if this $C_{S,ij}$ would be linear in these variables, the resulting cost term $C_{S,ij}$ of member i would be nonlinear.

Despite the above difficulties, the sawing cost can be expressed as in Eq. (3.104) in certain situations. For example, in the roof truss considered in Chapter 7, each bracing member is connected to the chord in a predefined angle. Then, the cost components $C_{S,ij}$ are constant. Their expression is

$$C_{S,ij} \;=\; c_S T_{NS}(L_i, \theta_{i1}, \theta_{i2}) + \sum_{\ell=1}^{2} T_{PS}(H_j, T_j, \theta_{i\ell}) \left(c_{CS}(\hat{A}_j, T_j, \theta_{i\ell}) + c_S + c_{EnS} \right) \tag{3.105}$$

where

$$T_{NS}(L_i, \theta_{i1}, \theta_{i2}) = 4.5 + 1 \cdot \lceil 1 - \cos\theta_{i1} \rceil + 1 \cdot \lceil 1 - \cos\theta_{i2} \rceil + \frac{1}{20000} L_i \tag{3.106}$$

$$T_{PS}(H_j, T_j, \theta_{i\ell}) = \frac{h(H_j, T_j)}{S(T_j, \theta_{i\ell}) \cdot S_m} + \frac{A_h(H_j, T_j, \theta_{i\ell})}{Q} \tag{3.107}$$

$$= \frac{H_j - 2T_j}{S(T_j, \theta_{i\ell}) \cdot S_m} + \frac{2H_j T_j}{Q \cos\theta_{i\ell}} \tag{3.108}$$

$$c_{CS}(\hat{A}_j, T_j, \theta_{i\ell}) = \frac{\hat{A}_j p_{SB}}{\cos\theta_{i\ell} \cdot Q \cdot F_s \cdot F_{sp}(T_j, \theta_{i\ell}) \cdot T_{PS}(H_j, T_j, \theta_{i\ell})} \tag{3.109}$$

The term $T_{PS} \cdot c_{CS}$ appears in Eq. (3.105) . Using Eq. (3.101), this can be simplified to

$$T_{PS} c_{CS} = \frac{A_t p_{SB}}{S_t} \tag{3.110}$$

Welding Cost

The truss is assembled by welding the members together. The assembly cost function is

$$C_A = T_{PA} \left(\frac{c_{LA} + c_{EqA} + c_{ReA} + c_{SeA}}{u_{PA}} + c_{EnA} \right) + c_{CA} \tag{3.111}$$

Here, the non-productive time and maintenance cost of the assembly are neglected, and the utilisation ratio $u_A = 1.0$.

The productive time, T_{PA}, consists of tack welding and welding time, that is

$$T_{PA} = T_{Ta} + T_{We} \tag{3.112}$$

Here, the tack welding time $T_{Ta} = 1.59$ [min] per part is used. The welding time depends on the weld type and welding technology. Here, gas metal arc welding with

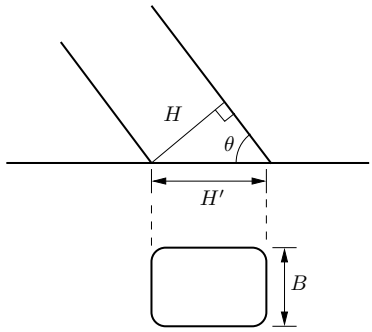

Figure 3.7: Length of the weld.

mixed gas (MAG M) is used as the welding technologyFor fillet welds, the welding time is computed from the formula

$$T_{We} = \frac{L_{fw}}{1000}\left(0.4988a^2 - 0.0005a + 0.0021\right) \text{ [min]} \tag{3.113}$$

where L_{fw} is the length of the weld [mm] and a is the filled weld size [mm]. The length of the weld is the circumference of the profile projected to the surface, where the profile is welded. In Fig. 3.7, a RHS with side lengths H and B and rounding outer radius R that is welded in angle θ is shown. From this figure, it can be seen that the projected side length $H' = H/\sin\theta$. Thus, the total circumference and weld length is

$$L_{fw} = 2(H' - 2R) + 2(B - 2R) + 4 \cdot \frac{1}{4} \cdot 2\pi R \tag{3.114}$$

$$= 2H' + 2B + (2\pi - 8)R \tag{3.115}$$

$$= \left(\frac{2H}{\sin\theta} + 2B\right) + (2\pi - 8)R \tag{3.116}$$

For steel grade S355, the weld size $a = 1.1t$ is used, where t is the wall thickness of the profile (Wardenier et al. 2010).

For single-bevel butt welds, the welding time is

$$T_{We} = \frac{L_{fw}}{1000}\left(0.249b^2 + 0.0096b - 0.0506\right) \text{ [min]} \tag{3.117}$$

where b is the depth of the weld [mm]. Here, $b = t$ is used. The length of the weld, L_{fw} is computed by Eq. (3.114) as for fillet welds.

The unit labor cost is $c_{LA} = 0.46$ [€/min]. The cost of the welding equipment $c_{EqA} = 0.01$ [€/min]. The real estate investment cost, c_{ReA}, and real estate maintenance cost, c_{SeA}, depend on the size of the truss. They can be obtained by using Eq. (2) from Haapio (2012). For fillet welds, the cost of non-time-related welding consumables, c_{CA}, is computed from the formula

$$c_{CA} = 7.85 \cdot 10^{-6} L_{fw} a^2 \cdot 6.35 \text{ [€]} \tag{3.118}$$

which includes the cost of welding wire and welding shield gas. For butt welds, the expression is

$$c_{CA} = 7.85 \cdot 10^{-6} L_{fw} \frac{b^2}{2} \cdot 6.35 \text{ [€]} \tag{3.119}$$

Finally, the cost of energy used by the welding equipment, $c_{EnA} = 0.01$ [€/min].

The assembling cost can be expressed in terms of the profile variables y_{ij} as

$$C_A(\mathbf{x}) = \sum_{i=1}^{n_E} \sum_{j=1}^{n_S} C_{A,ij} y_{ij} \tag{3.120}$$

The welding cost of each profile alternative must be determined for every member. Let $c_A = (c_{LA} + c_{EqA} + c_{ReA} + c_{SeA})/u_A + c_{EnA}$. Then

$$C_{A,ij} = c_A T_{Ta} + \sum_{\ell=1}^{2} (c_A T_{We,ij\ell} + c_{CA,ij\ell}) \tag{3.121}$$

where $c_{CA,ij\ell}$ is the cost of welding consumables, and $T_{We,ij\ell}$ is the welding time of the end ℓ of profile j of member i. They depend on the dimensions of the section and on the welding angle according to Eq. (3.118) and Eq. (3.113).

Painting Cost

The assembled truss is painted by a spray gun in a separate painting space. The painting cost function is

$$C_P = T_{PP} \cdot \left(\frac{c_{LP} + c_{ReP} + c_{SeP}}{u_P} \right) + c_{CP} \tag{3.122}$$

where T_{PP} is the productive time, c_{LP} is the labour cost, c_{ReP} is the real estate investment cost, c_{SeP} is the real estate maintenance cost, $u_P = 1.0$ is the utilisation ratio, and c_{CP} is the cost of painting consumables. Denote $c_P = (c_{LP} + c_{ReP} + c_{SeP})/u_P$.

Assuming a class C3/M alkyd painting system, the productive time is

$$T_{PP} = 5.7 \cdot 10^{-9} A_p \tag{3.123}$$

where A_p [mm^2] is the total area of the assembly to be painted. For plane trusses this is the sum of outer surfaces of the members. This is written as

$$A_u = \sum_{i=1}^{n_E} A_{u,i} L_i = \sum_{i=1}^{n_E} \sum_{j=1}^{n_S} L_i \hat{A}_{u,j} y_{ij} \tag{3.124}$$

The outer surfaces, $\hat{A}_{u,j}$, must be provided as input to the optimization.

The labour cost is $c_{LP} = 0.46$€/min. The real estate costs, c_{ReP} and c_{SeP}, depend on the size of the painting space.

For the class C3/M alkyd painting system, the cost of painting consumables, consisting of the paint and solvent, is

$$c_{CP} = 3.87 \cdot 10^{-6} A_u \quad [€] \tag{3.125}$$

Thus, the complete expression for the painting cost function is

$$C_P(\mathbf{x}) = \left(5.7 \cdot 10^{-9} c_P + 3.87 \cdot 10^{-6}\right) \sum_{i=1}^{n_E} \sum_{j=1}^{n_S} \left(L_i \hat{A}_{u,j} y_{ij}\right) \tag{3.126}$$

Cost Function

The cost function that can be used in optimization is the combination of expressions Eq. (3.94), Eq. (3.95), Eq. (3.104), Eq. (3.120), and Eq. (3.126), that is

$$C(\mathbf{x}) = C_M(\mathbf{x}) + C_B(\mathbf{x}) + C_S(\mathbf{x}) + C_A(\mathbf{x}) + C_P(\mathbf{x}) \tag{3.127}$$

This is a linear function in terms of the profile selection variables y_{ij}. Blasting cost can also be expressed in terms of member variables y_i, since it only depends on the length of the members.

3.5 Alternative Formulations

In the previous sections, various constraints and design variables were presented. From the perspective of the structural designer, the most applicable set of constraints includes member strength and buckling, chains, kinematic stability, and possibly member grouping. On the other hand, the choice of binary variables related to members is not obvious. Profile selection variables y_{ij} are necessarily present, but should the member selection variables y_i or the slack variables y_{i0} be included as well or not? Even though introducing these variables would increase the problem size, it is not evident that the problem becomes more difficult to solve. On the contrary, these optional variables might prove to be beneficial in the solution process.

In this section, the formulations of the constraints for three possibilities in choosing the binary variables is presented. In the next section, the solution aspects are discussed.

The three formulations are based on the following choice of variables:

1. Do not include variables y_i. The binary variables related to members are y_{ij}. A member is removed from the ground structure, if the left-hand side of Eq. (3.7) is zero.

2. Do not include variables y_i, but include the slack variables y_{i0}. A member is removed from the ground structure, if $y_{i0} = 1$. Eq. (3.8) is used instead of Eq. (3.7) for determining a unique profile for a member.

3. Include variables y_i in addition to y_{ij}. Eq. (3.7) is replaced by Eq. (3.12).

3.5.1 Formulation 1

In this case, the vector of design variables is denoted

$$\mathbf{x} = \{\mathbf{y}\ \mathbf{N}_1^1\ \mathbf{N}_2^1\ \ldots\ \mathbf{N}_{n_E}^1\ \mathbf{u}^1 \ldots \mathbf{N}_1^{n_L}\ \mathbf{N}_2^{n_L}\ \ldots\ \mathbf{N}_{n_E}^{n_L}\ \mathbf{u}^{n_L}\} \tag{3.128}$$

The number of binary variables is $n_E \cdot n_S$, and the number of continuous variables is $(n_E \cdot n_S + n_d) \cdot n_L$.

If nodal variables, $\mathbf{z}$, are included, the design variable vector becomes

$$\mathbf{x} = \{\mathbf{y}\ \mathbf{N}_1^1\ \mathbf{N}_2^1\ \ldots\ \mathbf{N}_{n_E}^1\ \mathbf{u}^1 \ldots \mathbf{N}_1^{n_L}\ \mathbf{N}_2^{n_L}\ \ldots\ \mathbf{N}_{n_E}^{n_L}\ \mathbf{u}^{n_L}\ \mathbf{z}\} \tag{3.129}$$

The number of design variables is increased to $n_E \cdot n_S + n_N + n_E \cdot n_S \cdot n_L + n_d \cdot n_L$.

If the loading condition for kinematic stability is included in the formulation, the force variables, $\tilde{N}_i$, are added, which leads to the following vector of design variables:

$$\mathbf{x} = \{\mathbf{y}\ \mathbf{N}_1^1\ \mathbf{N}_2^1\ \ldots\ \mathbf{N}_{n_E}^1\ \mathbf{u}^1 \ldots \mathbf{N}_1^{n_L}\ \mathbf{N}_2^{n_L}\ \ldots\ \mathbf{N}_{n_E}^{n_L}\ \mathbf{u}^{n_L}\ \mathbf{z}\ \tilde{\mathbf{N}}\} \tag{3.130}$$

The number of design variables is now $n_E \cdot n_S + n_N + n_E \cdot n_S \cdot n_L + n_d \cdot n_L + n_E$.

Several problem formulations can be constructed from the constraints and objective functions that have been presented in the previous sections. To facilitate the presentation, some additional notation is introduced for the constraints.

The constraints for member forces and unique profile selection are denoted by Ω_F:

$$\begin{aligned}\Omega_F = \{\, \mathbf{x} \mid\ & \underline{N}_{ij}^k y_{ij} \le N_{ij}^k \le \overline{N}_{ij}^k y_{ij} \\ & (1-y_{ij})\underline{N}_{ij}^k \le \frac{E_i}{L_i}\hat{A}_j \mathbf{b}_i^{\mathrm{T}}\mathbf{u}^k - N_{ij}^k \le (1-y_{ij})\overline{N}_{ij}^k \\ & \sum_{j=1}^{n_S} y_{ij} \le 1\ \forall\, i \in \mathcal{M},\ j \in \mathcal{P},\ k \in \mathcal{L}\,\}\end{aligned} \tag{3.131}$$

The nodal force equilibrium equations are denoted by

$$\Omega_{EQ} = \{\, \mathbf{x} \mid \hat{\mathbf{B}}\hat{\mathbf{N}}^k = \mathbf{p}^k,\ \forall\, k \in \mathcal{L}\,\} \tag{3.132}$$

$$\Omega_{EQ}^L = \{\, \mathbf{x} \mid \hat{\mathbf{B}}\hat{\mathbf{N}}^k - \mathbf{Q}^k\mathbf{y} = \mathbf{p}^k,\ \forall\, k \in \mathcal{L}\,\} \tag{3.133}$$

where the latter set is included, if the problem contains line loadings.

The strength constraints are denoted by

$$\Omega_S = \{\, \mathbf{x} \mid\ -\underline{\sigma}\hat{A}_j y_{ij} \le N_{ij}^k \le \overline{\sigma}\hat{A}_j y_{ij},\ \forall\, i \in \mathcal{M},\ j \in \mathcal{P},\ k \in \mathcal{L}\,\} \tag{3.134}$$

The buckling constraints are denoted by

$$\Omega_B^{EU} = \left\{ \mathbf{x} \mid N_{ij}^k \ge -\pi^2 \frac{E_i \hat{I}_j}{L_{ni}^2} y_{ij},\ \forall\, i \in \mathcal{M},\ j \in \mathcal{P},\ k \in \mathcal{L} \right\} \tag{3.135}$$

$$\Omega_B^{EC} = \{\, \mathbf{x} \mid N_{ij}^k \ge -\chi(\hat{A}_j, \hat{I}_j)\underline{\sigma}\hat{A}_j y_{ij}\ \forall\, i \in \mathcal{M},\ j \in \mathcal{P},\ k \in \mathcal{L}\,\} \tag{3.136}$$

The constraints related to chains are denoted by

$$\begin{aligned}\Omega_C = \{\, \mathbf{x} \mid & \sum_{i\in\mathcal{E}_c(s)} \sum_{j=1}^{n_S} y_{ij} \le 1 \quad \forall\, v_s \in \mathcal{V}_c \\ & \sum_{j=1}^{n_S} y_{ij} \le \sum_{r\in\mathcal{N}_c(s)} \sum_{j=1}^{n_S} y_{rj} \quad \forall\, v_s \in \mathcal{J}_c,\, i \in \mathcal{M}_c(s) \\ & \sum_{j=1}^{n_S} y_{ij} \le 1 - \sum_{j=1}^{n_S} y_{rj} \quad \forall\, r \in \mathcal{N}_c(s),\, s \in \mathcal{J}_c,\, i \in \mathcal{E}_c^o(s)\,\}\end{aligned} \tag{3.137}$$

The stabilizing loading condition is denoted by

$$\Omega_{ST} = \{\, \mathbf{x} \mid \mathbf{B}\tilde{\mathbf{N}} = \mathbf{P}\mathbf{z},\ -\underline{\sigma} \sum_{j=1}^{n_S} \hat{A}_j y_{ij} \le \tilde{N}_i \le \overline{\sigma} \sum_{j=1}^{n_S} \hat{A}_j y_{ij}\ \forall\, i \in \mathcal{M}\,\} \tag{3.138}$$

The constraints related to the nodal variables are denoted by

$$\begin{aligned}\Omega_N = \{\, \mathbf{x} \mid & \underline{\mathbf{u}}_\ell z_\ell \le \mathbf{u}_\ell^k \le \overline{\mathbf{u}}_\ell z_\ell \quad \forall\, \ell \in \mathcal{N},\, k \in \mathcal{L} \\ & \sum_{i\in\mathcal{M}_\ell} \sum_{j=1}^{n_S} y_{ij} \ge \underline{C}_\ell z_\ell \quad \forall\, \ell \in \mathcal{N} \\ & \sum_{j=1}^{n_S} y_{ij} \le z_\ell \quad \forall\, \ell \in \mathcal{N},\, i \in \mathcal{M}_\ell \\ & \sum_{i=1}^{n_E} \sum_{j=1}^{n_S} y_{ij} + \sum_{s\in\mathcal{N}_S} R_s z_s \ge 2 \sum_{\ell=1}^{n} z_\ell \\ & \sum_{\ell\in\mathcal{N}_S} z_\ell \ge 2\,\}\end{aligned} \tag{3.139}$$

The constraints of member grouping are denoted by

$$\Omega_G = \{\, \mathbf{x} \mid \sum_{j=1}^{n_S} w_j \le 1,\, y_{ij} \le w_j\ \forall\, i \in \mathcal{G},\, j \in \mathcal{P},\, \sum_{i\in\mathcal{G}} y_{ij} \ge w_j,\, \forall\, j \in \mathcal{P}\,\} \tag{3.140}$$

3.5.2 Formulation 2

In the second formulation, the variables y_{i0} are included. The design variable vector is then

$$\mathbf{x} = \{\mathbf{y}\ \mathbf{N}_1^1\ \mathbf{N}_2^1\ \ldots\ \mathbf{N}_{n_E}^1\ \mathbf{u}^1 \ldots \mathbf{N}_1^{n_L}\ \mathbf{N}_2^{n_L}\ \ldots\ \mathbf{N}_{n_E}^{n_L}\ \mathbf{u}^{n_L}\ \mathbf{y}_0\} \tag{3.141}$$

The number of binary variables is $n_E(n_S+1)$, and the number of continuous variables is $(n_E \cdot n_S + n_d)n_L$.

The constraints are identical with the previous formulation, except the constraint determining a unique selection, which is included in the member force constraints Ω_F.

In the present formulation, this set is

$$\begin{aligned}\Omega_F = \{\, \mathbf{x} \mid & \underline{N}_{ij}^k y_{ij} \le N_{ij}^k \le \overline{N}_{ij}^k y_{ij} \\ & (1-y_{ij})\underline{N}_{ij}^k \le \frac{E_i}{L_i}\hat{A}_j \mathbf{b}_i^{\mathrm{T}} \mathbf{u}^k - N_{ij}^k \le (1-y_{ij})\overline{N}_{ij}^k \\ & \sum_{j=0}^{n_S} y_{ij} = 1 \;\forall\, i \in \mathcal{M},\, j \in \mathcal{P},\, k \in \mathcal{L}\,\}\end{aligned} \tag{3.142}$$

As in the previous formulation, the design variable vector can be extended to include the nodal variables and the force variables related to the stabilizing loading condition.

3.5.3 Formulation 3

The third formulation differs from the other two substantially due to the binary variables y_i. The design variable vector, including nodal variables and the force variables related to the stabilizing loading condition is now

$$\mathbf{x} = \{\mathbf{y}\ \mathbf{N}_1^1\ \mathbf{N}_2^1\ \ldots\ \mathbf{N}_{n_E}^1\ \mathbf{u}^1 \ldots \mathbf{N}_1^{n_L}\ \mathbf{N}_2^{n_L}\ \ldots\ \mathbf{N}_{n_E}^{n_L}\ \mathbf{u}^{n_L}\ \mathbf{Y}\ \mathbf{z}\ \tilde{\mathbf{N}}\} \tag{3.143}$$

The constraints for member forces and profile selection are

$$\begin{aligned}\Omega_F = \{\, \mathbf{x} \mid & \underline{N}_{ij}^k y_{ij} \le N_{ij}^k \le \overline{N}_{ij}^k y_{ij}, \\ & (1-y_{ij})\underline{N}_{ij}^k \le \frac{E_i}{L_i}\hat{A}_j \mathbf{b}_i^{\mathrm{T}} \mathbf{u}^k - N_{ij}^k \le (1-y_{ij})\overline{N}_{ij}^k, \\ & y_i = \sum_{j=1}^{n_S} y_{ij}\ i \in \mathcal{M},\, j \in \mathcal{P},\, k \in \mathcal{L}\,\}\end{aligned} \tag{3.144}$$

The equilibrium equations for line loadings are

$$\Omega_{EQ}^L = \{\, \mathbf{x} \mid \hat{\mathbf{B}}\hat{\mathbf{N}}^k - \mathbf{Q}^k\mathbf{Y} = \mathbf{p}^k \;\forall k \in \mathcal{L}\,\} \tag{3.145}$$

If only point loads are included, the equilibrium equations are identical to the previous formulations. Also, member strength and buckling constraints, the constraints related to the stabilizing loading condition, and the constraints of member grouping do not change from the previous cases.

The constraints related to chains are

$$\begin{aligned}\Omega_C = \{\, \mathbf{x} \mid & \sum_{i \in \mathcal{E}_c(s)} y_i \le 1 \quad \forall\, v_s \in \mathcal{V}_c \\ & y_i \le \sum_{r \in \mathcal{N}_c(s)} y_r \quad \forall\, v_s \in \mathcal{J}_c,\, i \in \mathcal{M}_c(s) \\ & y_i \le 1 - y_r \quad \forall\, r \in \mathcal{N}_c(s),\, s \in \mathcal{J}_c,\, i \in \mathcal{E}_c^o(s)\,\}\end{aligned} \tag{3.146}$$

The constraints related to the nodal variables are

$$\begin{aligned}\Omega_N = \{\, \mathbf{x} \mid\ & \underline{\mathbf{u}}_\ell z_\ell \le \mathbf{u}_\ell^k \le \overline{\mathbf{u}}_\ell z_\ell \quad \forall\, \ell \in \mathcal{N},\, k \in \mathcal{L} \\ & \sum_{i \in \mathcal{M}_\ell} y_i \ge \underline{C}_\ell z_\ell \quad \forall\, \ell \in \mathcal{N} \\ & y_i \le z_\ell \quad \forall\, \ell \in \mathcal{N},\, i \in \mathcal{M}_\ell \\ & \sum_{i=1}^{n_E} y_i + \sum_{s \in \mathcal{N}_S} R_s z_s \ge 2 \sum_{\ell=1}^{n} z_\ell \\ & \sum_{\ell \in \mathcal{N}_S} z_\ell \ge 2 \,\}\end{aligned} \tag{3.147}$$

3.6 Discussion

The mixed variable approach for truss topology optimization possesses several advantages over the conventional NAND formulations. Most importantly, the mixed variable formulation circumvents the issues related to vanishing members completely. No special measures are required to handle zero cross-sections. The inherent difficulty plaguing topology optimization becomes a computational issue rather than a theoretical matter. Consequently, the applicability of the mixed variable formulations for treating problems with practical ground structures and profile alternatives depends solely on the numerical optimization algorithms and the available computational power. Fortunately, the solution methods and software have undergone a tremendous development in the recent years, and the boundaries of the problem size that can be solved within reasonable time are constantly pushed further.

Another powerful feature of the mixed variable approach is the application of binary variables in expressing topology-related conditions explicitly. All such constraints presented in this work are linear. For example, the binary variables can be employed to enforce the kinematic stability of the truss, which has proven to be difficult to achieve by the conventional formulations.

The binary variables can also be used to solve the difficult jump in the buckling length phenomenon by introducing member chains. This is an important original contribution of the present thesis, as it improves the direct applicability of the optimum designs. Chains can also be used to incorporate line loading in truss topology optimization without distorting the solution. The author is not aware of other satisfactory approaches to this issue in the literature.

It is remarkable that the problem formulations result in linear optimization problems for discrete cross-sections, even when buckling constraints are included. This is enabled by the binary profile selection variables. The complicated expressions for buckling strength are reduced to constants in the constraints as the buckling strength is evaluated separately for each profile alternative for every member. Also, important criteria can be written as linear functions of the binary variables. The "discrete" criteria such as the number of members and nodes are difficult to express in terms of cross-sectional areas, but employing binary variables leads to very simple expressions.

The mixed variable formulation can also be used for cost optimization. The cost function of Haapio (2012) allows a linear cost function in terms of the binary variables. Cost optimization requires that the details of the manufacturing process are known. Consequently, the cost function includes many parameters, some of which might be difficult to obtain reliably.

The price of the mixed variable approach is that the formulations lead to mixed-integer linear optimization problems, which are very difficult to solve in general. In practical design situations, these problems can be expected to become large-scale, as the problem size grows rapidly with respect to the number of ground structure members and available profiles. It is then interesting to study the capability of contemporary computers to solve the resulting optimization problems by modern algorithms. This issue is explored in the coming chapters of the present study.

CHAPTER 4

Solving Mixed Variable Problems

Something real and tangible, yet
fraught with infinite suggestions of
nighted mystery, now confronted me.
H.P. Lovecraft

4.1 Introduction

The optimization problems of this thesis are *mixed-integer linear programming (MILP)* problems. These problems have been widely studied in the optimization community, and several software packages –commercial and free– are available. In this chapter, a brief overview of the solution method implemented in most codes is discussed. As the focus of the study is on problem formulations rather than solution algorithms, the topic is not treated in detail.

Before the actual solution process is discussed, the issue of computational complexity needs to be addressed. It is a well-known result, that except for a limited number of instances, mixed-integer optimization problems are among the most difficult optimization problems to be solved. In the parlance of the theory of computational complexity, many mixed-integer problems are NP-hard, which means that an algorithm that would solve the problem in polynomial time is not known (Wolsey 1998). The consequence of this is that sooner or later, as the problem size is enlarged, any known algorithm will fail to give the optimum solution within the time and computational power available. Nevertheless, due to the significant advances in the methods and software in the last decade or so, it can be expected that practical truss topology optimization problems can be solved by modern computers using mixed variable formulations.

In the mixed variable formulations presented in Chapter 3, the problem size is essentially determined by the number of ground structure members, loading conditions and profile alternatives. The number of nodes also contributes to the problem size, but with less impact than the three other factors. Once the total number of ground structure members, loading conditions, and profile alternatives reaches a certain value –not known *a priori*– the solution algorithms stagnate and verifying that the global optimum of the problem has been found becomes intractable. One of the research issues addressed in this thesis is the determination of the problem size that can be solved with present software on a desktop computer within a given time limit.

The optimization problems to be solved are of the following form

$$\min_{(\mathbf{x},\mathbf{y})\in\Omega} f(\mathbf{x},\mathbf{y}) = \mathbf{c}^{\mathrm{T}}\mathbf{x} + \mathbf{d}^{\mathrm{T}}\mathbf{y} \qquad (P_{MIP})$$

where $\mathbf{x} \in \mathbb{R}^n$ and $\mathbf{y} \in \mathbb{B}^d = \{0,1\}^d$ are the continuous and binary variables, respectively. Vectors $\mathbf{c}$ and $\mathbf{d}$ are constants. Note that the notation used in this chapter is for general MILP problems, and it does not coincide with the notation of other chapters of the thesis.

The feasible set Ω is written as

$$\Omega = \{(\mathbf{x},\mathbf{y}) \,|\, \mathbf{A}\mathbf{x} + \mathbf{B}\mathbf{y} \leq \mathbf{b},\ \mathbf{C}\mathbf{x} + \mathbf{D}\mathbf{y} = \mathbf{g}, \mathbf{x} \in \mathbb{R}^n,\ \mathbf{y} \in \mathbb{B}^d\} \qquad (4.1)$$

where $\mathbf{A}$, $\mathbf{B}$, $\mathbf{C}$, $\mathbf{D}$, $\mathbf{b}$, and $\mathbf{g}$ are constant matrices and vectors. The *relaxation* of problem P_{MIP} plays an important role in the solution process. It is obtained by treating the binary variables $\mathbf{y}$ as continuous variables:

$$\min_{(\mathbf{x},\mathbf{y})\in\Omega_R} f(\mathbf{x},\mathbf{y}) = \mathbf{c}^{\mathrm{T}}\mathbf{x} + \mathbf{d}^{\mathrm{T}}\mathbf{y} \qquad (P_R)$$

where

$$\Omega_R = \{(\mathbf{x},\mathbf{y}) \,|\, \mathbf{A}\mathbf{x} + \mathbf{B}\mathbf{y} \leq \mathbf{b},\ \mathbf{C}\mathbf{x} + \mathbf{D}\mathbf{y} = \mathbf{g}, \mathbf{x} \in \mathbb{R}^n,\ \mathbf{y} \in \mathbb{R}^d\} \qquad (4.2)$$

Problem P_R is an LP problem. Since $\Omega_R \subseteq \Omega$, the solution of problem P_R provides a lower bound for the optimum of problem P_{MIP}.

4.2 Branch-and-Cut

Arguably the most successful solution approach for MILP problems is the family of *branch-and-cut* algorithms, which combine the well-known *branch-and-bound* method with *cutting planes*. In the following, the ideas of this approach are briefly introduced. A more detailed presentation can be found in (Nemhauser & Wolsey 1999) and (Wolsey 1998).

The foundation of branch-and-cut relies on the principle of branch-and-bound (Land & Doig 1960). The idea is to divide the feasible set Ω into subsets Ω^i such that $\cup_{i=1}^{k} \Omega^i = \Omega$ and to solve the optimization problem in each Ω^i. The presumption is that it is easier to find the minimum of f in the subsets Ω^i than it is in Ω. The division of Ω is done recursively and it can be represented as a tree-shaped graph, called the *search tree*, where Ω^i constitute the nodes.

At a given iteration of the branch-and-bound algorithm, a node of the search tree is selected for inspection. Minimizing f in Ω^i can be as difficult as solving problem P_{MIP}. Therefore, the relaxation of the problem at the node is considered, i.e. the problem

$$\min_{(\mathbf{x},\mathbf{y})\in\Omega^i_R} f(\mathbf{x},\mathbf{y}) \qquad (P^i_R)$$

Problem P^i_R is solved by an LP algorithm. There are three possible outcomes. Firstly, if $\Omega^i_R = \emptyset$, then $\Omega^i = \emptyset$, and the node need not be considered any further, i.e. it can be *pruned* (or *fathomed*). Secondly, if the solution $(\mathbf{x}^i_R, \mathbf{y}^i_R) \in \Omega^i$, then the optimum of f in the present node has been found and the node can be pruned. Furthermore, $f(\mathbf{x}^i_R, \mathbf{y}^i_R)$ provides an upper bound for the minimum of f. Thirdly, if $(\mathbf{x}^i_R, \mathbf{y}^i_R) \notin \Omega^i$, then $f(\mathbf{x}^i_R, \mathbf{y}^i_R)$ gives a lower bound for the minimum of f. If a solution $(\hat{\mathbf{x}}, \hat{\mathbf{y}}) \in \Omega$ with $f(\hat{\mathbf{x}}, \hat{\mathbf{y}}) \leq f(\mathbf{x}^i_R, \mathbf{y}^i_R)$ has been found earlier, it can be concluded that neither the present node nor any of its subnodes can contain a solution better than $\hat{\mathbf{x}}$, and the node can be pruned. Otherwise, Ω^i is divided into smaller subsets, and new nodes to be explored are generated.

For problems where all discrete variables are binary, the division of Ω^i is commonly performed as follows. A binary variable, say y_r, with a fractional value at $(\mathbf{x}^i_R, \mathbf{y}^i_R)$ is chosen. Then, Ω^i is divided into two new subsets (nodes), Ω^{i+1} and Ω^{i+2}, where $\Omega^{i+1} = \Omega^i \cap \{\mathbf{y} \in \mathbb{B}^d \,|\, y_r = 0\}$ and $\Omega^{i+2} = \Omega^i \cap \{\mathbf{y} \in \mathbb{B}^d \,|\, y_r = 1\}$.

Typically, there are many binary variables with a fractional value at the optimum of the relaxation. Choosing the branching variable is not a trivial task, and it has a significant impact on the overall performance of the algorithm. If the binary variables play different roles in the MILP model, the user might provide *branching priorities* where the binary variables are ordered such that the variables having a greater impact on the objective function are forced to integral values sooner than the others. Otherwise, a computational procedure is performed to find the branching variable. Common branching strategies can be found in (Nemhauser & Wolsey 1999, pp. 359). Further approaches and a computational comparison of branching strategies have been presented by Achterberg, Koch & Martin (2005).

Choosing the node to be investigated is another important issue in branch-and-bound. Common strategies are *depth-first*, *breath-first*, and *best-node first*. In the depth-first strategy, the next node to be explored is always the son of the previous node. In breath-first, all the nodes at a given level are considered before any nodes of the lower level. Finally, in best-node first strategy, the node having the lowest lower bound is chosen. For benefits of the different strategies, see (Nemhauser & Wolsey 1999, pp. 358).

The above procedure leads to an iterative algorithm, where sequences of non-decreasing lower bounds and non-increasing upper bounds are generated. The lower bounds are obtained by solving the relaxation at the nodes. The upper bounds are provided by feasible solutions that can be found either as solutions to the relaxations or by applying heuristic search methods at the nodes. The algorithm terminates, when there are no more nodes to be searched, or when the greatest lower bound and lowest upper bound are within a predefined tolerance of each other. At termination, the global optimum of problem P_{MIP} is obtained.

The number of steps in the branch-and-bound algorithm is finite. In its basic form, however, the method produces a rapidly growing search tree, and for solving practical problems, several enhancements must be introduced. These include heuristics for finding feasible solutions, preprocessing and probing techniques for tightening the problem formulation (Savelsbergh 1994), and valid inequalities and cutting planes to improve the quality of the relaxations.

An inequality $\mathbf{a}^{\mathrm{T}}\mathbf{x} + \mathbf{b}^{\mathrm{T}}\mathbf{y} \leq a_0$ is called a *valid inequality* for Ω, if it is satisfied by all points in Ω. The purpose of adding valid inequalities to the problem is to make the relaxations tighter, i.e. to remove fractional parts of the feasible set without removing any feasible solution. Valid inequalities can be devised for inequalities of specific structure or they can be generated for more general constraints, for example, by the *Chvátal-Gomory* procedure (Wolsey 1998).

A *cutting plane*, or simply *cut*, with respect to a point $(\hat{\mathbf{x}}, \hat{\mathbf{y}})$ is a valid inequality for Ω that is violated by $(\hat{\mathbf{x}}, \hat{\mathbf{y}})$. The purpose of cutting planes is to remove from the feasible set solutions of the relaxations that do not belong to Ω along with parts of Ω_R not containing points where the variables $\mathbf{y}$ obtain integer values. Similarly to valid inequalities, special cutting planes can be used for constraints having a specific structure, and more general cuts may be generated for general constraints.

Incorporating cutting planes to the branch-and-bound framework constitutes the branch-and-cut solution method. The idea is to get tight relaxations by adding cutting planes and to perform other techniques at every node of the search tree. The aim is to reduce the number of nodes that need to be explored and to find feasible solutions more quickly. On the other hand, as the cuts themselves are inequality constraints, adding cuts to the problem increases the size of the relaxation at the corresponding node of the search tree, slowing the computation of the lower bound. Also, the information related to the cuts needs to be stored in a separate *cut pool* and it needs to be indicated, which cuts are related to which nodes (Wolsey 1998, pp. 157).

Cutting planes provide a powerful enhancement to the branch-and-bound algorithm. Bixby & Rothberg (2007) performed a study, where the cutting planes were disabled from the solver CPLEX 8.0. Without cutting planes, the mean performance of the software was degraded by the factor of 53.7. Rasmussen & Stolpe (2008) solved truss topology optimization problems by branch-and-bound and by branch-and-cut with Combinatorial Benders' cuts (Codato & Fischetti 2006) and Projected Chvátal-Gomory cuts (Bonami, Cornuéjols, Dash, Fischetti & Lodi 2008). In their implementation, the cutting planes are created only at the root node of the search tree. Nevertheless, they obtain improvements of several orders of magnitude in computational time compared with branch-and-bound.

An important observation is that certain cutting planes work very well on specific problems while not contributing much enhancement for other problems. For example, Codato & Fischetti (2006) employ Combinatorial Benders' cuts for a set of problems well-suited for these cuts. As a result, they obtain a mean improvement of factor 21.1 over a general-purpose software. It can be deduced, that for every specific problem, the mathematical form of the constraints should be carefully inspected and several cutting planes considered for finding the most efficient solution approach.

For more on valid inequalities and cutting planes, see (Wolsey 1998, Marchand, Martin, Weismantel & Wolsey 2002, Cornuéjols 2008).

Bixby (2012) has presented an overview on the progress in the MILP methods and software. By comparing the performance of different versions of CPLEX from 1.2. to 11, he concluded that there has been an improvement in the software of a factor of over 29,000 since the early 1990s to 2007.

4.3 Solution Software

One of the research questions of this study is, what is the ability of contemporary software and computers to solve truss topology optimization problems using mixed variable formulations. Therefore, instead of developing an own research code, it was decided to use a commercial, state-of-the-art software for solving the MILP problems. Of the several available software packages, Gurobi 5.0 was chosen as the solver (Gurobi Optimization, Inc. 2012). It includes various preprocessing techniques, heuristics, and twelve cutting planes. The behaviour of the solver can be controlled by a set of parameters. For example, the branching strategy, cutting plane generation and various tolerances can be set by the user.

In this study, Gurobi 5.0 is used mostly with the default parameter settings. Only the variable branching strategy was switched to *pseudo reduced cost branching*, after some experimentation. In all cases, unless otherwise noted, the feasibility and termination tolerances were set to their default values. By default, Gurobi uses the values $\epsilon_g = 1 \cdot 10^{-6}$ and $\epsilon_f = 1 \cdot 10^{-4}$ for the constraint feasibility and relative optimality gap, respectively.

An important aspect of the branch-and-cut algorithm is the possibility to parallelize the computation. As many unexplored nodes as there are computing units, or *threads*, available can be investigated simultaneously. Gurobi is implemented to be intrinsically parallel, using all available threads by default.

4.4 Discussion

The theory of mixed integer programming is well-established, and powerful computer implementations are available. The recent progress in the software development opens the path for the mixed variable formulations of truss topology optimization to be employed in practical design situations.

Due to the computational complexity of mixed integer problems, problem-specific solution methods, cutting planes, or heuristics are often developed. Such developments should also be carried out for truss topology optimization problems. However, this research is beyond the scope of the present study. The general-purpose, state-of-the-art solver used in this thesis provides a reference to which further developments can be compared with.

CHAPTER 5

Benchmark Problems

Not only rules, but also examples are needed for establishing a practice. Our rules leave loop-holes open, and the practice has to speak for itself.

LUDWIG WITTGENSTEIN

5.1 Introduction

Before the mixed variable formulations are applied to practical design situations, it is important to verify them. It is also interesting to study the effect of the different constraints on the optimum solution. Furthermore, as there are three possibilities of choosing the design variables, it is necessary to compare them to find out if one formulation is computationally more favourable than the others. To this end, several benchmark problems are considered in the following. The problems are simple enough to be solved to global optimality without much effort, but versatile enough to display the above aspects. As the proven global optimum of each problem is found, the problems can be used in future research for testing new solution methods.

Two benchmark cases are treated. First, a cantilever truss with two ground structures is considered. The purpose is to verify the problem formulations and to demonstrate the effect of buckling constraints.

The second case is the well-known "L-shaped" truss. The instance reported by Rasmussen & Stolpe (2008) is considered and employed to study the computational effort related to the formulations of this thesis. This problem also serves to demonstrate the effect of the kinematic stability constraints. Then, another instance of the L-shape

is solved, where more sections are available and member buckling constraints are included. This problem is substantially larger than the first instance, and it includes most of the constraints that have been presented in Chapter 3.

In most instances, the weight of the truss is minimized. In the single exception, the material volume is minimized instead of weight. Because only one material is included, the minimum weight problem is equivalent to material volume minimization.

The minimum weight problem is stated as

$$\min_{\mathbf{x}\in\Omega} W(\mathbf{x}) \tag{5.1}$$

where the expression for the weight, W, is as in Eq. (3.86). The feasible set, Ω, varies for different sets of constraints, and the design variable vector also changes for different formulations. Different problem formulations are employed for the benchmark problems. Both the constraints and the choice of variables are varied in the formulations. The feasible sets of the different problems are given in conjunction with each problem.

5.2 Cantilever Truss

Consider a square-shaped design domain that is supported from the left-hand side and loaded by a point load at the lower right corner, as shown in Fig. 5.1. The members of the truss are made of steel with density $\rho = 7850\,\mathrm{kg/m^3} = 7.850 \cdot 10^{-6}\,\mathrm{kg/mm^3}$, Young's modulus $E = 210\,\mathrm{GPa}$, and yield strength $f_\mathrm{y} = 420\,\mathrm{MPa}$. The side length of the domain is $L = 2000\,\mathrm{mm}$, and the magnitude of the load is $F = 100\,\mathrm{kN}$. The bounds for the nodal displacements are in each case $\overline{u} = -\underline{u} = 50\,\mathrm{mm}$. Such displacements can be regarded large for the present design domain, and the main purpose of the displacement bounds is to provide bounds for the force variables.

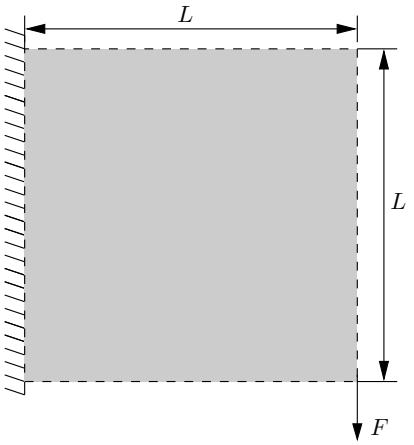

Figure 5.1: Design domain of the cantilever truss.

Two ground structures, shown in Fig. 5.2, are considered. The nodal coordinates and element connectivity tables are given in Appendix B.1. The idea is to solve the same

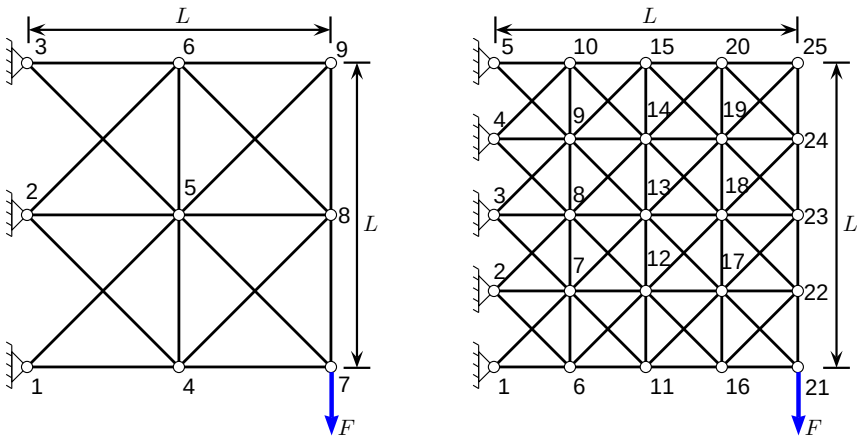

Figure 5.2: The two ground structures of the cantilever truss.

Table 5.1: Selection of profiles for the cantilever truss problem (see Fig. 2.1).

Profile	A [mm^2]	I [mm^4]	H [mm]	t [mm]
1	209	16900	25.0	2.5
2	241	18400	25.0	3.0
3	359	82200	40.0	2.5
4	541	194700	50.0	3.0
5	659	494100	70.0	2.5

optimization problems for both ground structures to see how the optimum topology varies with the ground structure and how chains work when buckling constraints are included.

The member profiles are square hollow sections. The data for the available profiles is shown in Table 5.1. The sections are chosen from the catalogue of a Finnish steel manufacturer (Ruukki 2011). The number of profile alternatives is kept small in order to reduce the computational effort.

The minimum weight problem, Eq. (5.1), is solved for both ground structures with varying feasible sets. Altogether nine problem formulations are considered. Formulation 1 (Section 3.5.1) is employed. In the simplest case, only strength constraints are included in the problem in addition to the equations of structural analysis. This problem is often called the stress-constrained minimum weight problem, and it is stated as

$$\min_{\mathbf{x}\in\Omega_1} W(\mathbf{x}) \tag{P_S}$$

where

$$\Omega_1 = \Omega_F \cap \Omega_{EQ} \cap \Omega_S \tag{5.2}$$

Note that neither chains nor nodal variables are included in this formulation. The first extension is obtained by adding member buckling constraints. If Euler buckling

is employed, the problem formulation becomes

$$\min_{\mathbf{x}\in\Omega_2} W(\mathbf{x}) \tag{P_{EU}}$$

where

$$\Omega_2 = \Omega_1 \cap \Omega_B^{EU} \tag{5.3}$$

Similarly, if buckling according to Eurocode 3 is used, the problem becomes

$$\min_{\mathbf{x}\in\Omega_3} W(\mathbf{x}) \tag{P_{EC}}$$

where

$$\Omega_3 = \Omega_1 \cap \Omega_B^{EC} \tag{5.4}$$

Chains and nodal variables can be added separately. First, if chains are included in the problem, the above three formulations are modified to

$$\min_{\mathbf{x}\in\Omega_1\cap\Omega_C} W(\mathbf{x}) \tag{P_{SC}}$$

$$\min_{\mathbf{x}\in\Omega_2\cap\Omega_C} W(\mathbf{x}) \tag{P_{EUC}}$$

$$\min_{\mathbf{x}\in\Omega_3\cap\Omega_C} W(\mathbf{x}) \tag{P_{ECC}}$$

These problems are then extended with nodal variables to the form

$$\min_{\mathbf{x}\in\Omega_1\cap\Omega_C\cap\Omega_N} W(\mathbf{x}) \tag{P_{SN}}$$

$$\min_{\mathbf{x}\in\Omega_2\cap\Omega_C\cap\Omega_N} W(\mathbf{x}) \tag{P_{EUN}}$$

$$\min_{\mathbf{x}\in\Omega_3\cap\Omega_C\cap\Omega_N} W(\mathbf{x}) \tag{P_{ECN}}$$

5.2.1 The 2-by-2 Ground Structure

The coarser ground structure, shown in Fig. 5.2a, has 9 nodes and 12 degrees of freedom. Without chains, the number of members is 18. If chains are added, the number of members increases to 25. The problem size depends on whether chains and nodal variables are included or not. In Table 5.2, the problem sizes of the different cases are given. For contemporary computers, all the problems can be considered small-scale. Indeed, each of the nine problems was solved in less than a second. Therefore, the computational aspects of the problem are not reported.

Table 5.2: Problem sizes of the 2-by-2 ground structure. '$\leq$' = number of inequality constraints, '=' = number of equality constraints.

Chains	Nodal variables	Members	Variables	Integer variables	$\leq$	=
NO	NO	18	192	90	378	12
YES	NO	25	262	125	582	12
YES	YES	25	271	134	667	12

Consider first the instance, where chains and nodal variables are not included. The same optimum topology is obtained for all problems P_S, P_{EU}, and P_{EC} (Fig. 5.3). This topology displays the appearance of intermediate, unstable nodes in the solution. When buckling constraints are included, the profiles of members 1 and 9 are selected using $L/2$ as buckling length. If the unstable node connecting members 1 and 9 is removed and the two members are combined with their common cross-section (profile 3 in Table 5.1), the buckling length becomes L and the buckling constraint is violated, both if Euler buckling or Eurocode 3 buckling is employed.

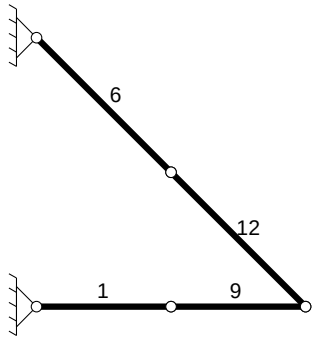

Figure 5.3: Minimum weight topology of the 2-by-2 ground structure without chains.

Table 5.3: Optimal solutions of the 2-by-2 ground structure, no chains.

Member	A [mm^2]	Strength [%]	Euler [%]	Eurocode [%]
No buckling, $W^* = 11.7546$ kg.				
1, 9	241	98.79	262.22	357.79
6, 12	359	93.79	–	–
Euler buckling, $W^* = 13.6072$ kg.				
1, 9	359	66.32	58.70	115.34
6, 12	359	93.79	–	–
Eurocode buckling, $W^* = 16.4646$ kg.				
1, 9	541	44.01	24.78	63.48
6, 12	359	93.79	–	–

In Table 5.3, the optimum member areas, and the utilization ratios with respect to strength and buckling constraints are given. The labels of the members correspond to the labels in Fig. 5.3. The utilization ratio of a constraint of the form $g(x) \leq \overline{g}$ is defined by

$$U_g(\mathbf{x}) = \frac{g(\mathbf{x})}{\overline{g}} \cdot 100\% \tag{5.5}$$

Thus, the utilization ratio is 100%, if the constraint is active, and greater than 100%, if

the constraint is violated. From Table 5.3, it can be seen that, the Eurocode 3 utilization of members 1 and 9 is 115, 34% for the solution of problem P_{EU}, so the optimum solution for Euler buckling constraints does not satisfy the Eurocode 3 buckling rule. This demonstrates the importance of incorporating the right buckling constraints in the problem formulation in order to guarantee the applicability of the solution.

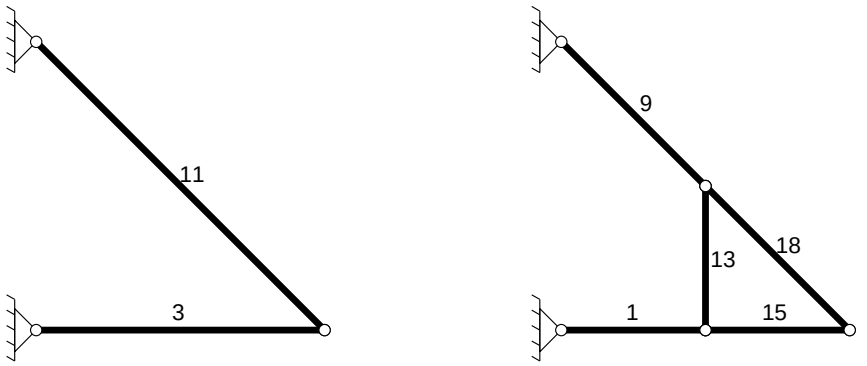

Figure 5.4: Minimum weight topology of the 2-by-2 ground structure with chains (a) without buckling; (b) with buckling (Euler and Eurocode). The number by each member corresponds to the numbering of the members in the ground structure with chains.

Table 5.4: Optimal solutions of the 2-by-2 ground structure with chains.

Member	A [mm^2]	Strength [%]	Euler [%]	Eurocode [%]
No buckling, $W^* = 11.7546$ kg.				
3	241	98.79	1048.87	1210.09
11	359	93.79	–	–
Euler buckling, $W^* = 15.2479$ kg.				
1, 15	359	66.32	58.70	115.34
9, 18	359	93.79	–	–
13	209	0	–	–
Eurocode buckling, $W^* = 18.1053$ kg.				
1, 15	541	44.01	24.78	63.48
9, 18	359	93.79	–	–
13	209	0	–	–

If chains are included in the problem, the optimum topology for buckling constraints changes. In Fig. 5.4a, the optimum topology without buckling constraints is depicted. The constraints Eq. (3.66) related to the chains have removed the unstable nodes from the structure. Without buckling constraints, the profiles of members 3 and 11 are identical to the profiles of members 6 and 12, and 1 and 9, respectively, of

the previous case. In Fig. 5.4b, the optimum topology for buckling constraints is shown. The vertical member 13 has been added to keep the buckling length as short as possible. The purpose of member 13 is to provide the part in compression (members 1 and 15) transversal support that allows the buckling length $L/2$ to be used instead of L. However, the topology is still clearly kinematically unstable, i.e. it is a mechanism, unable to support a vertical load at the node connecting members 1, 13, and 15. This can be verified by checking the necessary condition for kinematic stability, Eq. (3.27): $5 + 4 = 9 \ngeq 2 \cdot 5 = 10$. Thus, nodal variables are clearly needed in order to provide kinematically stable solutions.

The optimum solutions and the utilization ratios of the members are listed in Table 5.4. Note that member 13 in the optimum topology for buckling constraints does not carry any load.

The third problem type, where nodal variables are included in the problem formulation, leads to kinematically stable topologies, as shown in Fig. 5.5. In Fig. 5.5a, the optimum topology of problems P_{SN} and P_{ECN} is shown, and the optimum topology of problem P_{EUN} is shown in Fig. 5.5b. The corresponding member profiles and utilization ratios are given in Table 5.5. The reason for the difference in optimum topologies for the different buckling constraints is that an efficient cross-section for the buckling length $L/2$ is not available for Eurocode 3 buckling. For the given selection of profiles, it is more economical to use a longer member 3 with a larger cross-section than to add the diagonal member 5 which allows to use a shorter buckling length.

From the above, it can be seen that the type of buckling constraint affects both the optimum member profiles and the optimum topology. This observation highlights the importance of using the appropriate buckling constraint in the optimization problem.

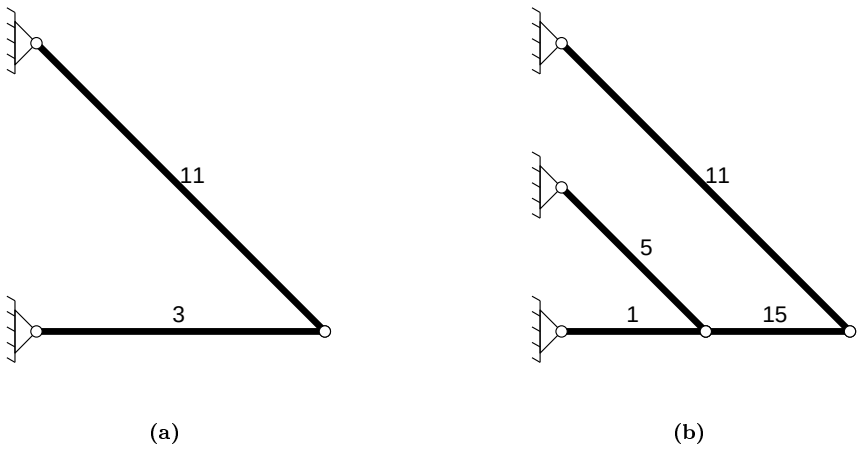

Figure 5.5: Minimum weight topology of the 2-by-2 ground structure with chains and nodal variables (a) without buckling and with Eurocode 3 buckling; (b) with Euler buckling. The numbers by each member corresponds to the numbering of the members in the ground structure with chains.

Table 5.5: Optimal solutions of the 2-by-2 ground structure with chains and nodal variables.

Member	A [mm^2]	Strength [%]	Euler [%]	Eurocode [%]
No buckling, $W^* = 11.7546$ kg.				
3	241	98.79	1048.87	1210.09
11	359	93.79	–	–
Euler buckling, $W^* = 15.9275$ kg.				
1, 15	359	66.32	58.70	115.34
11	359	93.79	–	–
5	209	0	–	–
Eurocode buckling, $W^* = 18.3172$ kg.				
3	659	36.13	39.06	69.85
11	359	93.79	–	–

5.2.2 The 4-by-4 Ground Structure

The denser ground structure, shown in Fig. 5.2b, contains 25 nodes and 40 degrees of freedom. As it was shown for the 2-by-2 ground structure, chains are essential for obtaining applicable solutions. Therefore, the problems without chains are not considered for the present case. Also, the problems without buckling constraints are excluded. Therefore, four different optimization problems are solved for this ground structure. With chains, the ground structure contains 150 members. The problem sizes are given in Table 5.6. The number of variables and constraints is considerably larger than for the 2-by-2 ground structure. However, the problems are still relatively small.

Table 5.6: Problem sizes of the 4-by-4 ground structure.

Chains	Nodal variables	Members	Variables	Integer variables	$\leq$	$=$
YES	NO	150	1540	750	3715	40
YES	YES	150	1565	775	4122	40

The optimum topology of problems P_{EUC} and P_{ECC} is shown in Fig. 5.6, and the optimum member sections and utilization ratios are given in Table 5.7. The same topology is obtained both problems. Again, due to the constraints related to chains, short members are added to provide transversal support for the part in compression (members 1, 45, 88, and 122). However, the topology is a mechanism and therefore not very practical.

When nodal variables are included in the problem, the optimum topologies become kinematically stable, but are not equal for the two types of buckling constraints. The optimum topologies for Euler buckling and Eurocode 3 buckling constraints are shown in Fig. 5.7a and Fig. 5.7b, respectively. The reason for the difference in optimum topologies is that for Eurocode 3 buckling constraints, more economical cross-sections are available for the buckling lengths $L/4$ and $3L/4$ than for $L/2$. On the other hand, members 1, 9, and 49 have different sections, which makes the fabrication of the joint connecting them more difficult than the joint connecting members 3, 90, and 20 in

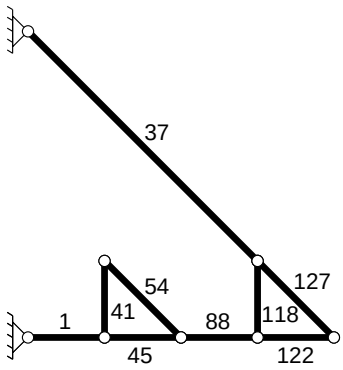

Figure 5.6: Minimum weight topology of the 4-by-4 ground structure with chains, and without nodal variables.

Table 5.7: Optimal solutions of the 4-by-4 ground structure with chains.

Member	A [mm^2]	Strength [%]	Euler [%]	Eurocode [%]
Euler buckling, $W^* = 14.5554$ kg.				
1, 45, 88, 122	241	98.79	65.55	151.29
37, 127	359	93.79	–	–
41, 54, 118	209	0	–	–
Eurocode buckling, $W^* = 16.4080$ kg.				
1, 45, 88, 122	359	66.32	14.67	77.17
37, 127	359	93.79	–	–
41, 54, 118	209	0	–	–

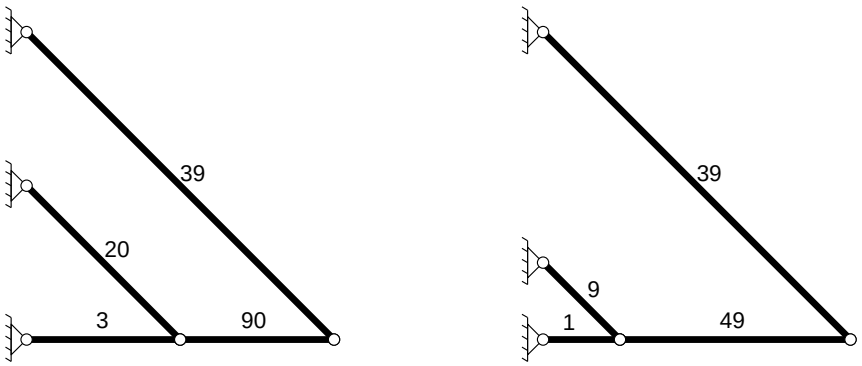

(a) (b)

Figure 5.7: Minimum weight topology of the 4-by-4 ground structure with chains, nodal variables, and (a) with Euler buckling; (b) with Eurocode buckling.

Figure 5.8: Optimal solutions of the 4-by-4 ground structure with chains and nodal variables.

Member	A [mm^2]	Strength [%]	Euler [%]	Eurocode [%]
Euler buckling, $W^* = 15.9275$ kg.				
3, 90	359	66.32	58.70	115.34
39	359	93.79	–	–
20	209	0	–	–
Eurocode buckling, $W^* = 16.9104$ kg.				
1	359	66.32	14.67	77.17
9	209	0	–	–
39	359	93.79	–	–
49	541	44.01	55.76	93.48

Fig. 5.7a. The optimum member sections and utilization ratios are given in Table 5.8 along with the minimum weight.

As the problem sizes are now substantially larger than for the 2-by-2 ground structure, the computational aspects of the solution process are more interesting. All problems were solved by Gurobi 5.0 on a computer with Intel Core 2 Quad (four threads) Q9400 processor, running at 2.66 GHz clock frequency with 3.25 GB RAM. In Table 5.8, some data of the computations are presented. First, the objective function values at the solution of the first relaxation, f_R, and at the first feasible solution, f_1, are given. Then, to measure the quality of the relaxation, the so-called *relative initial optimality gap* is computed. It is defined as

$$\text{Gap} = \frac{f^* - f_R}{f_R} \cdot 100\% \tag{5.6}$$

where f^* is the minimum value of the objective function. From Table 5.8 it can be seen that this gap is about 27% to 40%. The computation time, T_g, for finding the global optimum, as well as the total running time of the algorithm, T, are also given. The problem size poses no difficulties for the solver, as all instances are solved in less than 30 seconds. The global optimum is found relatively early compared with the total running time. Interestingly, less time is required to terminate the algorithm, when the nodal variables are included. The constraints related to the nodal variables seem to make the feasible set tighter.

Finally, the number of explored nodes of the search tree is given in Table 5.8. This value is a more objective measure for the computational effort, since the computation time is very much computer-depended and is likely to decrease as more powerful computers become available.

Table 5.8: Results of the computations for the 4-by-4 ground structure. The columns are: f_R = weight of the first relaxation, f_1 = the weight of the first feasible solution, Gap = the initial optimality gap, T_g = the elapsed time, when the global optimum was found, T = the elapsed time at termination, Nodes = explored nodes of the search tree, f^* = the minimum weight.

Problem	f_R [kg]	f_1 [kg]	Gap [%]	T_g [s]	T [s]	Nodes	f^* [kg]
P_{EUC}	11.2979	16.4646	28.8	4	19.66	4513	14.5540
P_{ECC}	16.4646	30.8234	40.3	3	27.42	8730	16.4080
P_{EUN}	12.1775	20.5056	30.8	4	9.17	691	15.9275
P_{ECN}	13.2888	31.8309	27.3	7	9.70	401	16.9104

5.3 L-Shaped Truss

Consider the design domain shown in Fig. 5.9a. The structure is supported from the top side and the load is in the middle of the rightmost vertical side. The ground structure, shown in Fig. 5.9b, has 21 nodes, and 36 degrees of freedom. Without chains, the number of members is 54. If chains are included, the number of members increases to 108. The nodal coordinates and element connectivity tables can be found in Appendix B.2.

In the following, two cases of this "L-shaped" truss, with different input data, are solved. First, the instance described by Rasmussen & Stolpe (2008) is considered. In this case, the members are made of aluminium, and the material volume is minimized instead of the weight. The number of profile alternatives is limited to two, and member buckling is not considered. As this problem has already been solved in the literature, it serves as a benchmark for verifying the formulations of this thesis. Also, the matter of kinematically stable optimum solutions is addressed in conjunction with this problem.

In the second case, the material of the members is changed to steel such that the constraints of Eurocode 3 can be applied. The number of profile alternatives is increased and the catalogue of a Finnish steel manufacturer is used for the profile data. The purpose of this case is to study the computational aspects and the optimum topologies of the different formulations for an increased problem size.

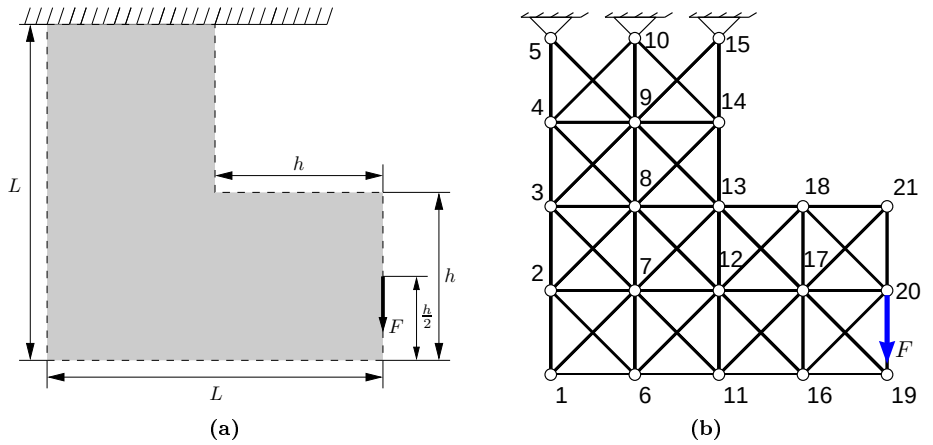

Figure 5.9: The design domain and the ground structure of the L-shaped truss.

5.3.1 Aluminium Members

Rasmussen & Stolpe (2008) considered the L-shaped truss with aluminium members. This problem is treated in the following using the original data. The Young's modulus is $E = 70\,\mathrm{GPa}$. The magnitude of the point load is $F = 450\,\mathrm{kN}$. The dimensions of the design domain, shown in Fig. 5.9a, are $L = 2000\,\mathrm{mm}$, and $h = 1000\,\mathrm{mm}$. The allowable stress in tension and in compression for the members is $\overline{\sigma} = 170\,\mathrm{MPa}$. The

cross-sectional areas of the members can be either $5000\,\mathrm{mm}^2$ or $10000\,\mathrm{mm}^2$. The bounds of the nodal displacements are $\overline{u} = -\underline{u} = 2000\,\mathrm{mm}$.

Three problems are considered using formulation 1 (Section 3.5.2). First, the material volume minimization with strength constraints is solved. This problem is stated as

$$\min_{\mathbf{x}\in\Omega_1} V(\mathbf{x}) \tag{P_V}$$

The second problem includes chains and nodal variables and it is formulated as

$$\min_{\mathbf{x}\in\Omega_1\cap\Omega_C\cap\Omega_N} V(\mathbf{x}) \tag{P_{VN}}$$

Finally, the loading condition for kinematic stability is introduced, which leads to the following problem:

$$\min_{\mathbf{x}\in\Omega_1\cap\Omega_C\cap\Omega_N\cap\Omega_{ST}} V(\mathbf{x}) \tag{P_{VS}}$$

As no information about the shape of the cross-sections is given, buckling constraints are not considered.

Rasmussen & Stolpe (2008) solved problem P_V and obtained the minimum material volume $V^* = 0.0466\,\mathrm{m}^3 = 46.6\cdot10^6\,\mathrm{mm}^3$. The optimum topology is shown in Fig. 5.10. The resulting structure is clearly kinematically unstable.

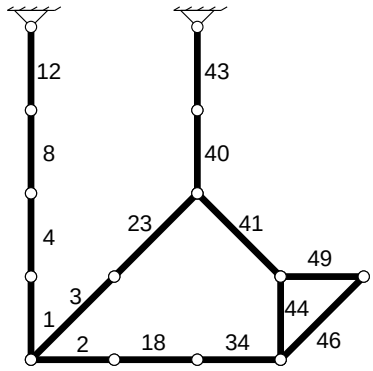

Figure 5.10: The optimum topology for the stress-constrained minimum weight problem with aluminium members obtained by Rasmussen & Stolpe (2008). The minimum material volume is $V^* = 0.0466\,\mathrm{m}^3 = 46.6\cdot10^6\,\mathrm{mm}^3$. Members 40 and 43 have the cross-sectional area $10000\,\mathrm{mm}^2$, whereas the area of all other members is $5000\,\mathrm{mm}^2$. The structure is kinematically unstable.

Problem P_V was solved by Gurobi 5.0 on a computer with Intel Core 2 Quad (four threads) Q9400 processor, running at 2.66 GHz clock frequency with 3.25 GB RAM. Rasmussen & Stolpe (2008) reported a total solution time of 508 seconds on a single thread. The speed up with 4 threads is 3.94, which means that for four threads, the solution was found in 129 s. Gurobi finds the optimum in 17.42 s, about 7.5 times faster

than Rasmussen & Stolpe (2008). Comparing a commercial state-of-the-art software with a research code is not straightforward. Nevertheless, it can be concluded that contemporary desktop computers are capable of solving truss topology optimization by mixed variable formulations using modern software much faster than what has been reported in the recent literature. This gives hope that the mixed variable approach need not be limited to small-scale ground structures with few profile alternatives.

In order to obtain a kinematically stable solution, nodal variables and chains were added to the problem. Consequently, the number of continuous and binary variables increased by 93% and 119%, respectively, and the number of inequality constraints increased by 237%. However, the optimum is now found in only 10.41 s. Thus, the larger problem was solved about 1.67 faster than the smaller one. The minimum material volume is $V^* = 54.142 \cdot 10^6\,\mathrm{mm}^2$, which is 16.2% greater than for problem P_V, where the necessary condition for kinematic stability was not included. The optimum topology is shown in Fig. 5.11a. Even though a constraint enforcing the necessary condition for kinematic stability was included in the problem, the obtained topology is unstable. The part of the truss defined by members 60, 62, and 90 cannot support a horizontal load, and the rest of the structure does not provide this support either. This demonstrates that the additional loading condition with small auxiliary loads at the nodes is required to guarantee kinematic stability.

When constraints Ω_{ST} were added to the problem for kinematic stability, the optimum solution was found in 29.25 s. The minimum material volume is $V^* = 57.25 \cdot 10^6\,\mathrm{mm}^3$. The optimum topology is depicted in Fig. 5.11b. The same solution was obtained by Rasmussen & Stolpe (2008), who included in the problem a loading condition where a small horizontal load is applied to the node 20. This is the node that is also loaded in the original setting. In the present instance, this approach is sufficient for kinematic stability. However, the solution time reported by Rasmussen & Stolpe (2008) is 85667 s (with 8 threads), which is several orders of magnitude greater than the solution time for problem P_{VS}.

The optimum member areas and strength utilization ratios are given in Table 5.10, where N_C and N_B are the number of continuous and binary variables, respectively. The problem sizes and solution times of the three problem instances are summarized in Table 5.9.

Table 5.9: Problem sizes and solution times for the L-shaped truss with aluminium members. N_C = number of continuous variables, N_B = number of binary variables, T = solution time, Nodes = number of explored nodes of the search tree, V^* = minimum material volume.

Problem	N_C	N_B	$\leq$	$=$	T [s]	Nodes	V^* [$10^6\mathrm{mm}^3$]
P_V	144	108	486	36	17.42	121172	46.6421
P_{VN}	252	237	1638	36	10.41	5257	54.1421
P_{VS}	360	237	1854	72	29.25	19430	57.2487

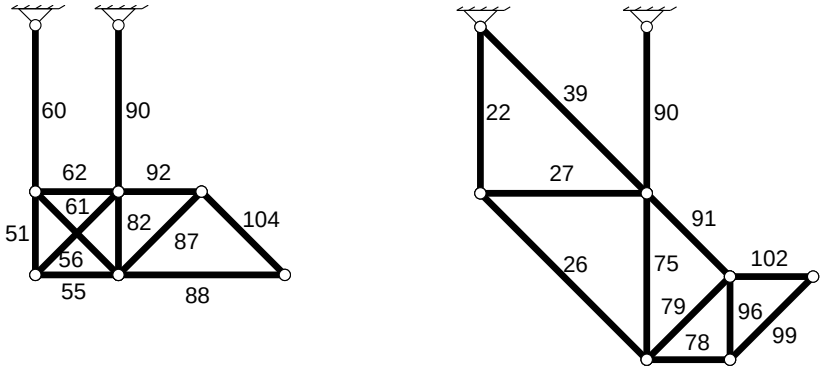

(a) **(b)**

Figure 5.11: Minimum weight topology of the L-shaped ground structure: (a) without stabilizing loads; (b) with stabilizing loads.

Table 5.10: Optimum solution of the L-shaped ground structure with aluminium members.

No stabilizing loads			With stabilizing loads		
$V^* = 54.14 \cdot 10^6$ mm^3			$V^* = 57.25 \cdot 10^6$ mm^3		
Member	A [mm^2]	Stress [%]	Member	A [mm^2]	Stress [%]
51, 55	5000	58.82	22, 27	5000	52.94
56	5000	83.19	26, 91, 99	5000	74.87
60, 92	10000	52.94	39, 79	5000	0.0
61	5000	66.55	75, 78	5000	52.94
62	5000	47.06	90	10000	52.94
82	5000	100.00	96, 102	5000	52.94
87, 104	5000	74.87			
88	5000	52.94			
90	10000	79.41			

5.3.2 Steel Members

In order to study the L-shaped ground structure under buckling constraints and with more profile alternatives, the material is altered to steel and profiles from a Finnish steel manufacturer (Ruukki 2011) are used (Table 5.11). To make buckling constraints relevant, the dimensions of the ground structure are doubled, that is $L = 4000\,\text{mm}$ and $h = 2000\,\text{mm}$. The load $F = 200\,\text{kN}$. The Young's modulus, density and yield strength for steel are $E = 210\,\text{GPa}$, $\rho = 7850\,\text{kg/m}^3$, and $f_\text{y} = 420\,\text{MPa}$, respectively. The bounds on the nodal displacements are set to $\overline{u} = -\underline{u} = 50\,\text{mm}$.

Table 5.11: Selection of profiles for the L-shaped ground structure with steel members.

Profile	H [mm]	t [mm]	A [10^2mm^2]	I [10^4mm^4]
1	40	4.0	5.35	11.07
2	50	2.0	3.74	14.15
3	50	3.0	5.41	19.47
4	50	4.0	6.95	23.74
5	50	5.0	8.36	27.04
6	60	2.0	4.54	25.14
7	60	3.0	6.61	35.13
8	60	4.0	8.55	43.55
9	60	5.0	10.36	50.49
10	70	3.0	7.81	57.53
11	70	4.0	10.15	72.12
12	70	5.0	12.36	84.63
13	80	3.0	9.01	87.84
14	80	4.0	11.75	111.04
15	80	5.0	14.36	131.44
16	80	6.0	16.83	149.18
17	90	3.0	10.21	127.28
18	90	4.0	13.35	161.92
19	90	5.0	16.36	192.93

As it has become clear from the previous problems, both nodal variables and the stabilizing loading condition are required to guarantee a kinematically stable optimum structure. Therefore, for the present case, these features are included in all problem formulations. In order to further study the influence of the buckling constraints, the minimum weight problem is solved both with Euler and Eurocode 3 buckling constraints. The two problems are stated as

$$\min_{\mathbf{x}\in\Omega_{EU}} W(\mathbf{x}) \qquad (P_{WEU})$$

where

$$\Omega_{EU} = \Omega_1 \cap \Omega_C \cap \Omega_N \cap \Omega_{ST} \cap \Omega_B^{EU} \qquad (5.7)$$

for Euler buckling constraints, and

$$\min_{\mathbf{x}\in\Omega_{EC}} W(\mathbf{x}) \qquad (P_{WEC})$$

Table 5.12: Problem sizes for the L-shaped truss with steel members. N_C = number of continuous variables, N_B = number of binary variables.

Formulation	Profiles	N_C	N_B	$\leq$	$=$
1	17	1980	1857	8334	72
1	19	2196	2073	9198	72
2	17	3921	21	8226	180
2	19	4356	21	9090	180
3	17	1980	1965	8718	180
3	19	2196	2181	9582	180

where

$$\Omega_{EC} = \Omega_1 \cap \Omega_C \cap \Omega_N \cap \Omega_{ST} \cap \Omega_B^{EC} \tag{5.8}$$

for Eurocode 3 buckling constraints.

Both problems P_{WEU} and P_{WEC} are solved with all three formulations presented in Section 3.5. Recall that the the three formulations differ in the binary variables used for profile selection. In formulation 1, the binary variables are related only to the selection of member profiles, and a unique profile is enforced by the inequality Eq. (3.7). In formulation 2, the variables y_{i0} are incorporated and the inequality Eq. (3.7) is replaced by the equality constraint Eq. (3.8). This approach allows to treat the profile selection constraint as a *type I Special Ordered Set (SOS)* (Beale & Tomlin 1970, Beale & Forrest 1976) and special branching rules can be applied. Furthermore, the profile selection variables need not be declared as binary variables, which reduces the number of integer variables in the problem considerably. Finally, formulation 3 includes the binary variables y_i for explicitly stating the existence of a member. In this formulation, Eq. (3.7) controls the unique selection of the profile, and the equality constraint Eq. (3.12) relates the member variables to the profile variables.

The problem sizes of the formulations differ from each other. However, by the nature of MILP problems, it is not clear, which formulation proves to be the easiest to solve. Therefore, the L-shaped truss is solved with each of the three formulations. Furthermore, to study the sensitivity of the solution algorithm to the number of available profiles, two separate cases are considered. In the first case, profiles 2 and 6 are removed from the list in Table 5.11. These profiles are chosen, since they have a wall thickness of 2.0 mm, which does not comply with the Eurocode 3 design rules for welded joints, requiring a minimum wall thickness of 2.5 mm (EN 1993–1–8 2005, Clause 7.1.1(5)). Consequently, 17 profiles are available in the first case, and 19 in the second case. The problem sizes are given in Table 5.12.

All instances were solved by Gurobi 5.0 on a computer with Intel Core i7-3770 processor (8 threads), running at 3.40 GHz clock frequency with 32.0 GB RAM. After some initial difficulties with the numerical solution, the feasibility tolerance was set to $1 \cdot 10^{-9}$ and the termination tolerance to $1 \cdot 10^{-3}$.

Consider first the case of 17 profile alternatives. The data of the solution process is shown in Table 5.13. Again, the objective function values of the first relaxation and the obtained minimum weight are given. The initial optimality gap, the elapsed time

Table 5.13: Results of the computations for the L-shaped truss with steel members and 17 profile alternatives. The columns are: f_R = weight of the first relaxation, Gap = the initial optimality gap, T_g = the elapsed time, when the global optimum was found, T = the elapsed time at termination, Nodes = explored nodes of the search tree, f^* = the minimum weight, Gap_F = the gap between the lower and upper bounds at termination.

Problem	f_R [kg]	f^* [kg]	Gap [%]	T_g [s]	T [s]	Nodes	Gap_F [%]
Formulation 1							
P_{WEU}	86.4986	108.9215	20.6	10	233.13	138895	0.10
P_{WEC}	94.2706	120.7334	21.9	52	1328	750096	4.10
Formulation 2							
P_{WEU}	83.6111	108.9215	30.3	41	97.42	9487	0.0
P_{WEC}	92.5686	120.7334	23.3	124	139.73	36023	0.09
Formulation 3							
P_{WEU}	86.4986	108.9215	20.6	11	55.94	4568	0.0
P_{WEC}	94.2707	120.7334	28.1	64	77.03	13348	0.04

to global optimum, the total running time, the number of nodes and the final gap between the lower and upper bounds are also reported.

For all problem formulations, the time limit for the algorithm was set to 2 hours, which equals 7200 s. Also, a limit on the number of nodes in the search tree was set to 750000. From Table 5.13, it can be seen that formulation 3 clearly outperforms the other two formulations. In most cases, the global optimum is found quickly, and most of the running time is spent on verifying the optimality, i.e. in increasing the lower bound. Formulation 1 is unable to verify the optimality for problem P_{WEC} within the node limit. At termination, the gap between the lower and upper bounds is 4.10%.

The optimum topologies of problems P_{WEU} and P_{WEC} are shown in Fig. 5.12a and Fig. 5.12b, respectively. In the figures, the line width of the members indicates the size of the cross-section. The optimum cross-sections and the utilization ratios are given in Table 5.14. The optimum topologies are nearly identical for the two buckling constraint types. For Eurocode 3 buckling constraints, member 82 is added to reduce the buckling length of the compression member 57 in Fig. 5.12a. Consequently member 57 is replaced by shorter members 55 and 86, for which a very efficient profile with buckling constraint utilization ratio 93.88% is found. Modifying the design from Euler buckling to Eurocode 3 buckling constraints increases the minimum weight from 108.92 kg to 120.73 kg, i.e by 10.8%.

When the problems with 19 profile alternatives were solved, the differences between the three formulations became very clear, as can be seen in Table 5.15. Formulation 1 failed to find the optimum solution within the node limit and terminated with 7.57% and 11.4% gaps. Formulation 2 found the optimum solution in both cases, but could not verify the optimality of the solution in problem P_{WEC} before the node limit was reached. At termination, the gap was 4.53%. Formulation 3 was able to find the optimum solutions of both problems. Also for this formulation, the computational effort required to verify optimality was much greater than in the case of 17 profile

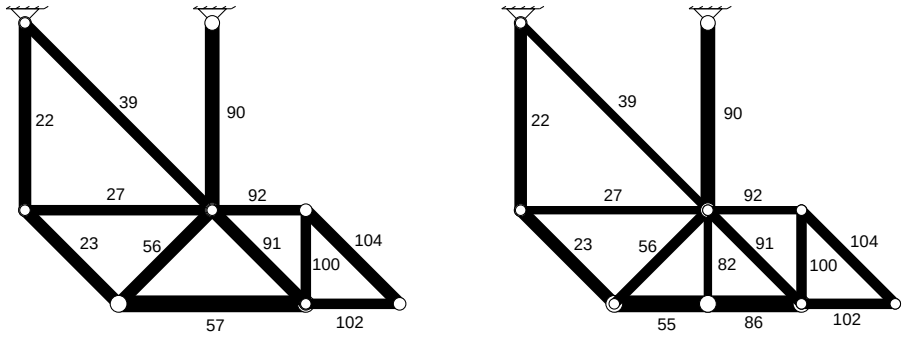

(a) **(b)**

Figure 5.12: Minimum weight topology of the L-shaped ground structure with 17 available steel profiles: (a) with Euler buckling; (b) with Eurocode 3 buckling.

Table 5.14: Optimum design of the L-shaped truss with 17 steel profile alternatives.

Member	A [mm^2]	Strength [%]	Euler [%]	Eurocode [%]
Euler buckling, $W^* = 108.9215$ kg.				
22	781	60.97	67.09	119.07
23	781	86.23	47.44	123.41
27, 92	535	89.01	–	–
39	535	0	–	–
56, 91, 104	695	96.90	–	–
57	1021	93.28	60.45	141.73
90	1015	93.83	–	–
100, 102	535	89.01	87.17	163.02
Eurocode buckling, $W^* = 120.7334$ kg.				
22	901	52.85	43.94	89.19
23	901	74.74	31.07	98.53
27, 92	535	89.01	–	–
39, 82	535	0	–	–
55, 86	1175	81.05	17.38	93.88
56, 91, 104	695	96.90	–	–
90	1015	93.83	–	–
100, 102	661	72.04	27.47	92.96

Table 5.15: Results of the computations for the L-shaped truss with steel members and 19 profile alternatives. The columns are: f_R = weight of the first relaxation, f^* = the minimum weight, Gap = the initial optimality gap, T_g = the elapsed time, when the global optimum was found, T = the elapsed time at termination, Nodes = explored nodes of the search tree, Gap_F = the gap between the lower and upper bounds at termination.

Problem	f_R [kg]	f^* [kg]	Gap [%]	T_g [s]	T [s]	Nodes	Gap_F [%]
Formulation 1							
P_{WEU}	80.4805	102.8258	21.7	–	1599.79	750057	7.57
P_{WEC}	88.1858	116.9331	23.2	–	1626.33	750051	11.4
Formulation 2							
P_{WEU}	79.3080	101.8995	22.2	218	1239.05	316270	0.09
P_{WEC}	87.4642	113.9675	23.3	83	2263.14	750083	4.53
Formulation 3							
P_{WEU}	80.4805	101.8995	21.0	108	391.23	116436	0.09
P_{WEC}	88.1994	113.9675	22.6	331	1843.78	674398	0.1

alternatives. This indicates that the solution method can be very sensitive to the number of profile alternatives.

The initial optimality gap in all cases was around 22%. The most time-consuming task of the algorithm is to reduce this gap, i.e. to increase the lower bound close to the upper bound. For example, it took the algorithm 331 seconds to find the optimum solution, and another 1512 seconds to verify optimality. By the time of finding the optimum, the gap between the lower and upper bounds was 6.07%.

The optimum topologies of the problems P_{WEU} and P_{WEC} are shown in Fig. 5.13, and the optimum profiles and utilizations are given in Table 5.16. The optimum topologies differ from each other clearly, and they also differ substantially from the optimum topologies of the previous case, where 17 profiles were available (see Fig. 5.12a). The optimum topology for Eurocode buckling is more economical from the manufacturing perspective, since it contains fewer members and nodes. In both cases, the utilization is high, which indicates that the profiles were selected economically, from the point of view of the weight.

5.4 Discussion

The benchmark problems solved in this chapter lead to the following observations.

Formulations The problems verify that the mixed variable formulations produce reasonable solutions. The cantilever truss shows that chains and nodal variables are essential in order to remove unstable nodes and to guarantee kinematic stability. They are also needed for buckling constraints. On the other hand, the L-shaped truss demonstrates that the constraint of the necessary condition for kinematic stability does not suffice, and the auxiliary loading condition is required.

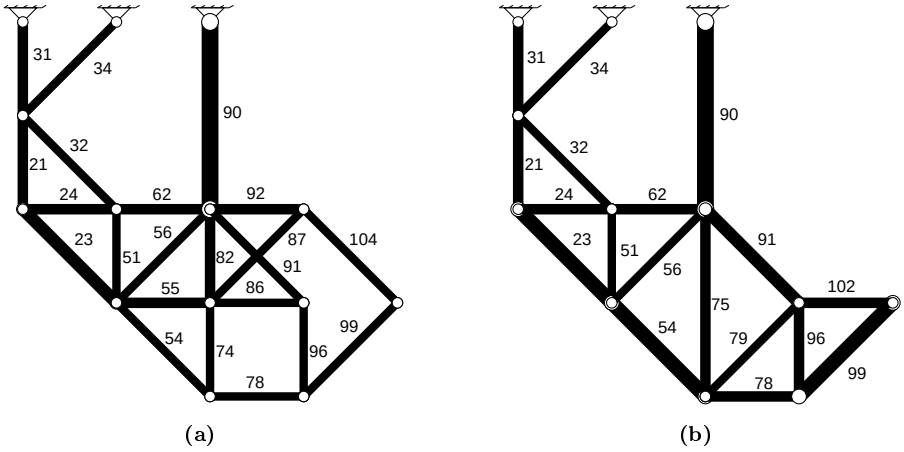

Figure 5.13: Minimum weight topology of the L-shaped ground structure with 19 available steel profiles: (a) with Euler buckling; (b) with Eurocode 3 buckling.

Table 5.16: Optimum design of the L-shaped truss with 19 steel profile alternatives.

Member	A [mm^2]	Strength [%]	Euler [%]	Eurocode [%]
Euler buckling, $W^* = 101.8995$ kg.				
21, 31, 55	535	89.01	87.17	163.02
23	781	86.23	47.44	123.41
24, 62, 82, 92	535	89.01	–	–
32, 34, 51	374	0	–	–
54, 87, 99	374	90.03	96.44	173.17
56, 91, 104	374	90.03	–	–
74, 96	374	63.66	–	–
78, 86	374	63.66	34.10	90.32
90	1015	93.83	–	–
Eurocode buckling, $W^* = 113.9676$ kg.				
21, 31, 78	661	72.04	27.47	92.96
23, 54, 99	901	74.74	31.07	98.53
24, 62, 75, 92, 102	535	89.01	–	–
32, 34, 51, 56, 79	374	0	–	–
90	1015	93.83	–	–
91	695	96.90	–	–

The jump in the buckling length issue is resolved by chains. The constraints related to chains lead to applicable solutions, and it can be concluded, that they control the behaviour of the chain members correctly.

Both the cantilever truss and the L-shaped truss showed that the optimum topology depends on the buckling constraints used. If the structure was optimized for Euler buckling, the solution was shown to be unsafe with respect to the buckling rule of Eurocode 3.

The L-shaped truss with steel members also displayed that the optimum topology depends on the selection of profile alternatives. Adding only two profiles to the set of alternatives changed the optimum topology completely.

From the most difficult problem solved (the L-shape with 17 and 19 profile alternatives), it can be seen that, of the three formulations presented in Section 3.5, formulation 3 was clearly the most efficient. An evident reason for this is not easy to find. It might be that branching with respect to the member variables tighten the feasible set of the child nodes quickly. For example, setting $y_i = 0$ forces $y_{ij} = 0$ for all $j \in \mathcal{N}$.

As formulation 3 outperforms the other formulations, it is chosen as the main formulation for the remainder of the thesis. However, it is not clear that this formulation is truly better than the others. Since the problems are solved with a commercial software with limited access to the details of the branch-and-cut algorithm, it is difficult to say, whether the properties of the formulations are fully exploited or not. For instance, it is unclear how Gurobi handles SOS branching.

Computational experience Generally, the benchmark problems indicate that modern algorithms and computers are able to solve moderate-sized truss topology optimization problems formulated as mixed variable problems. On the other hand, the L-shaped truss shows that the computation time can be sensitive to the problem size. Increasing the number of profile alternatives from 17 to 19 led to considerable increase in the computation time, even for the best formulation. When Euler buckling was used, this increase was of a factor of 7.0 and when Eurocode 3 buckling was considered, the factor was 24.

The L-shaped truss with 19 steel profile alternatives is a clear indication that the problem size is still limited. As the problem size depends strongly on both the number of members and the number of profiles, it is difficult to pin-point the limits. Furthermore, as the computing capacity increases constantly, the problem size limit is constantly pushed forward.

Most of the computing time is spent on increasing the lower bound. Gurobi finds feasible solutions without problems and often the optimum solution is found rather quickly. The initial gap between the lower bound and the optimum is about 20% for the L-shaped truss with steel members. In order to hasten the computations, a special-purpose modification of the branch-and-cut algorithm should be developed, with emphasis on the selection of cutting planes and branching strategies. Such further studies might prove to be necesessary in order to apply the mixed variable formulations to more complex situations.

CHAPTER 6

Multicriterion Formulations

A mind is like a parachute.
It doesn't work if it is not open.
FRANK ZAPPA

6.1 Introduction

So far, the optimization problems solved have contained a single objective (weight), and a single optimum design, where this objective function is minimized, is obtained as a solution. In many engineering design tasks, it is common that several conflicting and noncommensurable criteria should be minimized or maximized in order to achieve the most suitable design. The theory of *multicriterion (or multiobjective) optimization* provides the necessary tools for treating such design situations. In this chapter, multicriterion truss topology optimization problems are formulated and their properties are studied.

The standard form for multicriterion problems is

$$\min_{\mathbf{x}\in\Omega} \mathbf{f}(\mathbf{x}) = \{f_1(\mathbf{x}) \;\; f_2(\mathbf{x}) \;\ldots\; f_k(\mathbf{x})\} \qquad (P_{MO})$$

The objective function $\mathbf{f}$ is now vector-valued, with k component functions, f_i, that are called the *criteria*. The feasible set $\Omega \subseteq \mathbb{R}^n$ is as in Eq. (3.3). The space $\mathbb{R}^n$ is called the *design space* and the space $\mathbb{R}^k$ is called the *criterion space*. The image of the feasible set in the criterion space is called the *attainable set* and it is defined by

$$\Lambda = \{\mathbf{z} \in \mathbb{R}^k \mid \mathbf{z} = \mathbf{f}(\mathbf{x}),\, \mathbf{x} \in \Omega\} \qquad (6.1)$$

As there are now several functions to be optimized, the concept of optimality has to be extended from the conventional ordering of real numbers. The most fruitful approach has been proposed by Pareto (1896), stating that a design is optimal, if none of the criteria can be improved without deteriorating at least one other criterion. Formally, this can be stated as follows:

Definition 1 (Pareto optimality)**.** Consider problem P_{MO}. A design $\mathbf{x}^* \in \Omega$ is *Pareto optimal*, if there does not exist another point $\hat{\mathbf{x}} \in \Omega$ such that $f_i(\hat{\mathbf{x}}) \leq f_i(\mathbf{x}^*)$ for all $i = 1, 2, \ldots, k$ and $f_j(\hat{\mathbf{x}}) < f_j(\mathbf{x}^*)$ for at least one $j = 1, 2, \ldots, k$.

Often in the literature, both the optimal solutions in the design space and the corresponding points in the criterion space are called Pareto optimal. However, as these two spaces have completely different dimensions and units, it is advisable the make the distinction in terminology on whether a reference is made to optimal solutions in the design space or in the criterion space. The point $\mathbf{z}^* = \mathbf{f}(\mathbf{x}^*)$ of the criterion space corresponding to the Pareto optimal solution $\mathbf{x}^*$ is called a *minimal point*. The set of minimal points is sometimes called the *Pareto front*.

Some solution methods, while searching for Pareto optimal solutions, end up in points, where not all criteria cannot be improved simultaneously. These points are called *weakly Pareto optimal*, and they are formally defined as follows:

Definition 2 (Weak Pareto optimality)**.** A design $\mathbf{x}^* \in \Omega$ is *weakly Pareto optimal* for problem P_{MO}, if there does not exist another point $\hat{\mathbf{x}} \in \Omega$ such that $f_i(\hat{\mathbf{x}}) < f_i(\mathbf{x}^*)$ for all $i = 1, 2, \ldots, k$.

It is clear that every Pareto optimum is also a weak Pareto optimum, but the converse is not true. Usually the designer is not interested in those weak Pareto optima that are not Pareto optimal. In this thesis, such points are called *strictly weak Pareto optima*.

The above definitions are illustrated in Fig. 6.1, where the attainable set of a bicriterion discrete problem is depicted. The attainable set consists of separate points. The black dots are the minimal points, whereas the white dots are dominated. Points B and D are strictly weak minima, being dominated by A and C, respectively.

In this thesis, the aim is to find economical designs. To achieve this, the criteria presented in Section 3.4 are employed in formulating multicriterion problems. Firstly, a four-critera problem is proposed, where the weight is minimized simultaneously with the number of members, nodes and profiles. These cost factors have been identified by Sarma & Adeli (2000*b*) and they can be conveniently expressed without any cost data. The Pareto optimal solutions of this problem can be assessed for their economy and the most favourable design can be chosen for further considerations.

On the other hand, the cost of the truss can be minimized directly, if an appropriate cost function is available and if the parameters related to the details of the manufacturing process can be determined reliably. In this case, minimizing the cost simulatenously with weight as a bicriterion optimization problem offers quantitative information about the conflict of cost and mass. In this thesis, the cost function adopted from (Haapio 2012) as presented in Section 3.4 is employed for cost optimization.

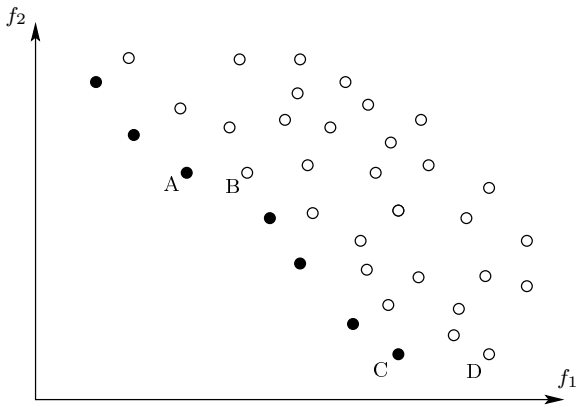

Figure 6.1: Attainable set of a bicriterion discrete problem. Minimal points are denoted by dots. White dots are dominated. Points B and D are strictly weak minima.

6.2 Problem Statements

The first approach for finding economical solutions is to minimize the weight, the number connections, members and profiles simultaneously. The rationale is that, as these four quantities affect the fabrication costs, economical designs can be found among the Pareto optima of the problem. The four-criteria problem is stated as

$$\min_{\mathbf{x}\in\Omega} \mathbf{f}(\mathbf{x}) = \{W(\mathbf{x}) \;\; N_y(\mathbf{x}) \;\; N_c(\mathbf{x}) \;\; N_p(\mathbf{x})\} \tag{P_{W3}}$$

Recall the expressions of the weight, the number of members and the number of nodes from Chapter 3:

$$W(\mathbf{x}) = \sum_{i=1}^{n_E}\sum_{j=1}^{n_S} \rho_i L_i \hat{A}_j y_{ij} \tag{6.2}$$

$$N_y(\mathbf{x}) = \sum_{i=1}^{n_E} y_i = \sum_{i=1}^{n_E}\sum_{j=1}^{n_S} y_{ij} \tag{6.3}$$

$$N_c(\mathbf{x}) = \sum_{i=1}^{n_N} z_i \tag{6.4}$$

The number of profiles, N_p, is expressed in the auxiliary binary variables α_j as

$$N_p = \sum_{j=1}^{n_S} \alpha_j \tag{6.5}$$

with the constraints in Eq. (3.90) relating α_j with y_{ij}.

The second problem considered is a bicriterion case, where the cost and weight are minimized simultaneously:

$$\min_{\mathbf{x}\in\Omega} \mathbf{f}(\mathbf{x}) = \{C(\mathbf{x}) \;\; W(\mathbf{x})\} \tag{P_{CW}}$$

This problem is discussed in Chapter 7 in conjuction with the design of a roof truss.

6.3 Conflict of Criteria

In multicriterion problems, the conflicting nature of the criteria is essential. In formulating a multicriterion problem, only conflicting quantities should be treated as separate criteria. If pair of quantities turn out to be not in conflict with each other, a single design optimizes both of them. From the computational point of view, the number of criteria should be kept as small as possible.

Koski (1994) has discussed the nature of conflict among criteria. He makes the distinction between *local* and *global* conflict. The local conflict is determined by the gradients of the criteria. Two criteria f_i and f_j have no conflict at a point $\mathbf{x}$, if there exists $c > 0$ such that $\nabla f_i(\mathbf{x}) = c\nabla f_j(\mathbf{x})$. Otherwise, the criteria are locally conflicting at $\mathbf{x}$. This means that the criteria are not locally conflicting, if their maximum improvements are achieved in the same direction.

For the global conflict, the constraints of the problem play a role. Koski (1994) proposes a definition, where two criteria are said to be globally conflicting in the feasible set, if they are minimized by different designs. This definition does not include the case, where the minimizer of a criterion is not unique. Thus, the definition of global conflict is generalized here as follows:

Definition 3. Two criteria f_i and f_j are *globally conflicting* in the feasible set Ω, if there does not exist a point $\mathbf{x}^* \in \Omega$ such that $f_i(\mathbf{x}^*) = \min_{\mathbf{x}\in\Omega} f_i(\mathbf{x})$ and $f_j(\mathbf{x}^*) = \min_{\mathbf{x}\in\Omega} f_j(\mathbf{x})$. Otherwise the criteria are called *globally conforming*.

By this definition, two globally conforming criteria can have several different minimizers, as long as there exist a common minimizer as well.

From the expressions of the criteria chosen above, it can be clearly seen that the criteria are locally conflicting everywhere as none of the pairs of gradients of the criteria are parallel. This is immediately apparent, if the formulation 3 (with member variables) is used, since then all the criteria depend on different variables, resulting in orthogonal gradients.

The global conflict of the criteria is not apparent from the problem formulation, but it can be conveniently explored by the principles of mechanics.

The weight of the structure can be lowered by reducing the size of the member profiles, the length and the number of members. As smaller members are able to carry less load, the normal forces should also be kept relatively small. This can be achieved by adding more members to the truss. For buckling constraints, smaller profiles can be chosen for the truss, if the members in compression are kept short. Thus, it can be concluded that weight and the number of members can be globally conflicting. On the other hand, it is also possible that the minimum weight design is obtained by the minimum number of members.

Similar reasoning holds for the global conflict of the weight and the number of nodes. In general, fewer nodes imply fewer and longer members, which leads to larger profiles,

especially for long members in compression. Thus, the weight and the number of nodes are globally conflicting in general, but there can also be cases, where the minimum weight design is obtained by the minimum number of nodes.

The number of profiles can be expected to be globally conflicting with the weight in most cases, which can be explained as follows. The number of profiles is minimized by selecting a single profile for all truss members. The choice of this profile is determined by the member under the most severe loading. As not all members are likely to be equally loaded, selecting the same profile for all members is likely to result in an unnecessarily heavy structure.

On the other hand, the number of profiles is not globally conflicting with the number of members and nodes, provided that appropriate profiles are available. For any number of members and nodes, the number of profiles can be set to 1 by choosing the profile of the most severely loaded member to all members. If the topology is statically indeterminate, increasing the member areas might lead to increased normal forces in some members. However, if large enough profiles are available, it should be expected that the largest profile is feasible for any topology.

As the number of profiles is globally conforming with the number of members and nodes, the following simplifying modification is made to problem P_{W3}. The number of profiles is not considered as a separate criterion, but it is combined with the number of members and nodes. Thus the number of criteria is reduced to three, and the modified problem is

$$\begin{aligned} \min_{\mathbf{x}\in\Omega} \mathbf{f}(\mathbf{x}) &= \{W(\mathbf{x}) \;\; N_y(\mathbf{x}) + N_p(\mathbf{x}) \;\; N_c(\mathbf{x}) + N_p(\mathbf{x})\} \\ &= \{f_1(\mathbf{x}) \;\; f_2(\mathbf{x}) \;\; f_3(\mathbf{x})\} \end{aligned} \qquad (P_{W2})$$

An important feature of this problem is that all of its Pareto optimal solutions are also Pareto optimal for problem P_{W3}, which can be shown by the more general result:

Lemma 1. Consider problem P_{MO} and the modified problem

$$\begin{aligned} \min_{\mathbf{x}\in\Omega} \mathbf{f}'(\mathbf{x}) = \{f_1(\mathbf{x}) \;\; f_2(\mathbf{x}) + f_r(\mathbf{x}) \;\ldots\; f_{r-1}(\mathbf{x}) + f_r(\mathbf{x}) \\ f_{r+1}(\mathbf{x}) + f_r(\mathbf{x}) \;\ldots\; f_k(\mathbf{x}) + f_r(\mathbf{x})\} \end{aligned} \qquad (P'_{MO})$$

where criterion f_r is added to all criteria except f_1, and removed from the objective function. Then if $\mathbf{x}^*$ is a Pareto optimal solution of problem P'_{MO}, it is also Pareto optimal for problem P_{MO}.

Proof. Suppose $\mathbf{x}^*$ is not Pareto optimal for problem P_{MO}. Then there exists a point $\hat{\mathbf{x}} \in \Omega$, $\hat{\mathbf{x}} \neq \mathbf{x}^*$ such that $f_i(\hat{\mathbf{x}}) \leq f_i(\mathbf{x}^*)$ for all $i = 1, 2, \ldots, k$ and $f_j(\hat{\mathbf{x}}) < f_j(\mathbf{x}^*)$ for some j. Without loss of generality, suppose that $j = 1$. Then, for all $i \neq j$ the following is true:

$$\begin{aligned} & f_i(\hat{\mathbf{x}}) \leq f_i(\mathbf{x}^*) \\ \Rightarrow \quad & f_i(\hat{\mathbf{x}}) + f_r(\mathbf{x}^*) \leq f_i(\mathbf{x}^*) + f_r(\mathbf{x}^*) \end{aligned}$$

Since $f_r(\hat{\mathbf{x}}) \leq f_r(\mathbf{x}^*)$, it follows that

$$f_i(\hat{\mathbf{x}}) + f_r(\hat{\mathbf{x}}) \leq f_i(\mathbf{x}^*) + f_r(\mathbf{x}^*)$$

This, together with $f_1(\hat{\mathbf{x}}) < f_1(\mathbf{x}^*)$ contradicts the assumption that $\mathbf{x}^*$ is Pareto optimal for problem P'_{MO}. Thus, the assumption that $\mathbf{x}^*$ is not Pareto optimal for problem P_{MO} is false, and the proof is complete. □

Note that the converse of Lemma 1 is not true, that is, not all Pareto optimal solutions of problem P_{MO} are Pareto optimal for problem P'_{MO}.

Koski & Silvennoinen (1987) have presented a result similar to Lemma 1. However, in their work, the combining of the criteria is carried out differently than here.

In the following, the modified problem P_{W2} is considered instead of problem P_{W3}. By reducing the number of criteria to three, the computational complexity of the problem is considerably reduced as well. Note that the number of profiles is still included in the criteria.

6.4 Generating Pareto Optimal Solutions

It follows from the definition of Pareto optimality that multicriterion problems have many optimal solutions. Continuous multicriterion problems have typically infinitely many Pareto optima, whereas the Pareto optimal set of a discrete problem consists of a finite number of solutions. Nevertheless, obtaining the entire Pareto optimal set of a discrete problem can be computationally prohibitive and instead, only a subset of Pareto optimal solutions can be generated within the available time limit.

Two philosophically different approaches are mainly used for solving multicriterion problems. In *interactive methods*, a human actor, called the *decision maker (DM)*, is involved. A single Pareto optimum is computed, and the DM either accepts the solution or guides the optimization process based on her preferences and using the information included in the solution at hand. Thus, an iterative loop is created, where new Pareto optima are generated, until the DM is satisfied with the results. An interactive approach might be preferable if an active DM is available, and if generating Pareto optima is computationally demanding. Interactive methods are discussed in detail in (Miettinen 1999). A survey of interactive methods for multicriterion MILP problems can be found in (Alves & Clímaco 2007).

The second approach for solving multicriterion problems is to automatically compute a representative subset of Pareto optimal points. Such methods are called in this thesis *generating methods*. The goal is to obtain a wide range of Pareto optima, and in the discrete case, possibly the entire Pareto optimal set. The classical approach is to scalarize the multicriterion problem by transforming the vector-valued objective function into a scalar-valued function which can be optimized by conventional solution algorithms. The scalarization is performed such that the solution of the scalarized problem is Pareto optimal. In most methods, the scalarization includes a set of parameters, which can be altered in order to obtain different Pareto optimal solutions. In a fully automated generating method, the varying of the scalarization parameters is done by some predefined rules. Generating methods can be computationally very expensive, since for each Pareto optimum, a single-criterion optimization problem must be solved. Thorough discussion on generating methods can be found in (Eschenauer,

Koski & Osyczka 1990) and in (Miettinen 1999), and a more recent review in (Marler & Arora 2004).

Recently, genetic algorithms and other population-based methods have become popular for generating Pareto optimal solutions (Osyczka 2002, Deb 2002). These methods seem to be well-suited for multicriterion problems, since they operate on a set of designs simultaneously, and they provide a set of solutions in a single run. On the other hand, population-based methods do not take full advantage of the mathematical structure of the optimization problem. Therefore, they are more appropriate for NAND formulations, where analytical expressions of the constraints and criteria are not available, and the number of variables and constraints is much smaller than in the SAND formulation that is employed in this thesis.

In this thesis, the aim is to generate all Pareto optimal solutions of the problems considered. For problem P_{W2}, this can be achieved by a procedure based on the *constraint method*. In the constraint method, the multicriterion problem is scalarized such that one criterion is minimized and the others are constrained by chosen parameters. In the general case of k criteria, the scalarized problem of the constraint method is

$$\begin{aligned} &\min_{\mathbf{x}\in\Omega} f_i(\mathbf{x}) \\ &\text{subject to } f_j(\mathbf{x}) \leq \epsilon_j \quad \forall\, j \neq i \end{aligned} \tag{P_{CM}}$$

A solution, $\mathbf{x}^*$, of problem P_{CM} is weakly Pareto optimal. It is also Pareto optimal, if it is the unique solution of problem P_{CM}, with $\epsilon_j = f_j(\mathbf{x}^*)$ for all $j \neq i$. Another condition for Pareto optimality is that $\mathbf{x}^*$ is a solution of problem P_{CM} for all $i = 1, 2, \ldots, k$, with $\epsilon_j = f_j(\mathbf{x}^*)$, for all $j \neq i$. (Miettinen 1999, pp. 85–86)

The proposed approach for generating the Pareto optimal solutions of problem P_{W2} is as follows. First, all three criteria are minimized separately. This yields the solutions $\mathbf{x}_i^*$, and $\mathbf{f}_i^* = \mathbf{f}(\mathbf{x}_i^*)$, $i = 1, 2, 3$. From these solutions, the lower and upper bounds are obtained for criteria f_2 and f_3 as $\underline{f}_j = f_j(\mathbf{x}_j^*)$, and $\overline{f}_j = \max_{i=1,2,3} \{f_{ij}^*\}$, $j = 2, 3$, where f_{ij}^* is the value of criterion j at the optimum of criterion i.

Next, the following problem is solved:

$$\begin{aligned} &\min_{\mathbf{x}\in\Omega} f_1(\mathbf{x}) \\ &\text{subject to } f_2(\mathbf{x}) = \underline{f}_2 + \epsilon_2 \\ &\qquad\qquad f_3(\mathbf{x}) = \underline{f}_3 + \epsilon_3 \end{aligned} \tag{6.6}$$

for every $\epsilon_j = 0, 1, \ldots, \overline{f}_j - \underline{f}_j$, $j = 2, 3$. Obviously, the solution of problem Eq. (6.6) is not necessarily Pareto optimal. However, every Pareto optimal solution $\hat{\mathbf{x}}$ with $f_j(\hat{\mathbf{x}}) \leq \overline{f}_j$, $j = 2, 3$, is the solution of Eq. (6.6) for $\epsilon_2 = f_2(\hat{\mathbf{x}}) - \underline{f}_2$ and $\epsilon_3 = f_3(\hat{\mathbf{x}}) - \underline{f}_3$. The proposed approach is not computationally appealing in general, but it is acceptable for the L-shaped truss considered in the following.

6.5 Multicriterion Optimization of L-Shaped Truss

The procedure described above is applied to find the Pareto optimal solutions of problem P_{W2} written for the L-shaped truss presented in Section 5.3. The ground structure

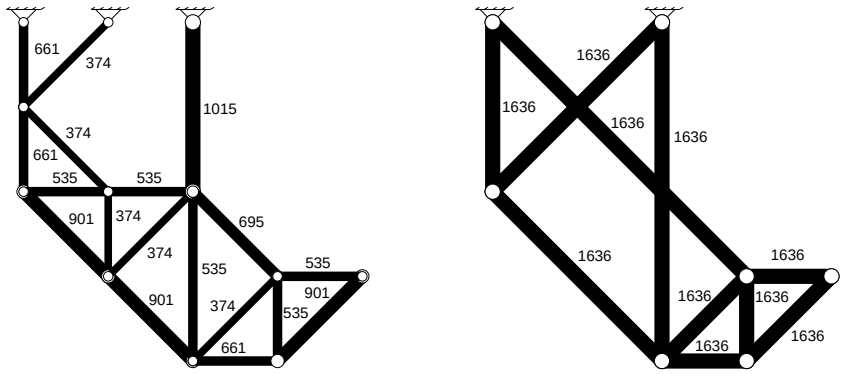

(a) $\mathbf{f}^1 = (113.968, 24, 18)$ **(b)** $\mathbf{f}^{13} = (279.043, 11, 8)$

Figure 6.2: Pareto optima minimizing (a) the weight; (b) criteria f_2 and f_3. The numbers by the members indicate the cross-sectional area. The values of the criteria are given in parenthesis.

is such that the sawing angles of the members cannot be determined *a priori*. Similarly, it is very difficult to determine, which members are to be welded. Therefore, direct cost optimization of the L-shaped truss is not treated.

The instance with steel members and 19 available profiles with Eurocode 3 buckling is considered. With the profile counting variables α_j, $j = 1, 2, \ldots, 19$, included, the problem has 4396 variables of which 2200 are binary. The number of inequality and equality constraints are 11653 and 180, respectively.

The minimum weight design and the design minimizing criteria f_2 and f_3 (see the formulation of problem P_{W2}) are shown in Fig. 6.2. A different solution was found in minimizing f_2, but this solution was dominated by the design shown in Fig. 6.2b, with both solutions having $f_2 = 11$. Thus, in this case, the number of members and nodes are globally conforming.

The minimal points corresponding to the Pareto optima are shown in Fig. 6.3, where the three-dimensional criterion space is projected to three two-dimensional spaces. The three projections reveal the conflicting nature of the criteria, and they provide an illustrative means to compare the solutions with one another.

First, it can be clearly seen that the design minimizing criteria f_2 and f_3 (number 13) is much heavier than the other Pareto optima. From this solution, the weight can be decreased by 62% by introducing a second profile. Thus, solution 13 is not a very favourable compromise.

A second observation from the graphical presentation of the minimal points is that there are no Pareto optimal solutions having either $f_2 \in \{21, 22, 23\}$ or $f_3 \in \{16, 17\}$. There is no evident reason for this that could be deduced from the ground structure or the selection of profiles. It is simply a result of the computations, that the solution 2 dominates the designs having the mentioned values for f_2 or f_3.

The Pareto optimal designs are shown in Fig. 6.4 and Fig. 6.5. From the figures, it can be seen that there are 7 Pareto optimal topologies.

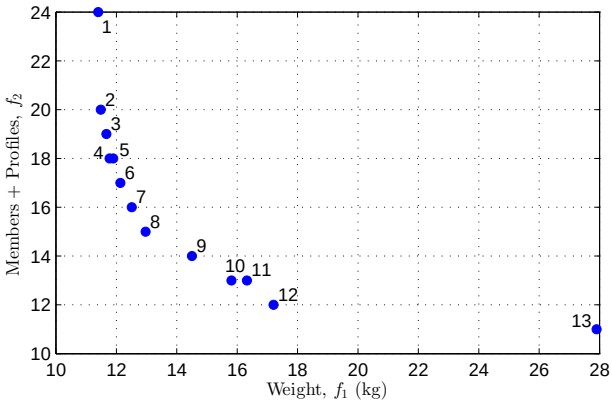

(a)

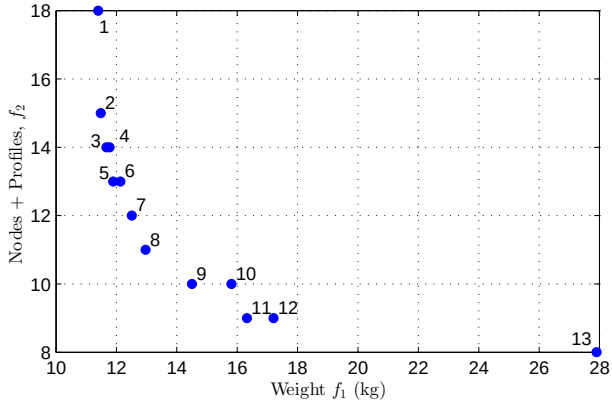

(b)

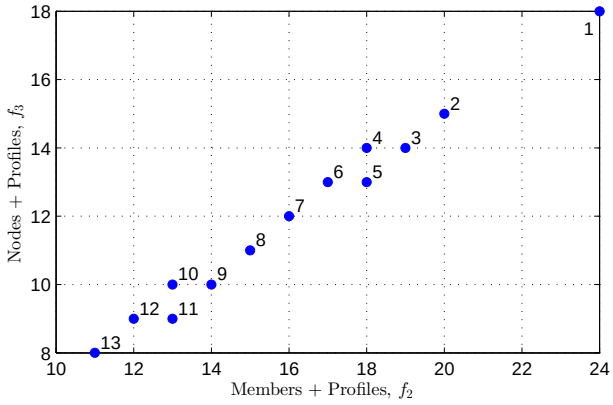

(c)

Figure 6.3: Minimal solutions of the L-shaped truss.

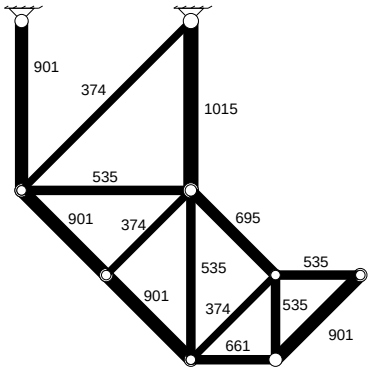

(a) Solution 2:
$\mathbf{f}^2 = (114.800, 20, 15)$

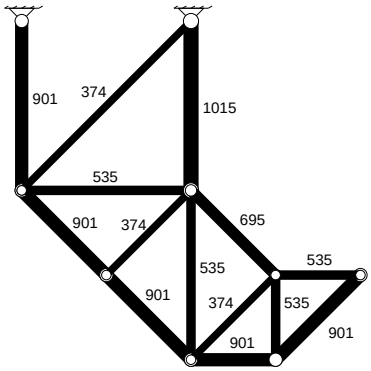

(b) Solution 3:
$\mathbf{f}^3 = (116.684, 19, 14)$

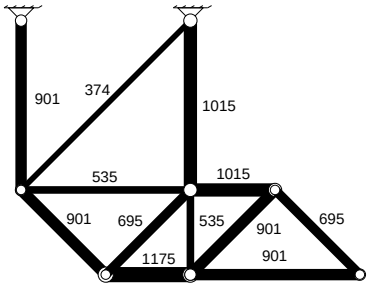

(c) Solution 4:
$\mathbf{f}^4 = (117.758, 18, 14)$

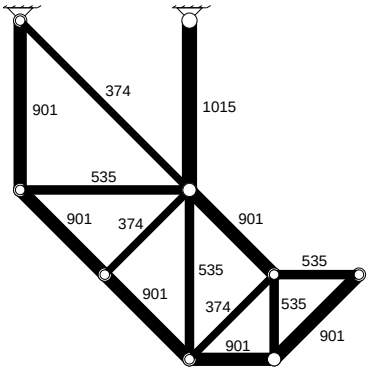

(d) Solution 5:
$\mathbf{f}^5 = (118.971, 18, 13)$

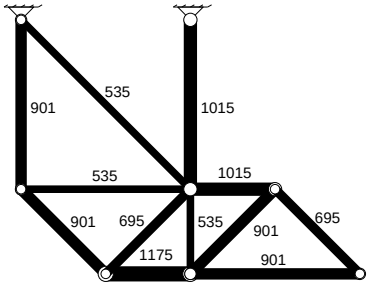

(e) Solution 6:
$\mathbf{f}^6 = (121.333, 17, 13)$

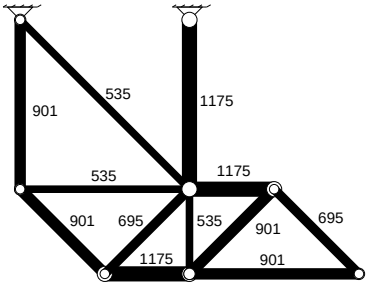

(f) Solution 7:
$\mathbf{f}^7 = (125.101, 16, 12)$

Figure 6.4: Pareto optimal designs of the L-shaped truss.

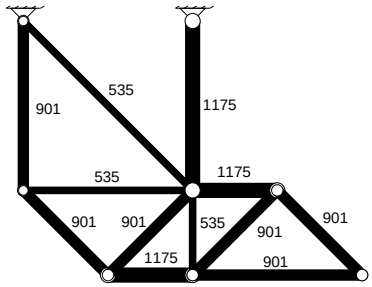

(a) Solution 8:
$\mathbf{f}^8 = (129.674, 15, 11)$

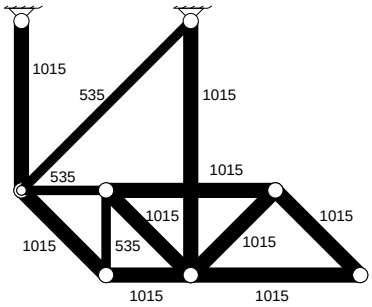

(b) Solution 9:
$\mathbf{f}^9 = (145.028, 14, 10)$

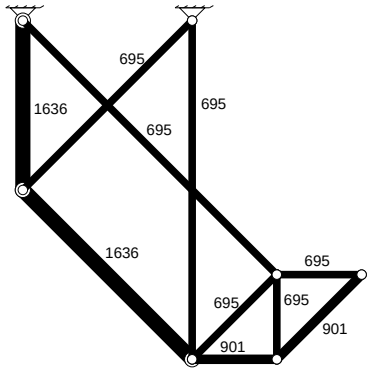

(c) Solution 10:
$\mathbf{f}^{10} = (158.113, 13, 10)$

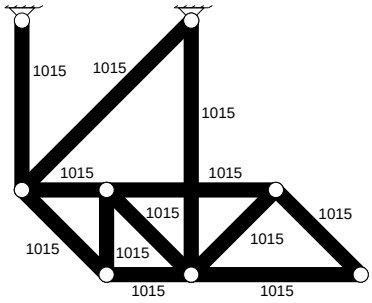

(d) Solution 11:
$\mathbf{f}^{11} = (163.222, 13, 9)$

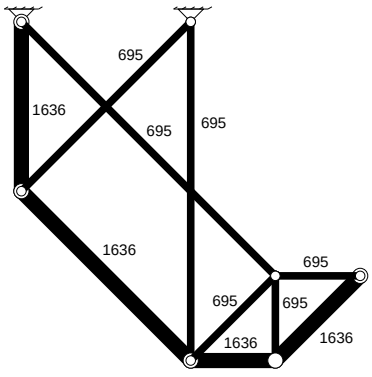

(e) Solution 12:
$\mathbf{f}^{12} = (172.042, 12, 9)$

Figure 6.5: Pareto optimal designs of the L-shaped truss.

As the standard problem in truss optimization is weight minimization, it is especially interesting to study how the weight varies among the Pareto optimal solutions. While Fig. 6.3 provides a graphical insight, it is also beneficial to have quantitative information about the solutions. First, the relative increase of weight from the minimum value is calculated as

$$r_i = \frac{f_1^i - f_1^*}{f_1^*} \cdot 100\% \tag{6.7}$$

The following values are obtained: $r_2 = 0.73\%$, $r_3 = 2.38\%$, $r_4 = 3.33\%$, $r_5 = 4.39\%$, $r_6 = 6.46\%$, $r_7 = 9.77\%$, $r_8 = 13.78\%$, $r_9 = 27.25\%$, $r_{10} = 38.74\%$, $r_{11} = 43.22\%$, $r_{12} = 50.96\%$, $r_{13} = 144.84\%$. The solutions 2 to 7 are within 10% of the minimum weight. The corresponding Pareto optimal trusses are depicted in Fig. 6.4. From the manufacturing point view, solution 2 seems especially appealing compared with the minimum weight design. This solution has 3 nodes and 4 members less than the minimum weight truss, but the difference in weight is only 0.73%. Solution 3 differs from the solution 2 in number of profiles, which is one less in solution 3. The increase in weight is 1.88 kg, which corresponds to 1.64%.

Moving from solution 3 to 4 and from 4 to 5 increases the weight by about 1.0% in both steps. The topology of solution 4 differs substantially from the topologies of 3 and 5, having two members and one node less, but more profiles. This topology appears also in solutions 6 and 7 with fewer profiles, but the difference in weight compared to solutions 1 and 2 is increased more clearly.

Having the Pareto optimal solutions at hand provides the designer more flexibility in finding a structure that is also favourable to the manufacturer. If only the minimum weight problem would have been solved, the designer would have only a single solution to proceed with. Instead, there are now 13 different designs that are proven compromise solutions with respect to the three criteria, and among these designs, very different topologies are represented. This is a great advantage of multicriterion optimization over the conventional single-criterion case.

6.6 Discussion

Many engineering design tasks are intrinsically multicriterion problems. Depending on the application, different design aspects are better suited as criteria than others. In this thesis, the main emphasis is on the economy of the solution. Two problem formulations aiming for economical designs were given. In both formulations, the weight of the truss was included as a criterion. Weight is an important quantity to minimize also for other reasons besides the economy of the structure. For example, assessing the environmental impact of the design, as performed according to the standard EN 15978 (2011), is strongly related to the amount of material used. In fact, if the truss is made of a single material, the environmental impact is proportional to the weight of the structure.

The greatest benefit of multicriterion optimization is arguably that the designer does not have to settle for one solution, but is provided with a set of compromise designs,

where the criteria are differently emphasized. By acknowledging the multicriterion nature of a design task, the competing criteria can be considered simultaneously without having to manipulate them in order to create a single-criterion problem.

Whenever a multicriterion problem is formulated, it is important to examine the conflict of the criteria before actually solving the problem. Criteria that are not severely in conflict can be combined to reduce the computational effort. This was done in the present study to transform four criteria into three.

As the main emphasis of this thesis is on the formulations and their mathematical properties, the methods for finding Pareto optimal solutions were not discussed. This is an interesting topic, that requires more involved research. Classical methods can be used to find individual Pareto optimal solutions of mixed variable problems as well, but generating the complete Pareto optimal set is generally very difficult, especially for problems with more than two or three criteria. The approach for finding the Pareto optimal solutions used in this thesis represents a brute force technique, where excessive computation is involved. Obviously, the goal of a solution method is to determine the Pareto optimal points with the least amount of computation.

CHAPTER 7

Case Study: Design of Roof Truss

Sometimes you get what you want
sometimes you get what you need
sometimes you get what you get
sometimes you get nothing.

EERO MURTOMÄKI

7.1 Introduction

In this chapter, the mixed variable formulation presented in Chapter 3 is applied to find the optimum topologies of a roof truss. The purpose is to examine, how the mixed variable formulations work in situations that are closer to actual design. This means that the number of available profiles is increased and denser ground structures are employed. Consequently, it is to be expected that the branch-and-cut algorithm is not able to verify the global optimum within a reasonable time.

The solution process is as follows. First, the optimum topology is solved for a relatively coarse ground structure and few available profiles. Then, both the number of profiles and the number of members in the ground structure are increased. New profiles are added such that for each ground structure, the solution of the previous problem with fewer profiles is feasible for the problem with added profiles. Thus, the solution of the previous case can be used as an initial solution for the next problem. However, the denser ground structures do not in general include the sparser ones.

The proposed approach could also be used in practice, since due to the exponential increase in problem size and solution time, starting the optimization with the max-

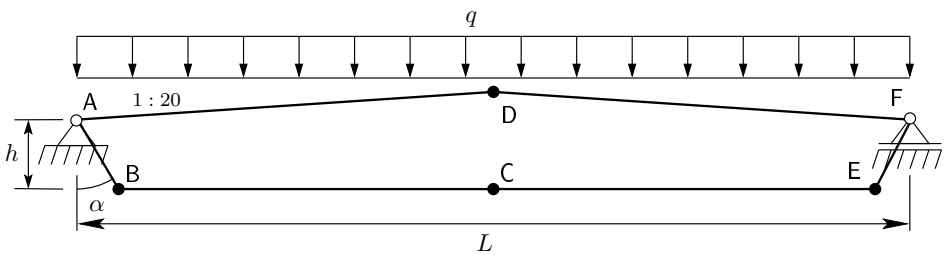

Figure 7.1: Main girder design domain.

imum number of profiles and the densest ground structure might lead to extremely slow progress in the computations.

The profiles are square hollow sections taken from the catalogue of a Finnish steel manufacturer (Ruukki 2011). Only profiles belonging to classes 1 and 2 of Eurocode 3 are included (see Section 2.3), and the "recommended series" is used. With these limitations, there are 53 available profiles. Furthermore, the largest profiles are eliminated by engineering judgment. Consequently, the greatest number of profiles is 40.

7.2 Problem Description

Consider the design domain of the main girder of a hall building show in Fig. 7.1. The boundary of the domain is fixed, and the goal is to determine the optimum layout of the bracing members, placed between the chords. The span of the truss $L = 24000\,\text{mm}$, and the height from the lower chord to the supports is $h = 2000\,\text{mm}$. The inclination of the upper chord is 1:20, which means a 2.86° angle with the x-axis. The angle of line segment AB with the y-axis is $\alpha = 30°$. The line load $q = 25.1\,\text{kN/m}$. This includes the snow load typical for southern Finland, and the weight of the roofing. These two loads are combined according to the Eurocode. The steel grade S355 is used, that is $f_\text{y} = 355\,\text{MPa}$, $E = 210\,\text{GPa}$, and $\rho = 7850\,\text{kg/m}^3$.

The ground structure is created as follows. The designer chooses the number of nodes on the half of the lower chord (line segment BC in Fig. 7.1). These nodes are placed equidistantly. The same number of nodes is placed on the upper chord, with x coordinates corresponding to the nodes of the lower chord. Then, a member is created between a pair of nodes, if the angle between the member and both chords is at least 30°. This restriction is to guarantee favourable welding conditions as stated in (EN 1993–1–8 2005).

Chains are created at the chords. A maximum chain member length, $L_\text{max} = 6000\,\text{mm}$ is prescribed in order to reduce the number of members. The purpose is to eliminate unrealistically long chord members by engineering judgment.

Symmetry of the ground structure with respect to the line defined by points C and D is enforced to keep the number of variables as small as possible. Note, however, that the true optimum structure might not be symmetric. The symmetry condition is included in the problem by relating the existence and profile variables of a member

with its symmetric counterpart. Similar procedure is applied for the nodal variables. In order to allow the node located at point C to vanish, members overlapping this node are created on the lower chord.

Six ground structures are considered. In the coarsest ground structure, 5 nodes are placed on the half of the lower chord. This number is then increased up to 10. The nodal coordinates and element connectivity tables can be found in Appendix B.3. For each ground structure, the number of profile alternatives is varied from 15 to 30 in steps of 5. In the last case, 40 profiles are available. The profile data can be found in Appendix A. The profiles of the different cases are as follows (see Table A.1): i) 16 to 30 (15 alternatives); ii) 11 to 30 (20 alternatives); iii) 11 to 35 (25 alternatives); iv) 6 to 35 (30 alternatives); v) all 40 profiles.

When the ground structure is fixed and only the number of profile alternatives is increased, the minimum weight solution of the previous problem can be used as a starting point for the next problem with more profiles.

For each ground structure, the minimum weight and minimum cost problems are solved. Member buckling is according to Eurocode 3, and a stabilizing loading condition is included to guarantee kinematic stability. Formulation 3 is employed, that is, member existence variables, nodal variables and profile variables are all included in the problem.

The cost function presented in Chapter 3 is employed and modified. For braces, the cost function components are easy to determine, since each bracing member is connected to both chords in constant angles defined by the ground structure.

The chords are manufactured as uniform long members to which the braces are welded. If the members of the structural model (pin-jointed truss) were used to determine the cost of the chords, unnecessarily many sawing and welding would be included in the cost objective function. Therefore, the cost components of the chords have to be treated separately.

The upper chord is made of two parts that are welded together using a butt weld. A similar weld is employed at the supports to take into account the cost of attaching the truss to the columns of the building. Thus, altogether four ends are sawn and three ends are welded. As the chord members are grouped to have the same profile, the grouping variables w_j can be employed to compute the sawing and welding costs of the entire upper chord. Denote by C_{Wj} and C_{Sj} the welding and sawing costs of profile j of the upper chord, respectively. The cost of the upper chord is then

$$C_{SW}^{up}(\mathbf{x}) = \sum_{j=1}^{n_S} (2C_{Sj} + 3C_{Wj})w_j \tag{7.1}$$

Note that C_{Sj} includes the sawing of both ends of one half of the chord. The components C_{Sj} and C_{Wj} can be determined as described in Chapter 3. For the welding, only the dimensions and the angles of the profile are needed. However, the length of the member is needed for the sawing cost. The length of one half of the upper chord is

$$L_{up} = \frac{24000\,\mathrm{mm}}{2\cos(2.86°)} = 12015.0\,\mathrm{mm} \tag{7.2}$$

This value is used for computing the C_{Sj}.

For the lower chord, only the sawing components must be determined. All the welding related to the lower chord is included in the cost components of the braces. During optimization, the length of the lower chord can vary. This possibility is neglected in the cost computation, and the length of the lower chord is determined from the ground structure:

$$L_{low} = 24000\,\text{mm} - 2 \cdot (2000\,\text{mm}) \cdot \tan(30°) = 21691.6\,\text{mm} \tag{7.3}$$

The lower chord sawing cost is then

$$C_S^{low}(\mathbf{x}) = \sum_{j=1}^{n_S} C_{Sj} w_j \tag{7.4}$$

The material, blasting, and painting costs of the chords can be included in the cost function for the chord members with respect to the variables y_{ij}.

The values for parameters of the cost function that depend on the size of the truss are as follows. For both painting and assembly by welding cost centers, the area of the working space is $(24 + 2) \times (2.6 + 2)\,\text{m}^2 = 119.6\,\text{m}^2$. Using Eq. (2) from Haapio (2012), the values $c_{ReA} = c_{ReP} = 0.0487\,€/\text{min}$ and $c_{SeA} = c_{SeP} = 0.0712\,€/\text{min}$ are obtained.

7.3 Results

Each problem instance is solved by Gurobi 5.0 on a computer with Intel Core i7-3770 processor (8 threads), running at 3.40 GHz clock frequency with 32.0 GB RAM. The time limit is set to 21600 s, which equals 6 hours. As described above, for each ground structure, the solution of the previous problem with fewer available profiles is used as a starting point for the next problem. The feasibility tolerance was set to $1 \cdot 10^{-9}$ and the termination tolerance to $1 \cdot 10^{-3}$.

Problem sizes and minimum weights are listed in Table 7.1. Note that due to symmetry, there are less member and nodal variables than ground structure members and nodes. These numbers can be found in Figs. 7.3–7.8, where N_Y is the number of member variables y_i and N_z is the number of nodal variables z_j. In Table 7.1, the computational times are also reported, and if the algorithm was not able to verify optimality of the solution in the given time limit, the gap between the lower and upper bounds is given. In the following, the ground structures and the problem instances are denoted by GS_i and $GS_{i,j}$, respectively, where i is the number of nodes on the upper chord between points A and D and and j is the number of profile alternatives.

The first observation is that, the computational time grows steeply as the ground structure is made denser and as the number of profiles is increased. For the instances $GS_{8,30}$, $GS_{8,40}$, $GS_{9,30}$, $GS_{9,40}$, $GS_{10,25}$, $GS_{10,30}$, and $GS_{10,40}$ the optimizer was unable to verify the global optimality of the solution in the given time limit. The gap between the lower and upper bounds at termination grows clearly, when the number of profiles is increased.

The minimum weight solution is found by the instance $GS_{5,40}$. However, as this ground structure is included in ground structure GS_{10}, the minimum weight design should also be feasible for GS_{10}. The minimum weight found in six hours is 1045 kg. However, there is a 22.62% gap between the lower bound and this solution. It was then decided to run the optimization again for GS_{10} using the minimum weight solution of $GS_{5,40}$ as an initial feasible point. The time limit was increased to 8 hours. In this time, the gap between the lower bound and this solution was decreased to 19.4%, and better feasible solutions could not be found. This indicates that the problem size is now too large for the computing capacity available to verify the optimality of the solution in an overnight computation. This suggests to favour a solution approach, where the optimization is first performed on a coarser ground structure, and the ground structure is made denser such that denser ground structures include the coarser as well.

In the minimum weight design, the upper chord corresponds to 48% of the total weight, and the lower chord 27%. Thus, the braces constitute 25% of the weight.

The results of cost minimization are displayed in Table 7.2. The problem sizes coincide with the minimum weight problems. Based on the experiences of the weight minimization, the time limit was set to 8 hours for the instance $GS_{10,40}$. This instance produces the minimum cost solution, even though there is a 9.93% gap when the time limit is reached. However, the best solution was found in 555 seconds, which corresponds to about 9 minutes. Thus, most of the computing time is spent on increasing the lower bound, which is indeed a very slow process.

It is remarkable that the computation times for cost minimization are substantially smaller than for weight minimization. Nevertheless, as the ground structure is made denser and more profiles are added, the progress of the algorithm saturates.

In Table 7.2, the weights of the minimum cost structures are also given. Comparing the minimum weight design with the weight of the minimum cost design indicates that the two are nearly identical. There is only a 12 kg difference in the weight, which corresponds to 1.2%. Similarly, the difference in cost is 25.6 €, which means 2.1%. On the other hand, the two designs are completely different, as can be seen from Fig. 7.8. Since the difference in the performance of the two solutions with respect both cost and weight is marginal, the multicriterion problem P_{CW} is not treated any further.

The profile selection and utilization ratios of the minimum weight and minimum cost designs of the different ground structures are given in Tables 7.3–7.8. In both cases, high degree of utility is obtained for both chords and most of the braces. On the other hand, both designs include braces that are not close to being fully utilized. Their purpose is mainly to reduce the buckling length of the upper chord members. At the same time they carry part of the load themselves.

In some instances, the side length of the largest braces are greater than the side length of the lower chord. For example, for GS_6 (Table 7.4), the largest side length of the braces is 100 mm, whereas the side length of the lower chord is 90 mm. Because of welding conditions, such dimensions are disadvantageous. Additional constraints should be included in the problem to enforce the side length of the braces to be sufficiently small compared with the dimensions of the chords.

The distribution of the cost factors of the minimum cost design is shown in Fig. 7.2. The material cost corresponds to 70% of the total cost. Therefore, it is understand-

Table 7.1: Minimum weight solutions of the main girder. n_x = number of lower chord half divisions; N_x = number of variables; W^* = minimum weight; T = running time of the solver; Gap = difference between the lower bound and the incumbent at termination.

n_x	n_S	N_x	N_B	$\leq$	$=$	W^* [kg]	T [s]	Gap [%]
5	15	1976	683	5946	169	1192.19	10.03	0
5	20	2576	893	7731	169	1141.87	11.25	0
5	25	3176	1103	9516	169	1141.87	24.91	0
5	30	3776	1313	11301	169	1078.84	52.92	0
5	40	4976	1733	14871	169	1034.89	218.7	0
6	15	3042	1037	9370	229	1236.27	40.15	0
6	20	3972	1357	12155	229	1172.07	135.1	0
6	25	4902	1677	14940	229	1172.07	633.25	0
6	30	5832	1997	17725	229	1100.76	544.18	0
6	40	7692	2637	23295	229	1047.12	8264.79	0
7	15	3772	1279	11660	275	1234.34	145.77	0
7	20	4927	1674	15115	275	1148.01	123.19	0
7	25	6082	2069	18570	275	1148.01	978.98	0
7	30	7237	2464	22025	275	1071.11	1366.74	0
7	40	9547	3254	28935	275	1037.68	14710.9	0
8	15	4870	1649	15504	336	1215.08	280.36	0
8	20	6365	2159	20024	336	1149.12	1375.27	0
8	25	7860	2669	24544	336	1149.12	5184.3	0
8	30	9355	3179	29064	336	1098.10	21600.1	3.91
8	40	12345	4199	38104	336	1061.15	21600.1	14.66
9	15	6032	2035	19274	400	1220.65	1028.89	0
9	20	7887	2665	24844	400	1163.21	4594.21	0
9	25	9742	3295	30414	400	1163.21	11563	0
9	30	11597	3925	35984	400	1103.03	21600.1	6.16
9	40	15307	5185	47124	400	1053.83	21600.2	10.09
10	15	7530	2533	24818	478	1187.57	2601.23	0
10	20	9850	3318	31828	478	1125.78	9701.83	0
10	25	12170	4103	38838	478	1125.78	21600.1	1.77
10	30	14490	4888	45848	478	1078.50	21600.1	10.34
10	40	19130	6458	59868	478	1045.00	21600.1	22.62
10	40	19130	6458	59868	478	1034.89	28800.1	19.41

Table 7.2: Minimum cost solutions of the main girder.

n_x	n_S	C^* [€]	T [s]	Gap [%]	$W(\mathbf{x}_c^*)$
5	15	1405.23	6.01	0	1192.19
5	20	1342.4	9.24	0	1141.87
5	25	1342.4	22.03	0	1141.87
5	30	1268.62	47.46	0	1078.84
5	40	1225.23	57.99	0	1041.8
6	15	1477.62	31.84	0	1236.27
6	20	1397.46	59	0	1172.07
6	25	1369.05	361.27	0	1172.97
6	30	1294.12	219.4	0	1148.39
6	40	1245.74	1720.42	0	1065.61
7	15	1424.83	49.89	0	1221.63
7	20	1344.97	177.19	0	1148.01
7	25	1344.97	509.16	0	1148.01
7	30	1287.97	710.11	0	1098.78
7	40	1248.82	7528.77	0	1064.35
8	15	1418.72	237.54	0	1209.37
8	20	1345.5	1610.63	0	1149.12
8	25	1345.5	1246.57	0	1149.12
8	30	1286.43	3415.79	0	1098.1
8	40	1243.13	21600.1	7.59	1061.15
9	15	1440.51	227.01	0	1228.18
9	20	1367.68	756.66	0	1169.35
9	25	1367.68	1890.62	0	1169.35
9	30	1299.48	7977.88	0	1110.88
9	40	1261.84	21600.2	2.32	1078.44
10	15	1398.45	3011.41	0	1188.33
10	20	1324.43	7244.59	0	1125.78
10	25	1324.43	582.53	0	1125.78
10	30	1253.53	21431.28	0	1091.08
10	40	1202.29	28800.2	9.93	1046.82

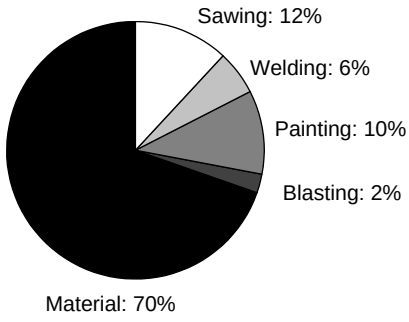

Figure 7.2: Distribution of cost components of the minimum cost design.

able that the cost of the minimum weight design is not significantly greater than the minimum cost obtained. The welding cost constitutes a relatively low portion of the total cost, which is a surprising result, since typically welding is a significant work phase.

The optimum designs of the different ground structures are depicted in Figs. 7.3–7.8. It can be seen that in many cases the minimum weight topology differs from the minimum cost topology. When the two topologies coincide, the designs are also nearly identical. For example, for the 6-by-1 ground structure, shown in Fig. 7.4, the two optima differ only in the upper chord. The minimum cost truss is obtained by choosing a profile which has a larger cross-sectional area but smaller outer dimensions, which leads to savings in painting, welding and sawing.

7.4 Discussion

The roof truss design problem demonstrates that the mixed variable approach can be applied to practical design situations. On the other hand, the limits of the formulations in terms of problem size and computational time start to emerge. It is clear that the choice of ground structures and profiles should be made with careful engineering discretion. For example, based on the loads and design domain dimensions, unnecessarily large or small profiles can be discarded and excessively long members can be disallowed from the ground structure.

Based on the computational experience on the ground structures GS_5 and GS_{10}, it can be recommended that the coarser ground structures should be included in the denser ground structures such that the optimum solutions of the coarser cases are feasible for the denser structures. Similarly, if the number of profiles is increased, the new profiles should be added to the existing alternatives in order to benefit from the earlier computations.

For the roof truss considered, the minimum cost and minimum weight designs obtained were substantially different. On the other hand, they were nearly equally good in both criteria. As cost and weight were only mildly conflicting, it was decided not to treat the multicriterion problem P_{CW} further.

Because the optimality of the minimum cost and minimum weight solutions was not verified, general conclusions about the conflict of the criteria cannot be drawn. The cost function used gave welding a rather small portion of the total cost. The cost function does not include the jig where the truss members are placed before welding. Also, tack welding time of the members might be inaccurate. Modifying the cost function regarding these aspects might lead to optimum solutions, where the material cost has a smaller share of the total cost, which might be reflected in the conflict of cost and weight.

Nevertheless, as the minimum cost design differs from the minimum weight design, it is advisable to develop and employ in optimization cost functions that take into account the various cost factors.

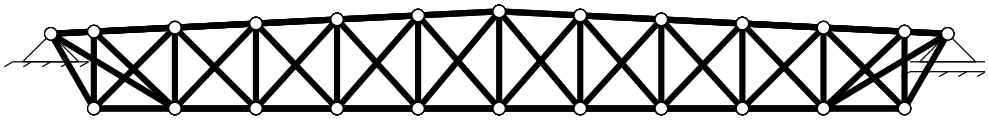

(a) Ground structure. $n_E = 78$, $n_N = 24$, $N_Y = 40$, $N_z = 13$.

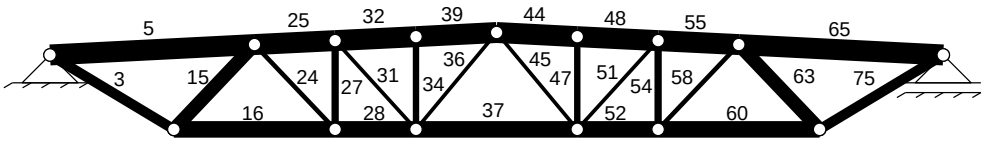

(b) Minimum weight design, $W^* = 1034.89\,\text{kg}$. (Cost: $C = 1227.92\,€$)

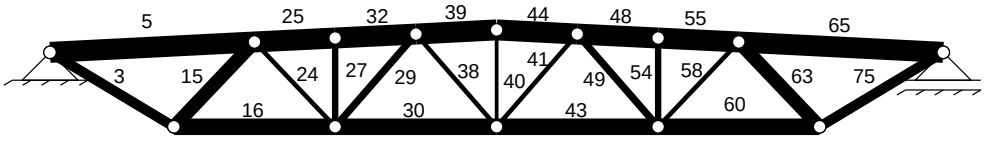

(c) Minimum cost design, $C^* = 1225.23\,€$. (Weight: $W = 1041.8\,\text{kg}$)

Figure 7.3: Ground structure with 5 nodes between the support and the top node, and the corresponding minimum weight and minimum cost designs, where 40 profiles are available.

Table 7.3: Minimum weight and minimum cost design utilization ratios.

Member	Profile	A [mm^2]	Strength [%]	Buckling [%]
Minimum weight design				
Upper chord	140×5	2636	75.07	99.60
Lower chord	110×5	2036	96.17	–
3, 75	80×4	1175	99.71	–
15, 63	110×4	1655	50.43	89.20
24, 58	40×3	421	95.36	–
27, 54	70×3	781	37.20	81.10
31, 51	30×3	301	58.95	–
34, 47	60×3	661	23.20	67.46
36, 45	30×3	301	9.58	–
Minimum cost design				
Upper chord	140×5	2636	74.37	99.60
Lower chord	110×5	2036	97.07	–
3, 75	80×4	1175	99.71	–
15, 63	110×4	1655	50.43	89.20
24, 58	40×3	421	95.36	–
27, 54	60×3	661	23.20	63.18
29, 49	70×3	781	23.29	81.37
38, 41	40×3	421	6.68	66.27
40	30×3	301	14.10	–

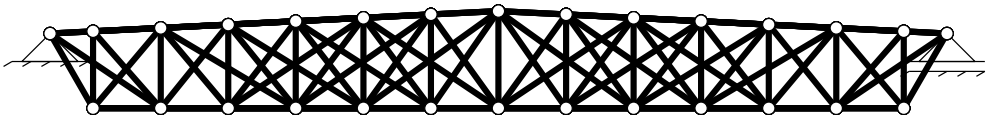

(a) Ground structure. $n_E = 122$, $n_N = 28$, $N_Y = 62$, $N_z = 15$.

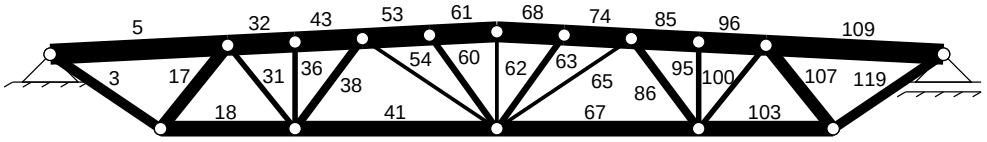

(b) Minimum weight design, $W^* = 1047.12\,\text{kg}$. (Cost: $C = 1253.62\,€$)

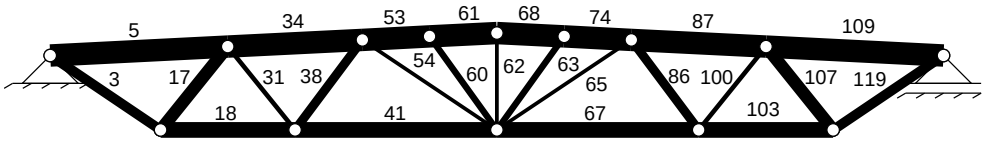

(c) Minimum cost design, $C^* = 1245.74\,€$. (Weight: $W = 1065.61\,\text{kg}$)

Figure 7.4: Ground structure with 6 nodes between the support and the top node, and the corresponding minimum weight and minimum cost designs, with 40 available profiles.

Table 7.4: Minimum weight and minimum cost design utilization ratios of the 6-by-1 ground structure.

Member	Profile	A [mm^2]	Strength [%]	Buckling [%]
Minimum weight design				
Upper chord	140×5	2636	77.75	88.35
Lower chord	90×6	1923	99.49	–
3, 119	100×3	1141	99.14	–
17, 107	100×4	1495	54.42	97.37
31, 100	40×4	535	86.57	–
36, 95	50×3	541	23.62	83.67
38, 86	80×3	901	32.22	79.83
54, 65	30×3	301	53.38	–
60, 63	60×3	661	23.00	94.10
62	30×3	301	22.59	–
Minimum cost design				
Upper chord	150×5	2836	72.26	90.53
Lower chord	90×6	1923	99.49	–
3, 119	100×3	1141	99.14	–
17, 107	100×4	1495	54.42	97.37
31, 100	40×3	421	91.26	–
38, 86	90×3	1021	36.54	77.09
54, 65	30×3	301	53.38	–
60, 63	60×3	661	23.00	94.10
62	30×3	301	22.59	–

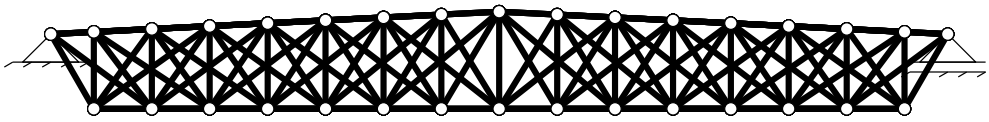

(a) Ground structure. $n_E = 152$, $n_N = 32$, $N_Y = 77$, $N_z = 17$.

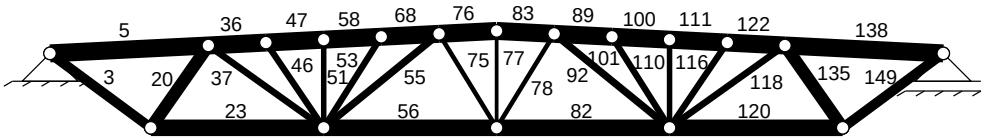

(b) Minimum weight design, $W^* = 1037.68\,\text{kg}$. (Cost: $C = 1281.16\,€$)

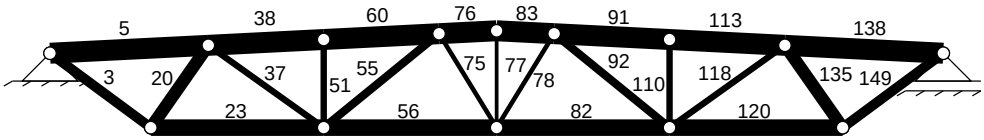

(c) Minimum cost design, $C^* = 1248.82\,€$. (Weight: $W = 1064.35\,\text{kg}$)

Figure 7.5: Ground structure with 7 nodes between the support and the top node, and the corresponding minimum weight and minimum cost designs, with 40 profiles available.

Table 7.5: Minimum weight and minimum cost design utilization ratios of the 7-by-1 ground structure.

Member	Profile	A [mm^2]	Strength [%]	Buckling [%]
Minimum weight design				
Upper chord	120×5	2236	87.67	99.83
Lower chord	110×5	2036	97.47	–
3, 149	100×3	1141	96.37	–
20, 135	100×4	1495	53.39	89.80
37, 118	50×4	695	98.54	–
46, 116	60×3	661	19.35	66.06
51, 110	50×3	541	20.25	73.63
53, 101	60×3	661	20.26	74.40
55, 92	70×3	781	14.07	67.26
75, 78	40×3	421	12.02	97.66
77	30×3	301	28.66	–
Minimum cost design				
Upper chord	140×5	2636	74.37	99.32
Lower chord	110×5	2036	97.47	–
3, 149	100×3	1141	96.37	–
20, 135	100×4	1495	53.39	89.80
37, 118	60×3	661	90.28	–
51, 110	60×3	661	33.14	89.41
55, 92	80×3	901	22.45	85.02
75, 78	40×3	421	12.02	97.66
77	30×3	301	28.66	–

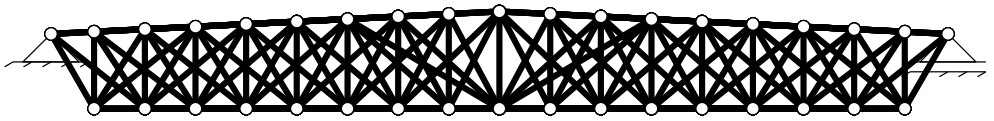

(a) Ground structure. $n_E = 197$, $n_N = 36$, $N_Y = 100$, $N_z = 19$.

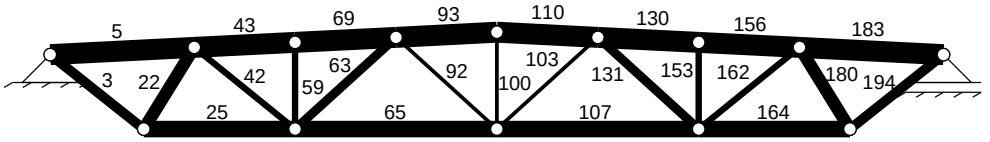

(b) Minimum weight design, $W^* = 1061.15\,\text{kg}$. (Cost: $C = 1243.13\,€$)

Figure 7.6: Ground structure with 8 nodes between the support and the top node, and the corresponding minimum weight and minimum cost design, with 40 profiles available. Note that a single truss optimizes both the weight and cost.

Table 7.6: Minimum weight and minimum cost design utilization ratios of the 8-by-1 ground structure.

Member	Profile	A [mm^2]	Strength [%]	Buckling [%]
Upper chord	140×5	2636	74.37	98.36
Lower chord	110×5	2036	96.28	–
3, 194	100×3	1141	94.20	–
22, 180	100×4	1495	52.67	84.93
42, 162	60×3	661	94.36	0.00
59, 153	60×3	661	29.00	76.40
63, 131	90×3	1021	29.21	79.98
92, 103	30×3	301	1.01	22.20
100	30×3	301	1.36	–

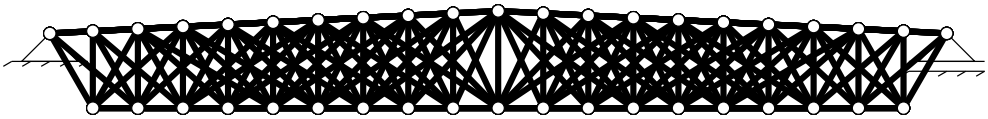

(a) Ground structure. $n_E = 245$, $n_N = 40$, $N_Y = 124$, $N_z = 21$.

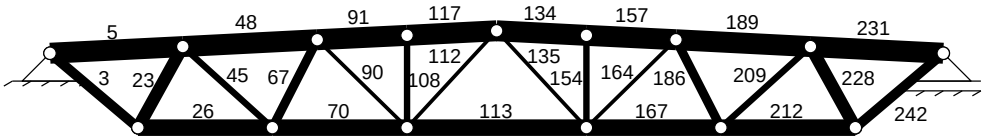

(b) Minimum weight design, $W^* = 1053.83\,\text{kg}$. (Cost: $C = 1247.45\,€$)

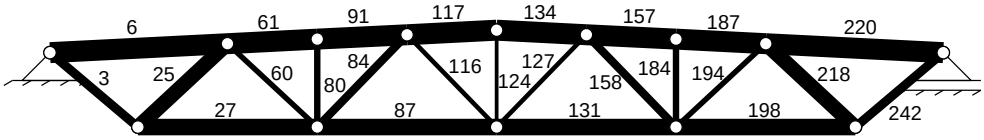

(c) Minimum cost design, $C^* = 1261.84\,€$. (Weight: $W^* = 1078.44\,\text{kg}$)

Figure 7.7: Ground structure with 9 nodes between the support and the top node, and the corresponding minimum weight and minimum cost designs, with 40 profiles available.

Table 7.7: Minimum weight and minimum cost design utilization ratios of the 9-by-1 ground structure.

Member	Profile	A [mm^2]	Strength [%]	Buckling [%]
Minimum weight design				
Upper chord	140×5	2636	74.83	98.50
Lower chord	110×5	2036	96.17	–
3, 242	100×3	1141	92.47	–
23, 228	100×4	1495	52.15	81.64
45, 209	60×3	661	87.55	–
67, 186	90×3	1021	42.68	77.52
90, 164	30×3	301	74.61	–
108, 154	60×3	661	25.78	74.42
112, 135	30×3	301	6.03	–
Minimum cost design				
Upper chord	140×5	2636	74.37	93.07
Lower chord	110×5	2036	96.77	–
3, 242	70×4	1015	97.82	–
25, 218	120×4	1815	51.97	87.94
60, 194	40×4	535	92.15	–
80, 184	60×3	661	25.78	69.17
84, 158	80×3	901	25.56	77.09
116, 127	40×3	421	4.21	45.36
124	30×3	301	8.44	–

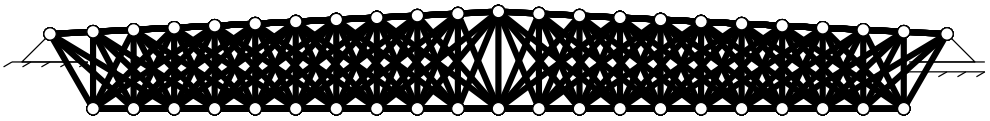

(a) Ground structure. $n_E = 307$, $n_N = 44$, $N_Y = 155$, $N_z = 23$.

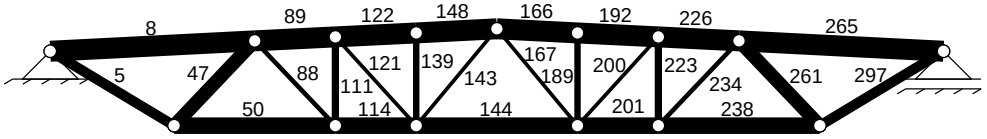

(b) Minimum weight design, $W^* = 1034.89\,\text{kg}$. (Cost: $C = 1227.92\,€$)

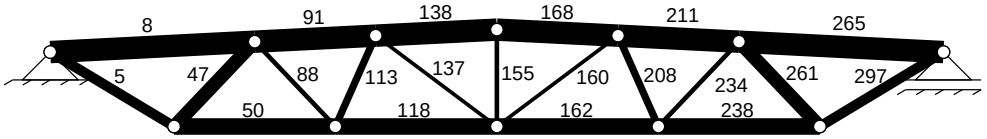

(c) Minimum cost design, $C^* = 1202.29\,€$. (Weight: $W^* = 1046.82\,\text{kg}$)

Figure 7.8: Ground structure with 10 nodes between the support and the top node, and the corresponding minimum weight and minimum cost designs, with 40 profiles available.

Table 7.8: Minimum weight and minimum cost design utilization ratios of the 10-by-1 ground structure.

Member	Profile	A [mm^2]	Strength [%]	Buckling [%]
Minimum weight design				
Upper chord	140×5	2636	75.07	99.60
Lower chord	110×5	2036	96.17	–
5, 297	80×4	1175	99.71	–
47, 261	110×4	1655	50.43	89.20
88, 234	40×3	421	95.36	–
111, 223	70×3	781	37.20	81.10
121, 200	30×3	301	58.95	–
139, 189	60×3	661	23.20	67.46
143, 167	30×3	301	9.58	–
Minimum cost design				
Upper chord	150×5	2836	69.13	97.43
Lower chord	110×5	2036	95.04	–
5, 297	80×4	1175	99.71	–
47, 261	110×4	1655	50.43	89.20
88, 234	40×3	421	83.35	–
113, 208	70×3	781	35.59	90.19
137, 160	30×3	301	9.49	–
155	40×3	421	8.13	52.39

CHAPTER 8

Summary and Conclusions

Following our will and wind
we may just go where no one's been
we ride the spiral to the end
and may just go where no one's been
MAYNARD JAMES KEENAN

The primary purpose of this thesis was to devise new formulations for truss topology optimization that would lead to applicable designs, whose global optimality could be guaranteed. The mixed variable approach was chosen as the basis for developing more advanced formulations. The main advantage of this approach is that it avoids all the difficulties related to vanishing members that haunt truss topology optimization theory. Furthermore, as all the functions of the optimization problems are explicitly written in terms of the optimization variables, the mathematical structure of the problem can be fully exploited in the solution. Finally, the formulations studied in this thesis lead to linear mixed-integer optimization problems, for which powerful algorithms are available.

The mixed variable approach was successfully employed in addressing the issues of member buckling and kinematic stability of the optimum structure. For member buckling, chains of members were introduced in order to avoid the jump in the buckling length problem. This issue had not been fully resolved in the literature. Chains also proved to be helpful in ensuring the kinematic stability of the optimum solution. By an auxiliary loading condition, where every node of the ground structure present in the current topology is loaded by small forces, structures that are mechanisms but still satisfy the equilibrium equations with respect to the original loads could be avoided.

The mixed variable formulations and especially chains allowed to incorporate line loading properly in truss topology optimization. In truss analysis, line loads are trans-

formed to equivalent point loads at the nodes. As all loaded nodes must be present in the optimum structure, making the ground structure denser leads to solutions where unnecessarily many nodes are present. The proposed approach for this issue allows nodes under line loading to vanish, and it was successfully demonstrated on the roof truss design problem.

The above extensions to the mixed variable formulations found in the literature bring truss topology optimization closer to the structural designer. The ultimate goal of structural optimization is to provide practicing engineers tools that lead to improved designs in given time. Therefore, it is important to formulate the optimization problem in a manner that is relevant for the designer. This means that not only must the objective function reflect the goal of the designer, but also the constraints must ensure that as many design aspects as possible are taken into account.

In this thesis, the design of tubular trusses according to Eurocode 3 was chosen for a special case for developing designer-oriented formulations. First, the objective was to find the most economical structure. This was realized by minimizing the weight together with the number of members, nodes and profiles in a multicriterion setting. Additionally, a detailed cost function was devised based on earlier research found in the literature. The design constraints were adopted from Eurocode 3. The most important constraint type presented in this thesis was member buckling according to the design rules of Eurocode 3. A remarkable outcome of the study is that the Eurocode 3 buckling constraints can also be formulated as linear constraints, when the member profiles are to be chosen from a predefined list of alternatives.

In addition to problem formulations, the numerical solution of the mixed variable problems was a major topic of the thesis. A state-of-the-art commercial software was used to solve the optimization problems. In recent years, the capabilities of the branch-and-cut algorithms have increased remarkably, and this development could be seen in the optimization problems solved in the thesis.

Even though the algorithm performed well, the limits in problem size became apparent especially in solving the roof truss design problem. Finding feasible designs did not pose a problem, but improving the lower bound proved to be a very slow process. This suggests that special cutting planes or other techniques must be employed to improve the convergence of the algorithm.

Further Research Avenues

The mixed variable formulations transform the theoretical difficulties of truss topology optimization into computational matters. For further developments there are two clear paths.

For applications related to structural design, it would be important to extend the formulations to include more of the design rules of the Eurocodes. For example, the joint strength, and fire design are important aspects that the designer needs to consider. Also, bending, shear and torsion effects should be incorporated in the optimization problem, when they are present. This would mean an extension of the formulations from trusses to frames. Such an extension is not straightforward. Even if the equations of frame analysis could be included as linear constraints, the linearity of strength

and stability constraints is not apparent. Any nonlinearities in the formulation will introduce severe difficulties in the numerical solution.

The second future research path is related to the solution methods for the mixed variable formulations. It is clear that if the optimality of the solution needs to be verified in an overnight computation, the problem size is rather limited. One possibility to enhance the solution process is to employ parallel computation. However, this might be a costly effort when compared with the gain in solution quality or time. On the other hand, there are numerous examples in the literature, where special-purpose methods have decreased the solution time by orders of magnitude from general algorithms.

In the branch-and-cut algorithm, the choice of branching strategy and the type of cutting planes used are the two main ingredients for improving the performance. For branching, prioritizing the binary variables should be considered. Also, the special-ordered-set-nature of the profile variables could be exploited in the branching. Gurobi has this capability but it is not clear how the SOS-branching is carried out.

The present study shows that even though truss topology optimization is a mature topic, there are still research avenues that can provide both the academic community and the practicing engineers valuable information and tools.

APPENDIX A

Selection of Profiles

Properites of the square hollow section profiles used in Chapter 7 for the members of the roof truss are listed in Table A.1. In the table, H is the side length, t is the wall thickness, A cross-sectional area, I moment of inertia, and A_u external sufrace are per unit length.

Table A.1: Profile data for square hollow sections, taken from (Ruukki 2011).

	H[mm]	t[mm]	A [10^2 mm^2]	I [10^4 mm^4]	A_u [10^2 mm^2/mm]
1	30	3	3.01	3.50	1.10
2	40	3	4.21	9.32	1.50
3	40	4	5.35	11.07	1.46
4	50	3	5.41	19.47	1.90
5	60	3	6.61	35.13	2.30
6	50	4	6.95	23.74	1.86
7	70	3	7.81	57.53	2.70
8	50	5	8.36	27.04	1.83
9	60	4	8.55	43.55	2.26
10	80	3	9.01	87.84	3.10
11	70	4	10.15	72.12	2.66
12	90	3	10.21	127.28	3.50
13	60	5	10.36	50.49	2.23
14	100	3	11.41	177.05	3.90
15	80	4	11.75	111.04	3.06
16	70	5	12.36	84.63	2.63
17	90	4	13.35	161.92	3.46
18	80	5	14.36	131.44	3.03
19	100	4	14.95	226.35	3.86
20	90	5	16.36	192.93	3.43
21	110	4	16.55	305.94	4.26
22	80	6	16.83	149.18	2.99
23	120	4	18.15	402.28	4.66
24	100	5	18.36	271.10	3.83
25	90	6	19.23	220.48	3.39
26	110	5	20.36	367.95	4.23
27	100	6	21.63	311.47	3.79
28	120	5	22.36	485.47	4.63
29	110	6	24.03	424.57	4.19
30	140	5	26.36	790.56	5.43
31	120	6	26.43	562.16	4.59
32	100	8	27.24	365.94	3.66
33	150	5	28.36	982.12	5.83
34	140	6	31.23	920.43	5.39
35	150	6	33.63	1145.91	5.79
36	120	8	33.64	676.88	4.46
37	140	8	40.04	1126.77	5.26
38	120	10	40.57	776.81	4.37
39	150	8	43.24	1411.83	5.66
40	160	8	46.44	1741.23	6.06

APPENDIX B

Ground Structures

Below, the nodal coordinates and element connectivity tables of all the problems considered in this thesis are given. The nodal coordinates are given in metres.

B.1 Cantilever Truss

Table B.1: Nodal coordinates [m] of the 2-by-2 ground structure

i	x	y	i	x	y	i	x	y
1	0.0	0.0	4	1.0	0.0	7	2.0	0.0
2	0.0	1.0	5	1.0	1.0	8	2.0	1.0
3	0.0	2.0	6	1.0	2.0	9	2.0	2.0

Table B.2: Element connectivity table of the 2-by-2 ground structure, no chains.

e	1	2	e	1	2	e	1	2
1	1	4	7	3	6	13	5	8
2	1	5	8	4	5	14	5	9
3	2	4	9	4	7	15	6	8
4	2	5	10	4	8	16	6	9
5	2	6	11	5	6	17	7	8
6	3	5	12	5	7	18	8	9

Table B.3: Element connectivity table of the 2-by-2 ground structure, with chains.

e	1	2	e	1	2	e	1	2
1	1	4	10	3	6	19	5	8
2	1	5	11	3	7	20	5	9
3	1	7	12	3	9	21	6	8
4	1	9	13	4	5	22	6	9
5	2	4	14	4	6	23	7	8
6	2	5	15	4	7	24	7	9
7	2	6	16	4	8	25	8	9
8	2	8	17	5	6			
9	3	5	18	5	7			

Table B.4: Nodal coordinates [m] of the 4-by-4 ground structure.

i	x	y	i	x	y	i	x	y	i	x	y	i	x	y
1	0.0	0.0	6	0.5	0.0	11	1.0	0.0	16	1.5	0.0	21	2.0	0.0
2	0.0	0.5	7	0.5	0.5	12	1.0	0.5	17	1.5	0.5	22	2.0	0.5
3	0.0	1.0	8	0.5	1.0	13	1.0	1.0	18	1.5	1.0	23	2.0	1.0
4	0.0	1.5	9	0.5	1.5	14	1.0	1.5	19	1.5	1.5	24	2.0	1.5
5	0.0	2.0	10	0.5	2.0	15	1.0	2.0	20	1.5	2.0	25	2.0	2.0

Table B.5: Element connectivity table of the 4-by-4 ground structure, with chains.

e	1	2	e	1	2	e	1	2	e	1	2	e	1	2
1	1	6	31	4	19	61	8	9	91	11	23	121	16	20
2	1	7	32	4	24	62	8	10	92	12	13	122	16	21
3	1	11	33	5	9	63	8	12	93	12	14	123	16	22
4	1	13	34	5	10	64	8	13	94	12	15	124	17	18
5	1	16	35	5	13	65	8	14	95	12	16	125	17	19
6	1	19	36	5	15	66	8	16	96	12	17	126	17	20
7	1	21	37	5	17	67	8	18	97	12	18	127	17	21
8	1	25	38	5	20	68	8	20	98	12	22	128	17	22
9	2	6	39	5	21	69	8	23	99	12	24	129	17	23
10	2	7	40	5	25	70	9	10	100	13	14	130	18	19
11	2	8	41	6	7	71	9	13	101	13	15	131	18	20
12	2	12	42	6	8	72	9	14	102	13	17	132	18	22
13	2	14	43	6	9	73	9	15	103	13	18	133	18	23
14	2	17	44	6	10	74	9	17	104	13	19	134	18	24
15	2	20	45	6	11	75	9	19	105	13	21	135	19	20
16	2	22	46	6	12	76	9	21	106	13	23	136	19	23
17	3	7	47	6	16	77	9	24	107	13	25	137	19	24
18	3	8	48	6	18	78	10	14	108	14	15	138	19	25
19	3	9	49	6	21	79	10	15	109	14	18	139	20	24
20	3	11	50	6	24	80	10	18	110	14	19	140	20	25
21	3	13	51	7	8	81	10	20	111	14	20	141	21	22
22	3	15	52	7	9	82	10	22	112	14	22	142	21	23
23	3	18	53	7	10	83	10	25	113	14	24	143	21	24
24	3	23	54	7	11	84	11	12	114	15	19	144	21	25
25	4	8	55	7	12	85	11	13	115	15	20	145	22	23
26	4	9	56	7	13	86	11	14	116	15	23	146	22	24
27	4	10	57	7	17	87	11	15	117	15	25	147	22	25
28	4	12	58	7	19	88	11	16	118	16	17	148	23	24
29	4	14	59	7	22	89	11	17	119	16	18	149	23	25
30	4	16	60	7	25	90	11	21	120	16	19	150	24	25

B.2 L-Shaped Truss

Table B.6: Nodal coordinates [m] of the L-shaped truss ground structure.

i	x	y	i	x	y	i	x	y
1	0.0	0.0	8	1.0	2.0	15	2.0	4.0
2	0.0	1.0	9	1.0	3.0	16	3.0	0.0
3	0.0	2.0	10	1.0	4.0	17	3.0	1.0
4	0.0	3.0	11	2.0	0.0	18	3.0	2.0
5	0.0	4.0	12	2.0	1.0	19	4.0	0.0
6	1.0	0.0	13	2.0	2.0	20	4.0	1.0
7	1.0	1.0	14	2.0	3.0	21	4.0	2.0

Table B.7: Element connectivity table of the L-shaped truss ground structure.

e	1	2	e	1	2	e	1	2	e	1	2	e	1	2
1	1	2	23	3	7	45	6	10	67	9	10	89	13	14
2	1	3	24	3	8	46	6	11	68	9	13	90	13	15
3	1	4	25	3	9	47	6	12	69	9	14	91	13	17
4	1	5	26	3	11	48	6	16	70	9	15	92	13	18
5	1	6	27	3	13	49	6	18	71	9	17	93	13	19
6	1	7	28	3	15	50	6	19	72	9	19	94	13	21
7	1	11	29	3	18	51	7	8	73	10	14	95	14	15
8	1	13	30	3	21	52	7	9	74	11	12	96	16	17
9	1	16	31	4	5	53	7	10	75	11	13	97	16	18
10	1	19	32	4	8	54	7	11	76	11	14	98	16	19
11	2	3	33	4	9	55	7	12	77	11	15	99	16	20
12	2	4	34	4	10	56	7	13	78	11	16	100	17	18
13	2	5	35	4	12	57	7	17	79	11	17	101	17	19
14	2	6	36	4	14	58	7	20	80	11	19	102	17	20
15	2	7	37	4	16	59	8	9	81	11	21	103	17	21
16	2	8	38	5	9	60	8	10	82	12	13	104	18	20
17	2	12	39	5	13	61	8	12	83	12	14	105	18	21
18	2	14	40	5	17	62	8	13	84	12	15	106	19	20
19	2	17	41	5	19	63	8	14	85	12	16	107	19	21
20	2	20	42	6	7	64	8	16	86	12	17	108	20	21
21	3	4	43	6	8	65	8	18	87	12	18			
22	3	5	44	6	9	66	8	21	88	12	20			

B.3 Roof Truss

B.3.1 Ground Structure 1

Table B.8: Nodal coordinates [m] of the ground structure GS_5.

i	x	y	i	x	y	i	x	y
1	0.000	0.000	9	7.662	0.383	17	16.338	-2.000
2	1.155	-2.000	10	9.831	-2.000	18	18.507	0.275
3	1.155	0.058	11	9.831	0.492	19	18.507	-2.000
4	3.324	-2.000	12	12.000	-2.000	20	20.676	0.166
5	3.324	0.166	13	12.000	0.600	21	20.676	-2.000
6	5.493	-2.000	14	14.169	0.492	22	22.845	0.058
7	5.493	0.275	15	14.169	-2.000	23	22.845	-2.000
8	7.662	-2.000	16	16.338	0.383	24	24.000	0.000

Table B.9: Element connectivity table of the ground structure GS_5.

e	1	2	e	1	2	e	1	2	e	1	2	e	1	2
1	1	2	17	5	6	33	9	13	49	14	17	65	18	24
2	1	3	18	5	7	34	10	11	50	14	18	66	19	20
3	1	4	19	5	9	35	10	12	51	15	16	67	19	21
4	1	5	20	6	7	36	10	13	52	15	17	68	19	23
5	1	7	21	6	8	37	10	15	53	15	19	69	20	21
6	2	3	22	6	9	38	11	12	54	16	17	70	20	22
7	2	4	23	6	10	39	11	13	55	16	18	71	20	23
8	2	5	24	7	8	40	12	13	56	16	19	72	20	24
9	2	6	25	7	9	41	12	14	57	16	20	73	21	22
10	3	4	26	7	11	42	12	15	58	17	18	74	21	23
11	3	5	27	8	9	43	12	17	59	17	19	75	21	24
12	3	7	28	8	10	44	13	14	60	17	21	76	22	23
13	4	5	29	8	11	45	13	15	61	18	19	77	22	24
14	4	6	30	8	12	46	13	16	62	18	20	78	23	24
15	4	7	31	9	10	47	14	15	63	18	21			
16	4	8	32	9	11	48	14	16	64	18	22			

B.3.2 Ground Structure 2

Table B.10: Nodal coordinates [m] of the ground structure GS_6.

i	x	y	i	x	y	i	x	y	i	x	y
1	0.000	0.000	8	6.577	-2.000	15	12.000	0.600	22	19.230	0.238
2	1.155	-2.000	9	6.577	0.329	16	13.808	0.510	23	19.230	-2.000
3	1.155	0.058	10	8.385	-2.000	17	13.808	-2.000	24	21.038	0.148
4	2.962	-2.000	11	8.385	0.419	18	15.615	0.419	25	21.038	-2.000
5	2.962	0.148	12	10.192	-2.000	19	15.615	-2.000	26	22.845	0.058
6	4.770	-2.000	13	10.192	0.510	20	17.423	0.329	27	22.845	-2.000
7	4.770	0.238	14	12.000	-2.000	21	17.423	-2.000	28	24.000	0.000

Table B.11: Element connectivity table of the ground structure GS_6.

e	1	2	e	1	2	e	1	2	e	1	2	e	1	2
1	1	2	26	6	8	51	10	15	76	16	20	101	21	23
2	1	3	27	6	9	52	11	12	77	16	21	102	21	24
3	1	4	28	6	10	53	11	13	78	16	22	103	21	25
4	1	5	29	6	11	54	11	14	79	17	18	104	21	27
5	1	7	30	6	12	55	11	15	80	17	19	105	22	23
6	2	3	31	7	8	56	12	13	81	17	20	106	22	24
7	2	4	32	7	9	57	12	14	82	17	21	107	22	25
8	2	5	33	7	10	58	12	15	83	17	23	108	22	26
9	2	6	34	7	11	59	12	17	84	18	19	109	22	28
10	2	8	35	7	13	60	13	14	85	18	20	110	23	24
11	3	4	36	8	9	61	13	15	86	18	21	111	23	25
12	3	5	37	8	10	62	14	15	87	18	22	112	23	27
13	3	7	38	8	11	63	14	16	88	18	23	113	24	25
14	3	9	39	8	12	64	14	17	89	18	24	114	24	26
15	4	5	40	8	13	65	14	18	90	19	20	115	24	27
16	4	6	41	8	14	66	14	19	91	19	21	116	24	28
17	4	7	42	9	10	67	14	21	92	19	22	117	25	26
18	4	8	43	9	11	68	15	16	93	19	23	118	25	27
19	4	10	44	9	12	69	15	17	94	19	25	119	25	28
20	5	6	45	9	13	70	15	18	95	20	21	120	26	27
21	5	7	46	9	15	71	15	19	96	20	22	121	26	28
22	5	8	47	10	11	72	15	20	97	20	23	122	27	28
23	5	9	48	10	12	73	16	17	98	20	24			
24	5	11	49	10	13	74	16	18	99	20	26			
25	6	7	50	10	14	75	16	19	100	21	22			

B.3.3 Ground Structure 3

Table B.12: Nodal coordinates [m] of the ground structure GS_7.

i	x	y	i	x	y	i	x	y	i	x	y
1	0.000	0.000	9	5.803	0.290	17	12.000	0.600	25	18.197	-2.000
2	1.155	-2.000	10	7.352	-2.000	18	13.549	0.523	26	19.747	0.213
3	1.155	0.058	11	7.352	0.368	19	13.549	-2.000	27	19.747	-2.000
4	2.704	-2.000	12	8.901	-2.000	20	15.099	0.445	28	21.296	0.135
5	2.704	0.135	13	8.901	0.445	21	15.099	-2.000	29	21.296	-2.000
6	4.253	-2.000	14	10.451	-2.000	22	16.648	0.368	30	22.845	0.058
7	4.253	0.213	15	10.451	0.523	23	16.648	-2.000	31	22.845	-2.000
8	5.803	-2.000	16	12.000	-2.000	24	18.197	0.290	32	24.000	0.000

Table B.13: Element connectivity table of the ground structure GS_7.

e	1	2	e	1	2	e	1	2	e	1	2	e	1	2
1	1	2	32	6	10	63	12	14	94	19	20	125	24	29
2	1	3	33	6	11	64	12	15	95	19	21	126	24	30
3	1	4	34	6	12	65	12	16	96	19	22	127	24	32
4	1	5	35	7	8	66	12	17	97	19	23	128	25	26
5	1	7	36	7	9	67	13	14	98	19	25	129	25	27
6	1	9	37	7	10	68	13	15	99	20	21	130	25	28
7	2	3	38	7	11	69	13	16	100	20	22	131	25	29
8	2	4	39	7	13	70	13	17	101	20	23	132	25	31
9	2	5	40	8	9	71	14	15	102	20	24	133	26	27
10	2	6	41	8	10	72	14	16	103	20	25	134	26	28
11	2	7	42	8	11	73	14	17	104	20	26	135	26	29
12	2	8	43	8	12	74	14	19	105	21	22	136	26	30
13	3	4	44	8	13	75	15	16	106	21	23	137	26	31
14	3	5	45	8	14	76	15	17	107	21	24	138	26	32
15	3	6	46	9	10	77	16	17	108	21	25	139	27	28
16	3	7	47	9	11	78	16	18	109	21	27	140	27	29
17	3	9	48	9	12	79	16	19	110	22	23	141	27	30
18	4	5	49	9	13	80	16	20	111	22	24	142	27	31
19	4	6	50	9	15	81	16	21	112	22	25	143	28	29
20	4	7	51	10	11	82	16	23	113	22	26	144	28	30
21	4	8	52	10	12	83	17	18	114	22	27	145	28	31
22	4	9	53	10	13	84	17	19	115	22	28	146	28	32
23	4	10	54	10	14	85	17	20	116	23	24	147	29	30
24	5	6	55	10	15	86	17	21	117	23	25	148	29	31
25	5	7	56	10	16	87	17	22	118	23	26	149	29	32
26	5	8	57	11	12	88	18	19	119	23	27	150	30	31
27	5	9	58	11	13	89	18	20	120	23	29	151	30	32
28	5	11	59	11	14	90	18	21	121	24	25	152	31	32
29	6	7	60	11	15	91	18	22	122	24	26			
30	6	8	61	11	17	92	18	23	123	24	27			
31	6	9	62	12	13	93	18	24	124	24	28			

B.3.4 Ground Structure 4

Table B.14: Nodal coordinates [m] of the ground structure GS_8.

i	x	y	i	x	y	i	x	y	i	x	y
1	0.000	0.000	10	6.577	-2.000	19	12.000	0.600	28	18.778	0.261
2	1.155	-2.000	11	6.577	0.329	20	13.356	0.532	29	18.778	-2.000
3	1.155	0.058	12	7.933	-2.000	21	13.356	-2.000	30	20.134	0.193
4	2.510	-2.000	13	7.933	0.397	22	14.711	0.464	31	20.134	-2.000
5	2.510	0.126	14	9.289	-2.000	23	14.711	-2.000	32	21.490	0.126
6	3.866	-2.000	15	9.289	0.464	24	16.067	0.397	33	21.490	-2.000
7	3.866	0.193	16	10.644	-2.000	25	16.067	-2.000	34	22.845	0.058
8	5.222	-2.000	17	10.644	0.532	26	17.423	0.329	35	22.845	-2.000
9	5.222	0.261	18	12.000	-2.000	27	17.423	-2.000	36	24.000	0.000

Table B.15: Element connectivity table of the ground structure GS_8.

e	1	2	e	1	2	e	1	2	e	1	2	e	1	2	e	1	2
1	1	2	34	6	8	67	11	13	100	18	19	133	22	30	166	28	29
2	1	3	35	6	9	68	11	14	101	18	20	134	23	24	167	28	30
3	1	4	36	6	10	69	11	15	102	18	21	135	23	25	168	28	31
4	1	5	37	6	11	70	11	17	103	18	22	136	23	26	169	28	32
5	1	7	38	6	12	71	11	19	104	18	23	137	23	27	170	28	33
6	1	9	39	6	14	72	12	13	105	18	24	138	23	29	171	28	34
7	2	3	40	7	8	73	12	14	106	18	25	139	23	31	172	28	36
8	2	4	41	7	9	74	12	15	107	18	27	140	24	25	173	29	30
9	2	5	42	7	10	75	12	16	108	19	20	141	24	26	174	29	31
10	2	6	43	7	11	76	12	17	109	19	21	142	24	27	175	29	32
11	2	7	44	7	13	77	12	18	110	19	22	143	24	28	176	29	33
12	2	8	45	7	15	78	13	14	111	19	23	144	24	29	177	29	35
13	2	10	46	8	9	79	13	15	112	19	24	145	24	30	178	30	31
14	3	4	47	8	10	80	13	16	113	19	26	146	24	32	179	30	32
15	3	5	48	8	11	81	13	17	114	20	21	147	25	26	180	30	33
16	3	6	49	8	12	82	13	18	115	20	22	148	25	27	181	30	34
17	3	7	50	8	13	83	13	19	116	20	23	149	25	28	182	30	35
18	3	9	51	8	14	84	14	15	117	20	24	150	25	29	183	30	36
19	3	11	52	8	16	85	14	16	118	20	25	151	25	31	184	31	32
20	4	5	53	9	10	86	14	17	119	20	26	152	25	33	185	31	33
21	4	6	54	9	11	87	14	18	120	20	28	153	26	27	186	31	34
22	4	7	55	9	12	88	14	19	121	21	22	154	26	28	187	31	35
23	4	8	56	9	13	89	14	23	122	21	23	155	26	29	188	32	33
24	4	9	57	9	15	90	15	16	123	21	24	156	26	30	189	32	34
25	4	10	58	9	17	91	15	17	124	21	25	157	26	31	190	32	35
26	4	12	59	10	11	92	15	18	125	21	27	158	26	32	191	32	36
27	5	6	60	10	12	93	15	19	126	21	29	159	26	34	192	33	34
28	5	7	61	10	13	94	16	17	127	22	23	160	27	28	193	33	35
29	5	8	62	10	14	95	16	18	128	22	24	161	27	29	194	33	36
30	5	9	63	10	15	96	16	19	129	22	25	162	27	30	195	34	35
31	5	11	64	10	16	97	16	21	130	22	26	163	27	31	196	34	36
32	5	13	65	10	18	98	17	18	131	22	27	164	27	33	197	35	36
33	6	7	66	11	12	99	17	19	132	22	28	165	27	35			

B.3.5 Ground Structure 5

Table B.16: Nodal coordinates [m] of the ground structure GS_9.

i	x	y
1	0.000	0.000
2	1.155	-2.000
3	1.155	0.058
4	2.360	-2.000
5	2.360	0.118
6	3.565	-2.000
7	3.565	0.178
8	4.770	-2.000
9	4.770	0.238
10	5.975	-2.000
11	5.975	0.299
12	7.180	-2.000
13	7.180	0.359
14	8.385	-2.000
15	8.385	0.419
16	9.590	-2.000
17	9.590	0.479
18	10.795	-2.000
19	10.795	0.540
20	12.000	-2.000
21	12.000	0.600
22	13.205	0.540
23	13.205	-2.000
24	14.410	0.479
25	14.410	-2.000
26	15.615	0.419
27	15.615	-2.000
28	16.820	0.359
29	16.820	-2.000
30	18.025	0.299
31	18.025	-2.000
32	19.230	0.238
33	19.230	-2.000
34	20.435	0.178
35	20.435	-2.000
36	21.640	0.118
37	21.640	-2.000
38	22.845	0.058
39	22.845	-2.000
40	24.000	0.000

Table B.17: Element connectivity table of the ground structure GS_9.

e	1	2	e	1	2	e	1	2	e	1	2	e	1	2	e	1	2
1	1	2	42	6	14	83	12	16	124	20	21	165	25	29	206	30	40
2	1	3	43	7	8	84	12	17	125	20	22	166	25	30	207	31	32
3	1	4	44	7	9	85	12	18	126	20	23	167	25	31	208	31	33
4	1	5	45	7	10	86	12	19	127	20	24	168	25	33	209	31	34
5	1	7	46	7	11	87	12	20	128	20	25	169	26	27	210	31	35
6	1	9	47	7	12	88	13	14	129	20	26	170	26	28	211	31	36
7	1	11	48	7	13	89	13	15	130	20	27	171	26	29	212	31	37
8	2	3	49	7	15	90	13	16	131	20	29	172	26	30	213	31	39
9	2	4	50	8	9	91	13	17	132	21	22	173	26	31	214	32	33
10	2	5	51	8	10	92	13	18	133	21	23	174	26	32	215	32	34
11	2	6	52	8	11	93	13	19	134	21	24	175	26	33	216	32	35
12	2	7	53	8	12	94	13	21	135	21	25	176	26	34	217	32	36
13	2	8	54	8	13	95	14	15	136	21	26	177	27	28	218	32	37
14	2	10	55	8	14	96	14	16	137	21	27	178	27	29	219	32	38
15	3	4	56	8	15	97	14	17	138	21	28	179	27	30	220	32	40
16	3	5	57	8	16	98	14	18	139	22	23	180	27	31	221	33	34
17	3	6	58	9	10	99	14	19	140	22	24	181	27	32	222	33	35
18	3	7	59	9	11	100	14	20	141	22	25	182	27	33	223	33	36
19	3	9	60	9	12	101	14	21	142	22	26	183	27	35	224	33	37
20	3	11	61	9	13	102	15	16	143	22	27	184	28	29	225	33	39
21	4	5	62	9	14	103	15	17	144	22	28	185	28	30	226	34	35
22	4	6	63	9	15	104	15	18	145	22	29	186	28	31	227	34	36
23	4	7	64	9	17	105	15	19	146	22	30	187	28	32	228	34	37
24	4	8	65	10	11	106	15	20	147	23	24	188	28	33	229	34	38
25	4	9	66	10	12	107	15	21	148	23	25	189	28	34	230	34	39
26	4	10	67	10	13	108	16	17	149	23	26	190	28	35	231	34	40
27	4	12	68	10	14	109	16	18	150	23	27	191	28	36	232	35	36
28	5	6	69	10	15	110	16	19	151	23	28	192	29	30	233	35	37
29	5	7	70	10	16	111	16	20	152	23	29	193	29	31	234	35	38
30	5	8	71	10	17	112	16	21	153	23	31	194	29	32	235	35	39
31	5	9	72	10	18	113	16	25	154	24	25	195	29	33	236	36	37
32	5	10	73	11	12	114	17	18	155	24	26	196	29	34	237	36	38
33	5	11	74	11	13	115	17	19	156	24	27	197	29	35	238	36	39
34	5	13	75	11	14	116	17	20	157	24	28	198	29	37	239	36	40
35	6	7	76	11	15	117	17	21	158	24	29	199	30	31	240	37	38
36	6	8	77	11	16	118	18	19	159	24	30	200	30	32	241	37	39
37	6	9	78	11	17	119	18	20	160	24	31	201	30	33	242	37	40
38	6	10	79	11	19	120	18	21	161	24	32	202	30	34	243	38	39
39	6	11	80	12	13	121	18	23	162	25	26	203	30	35	244	38	40
40	6	12	81	12	14	122	19	20	163	25	27	204	30	36	245	39	40
41	6	13	82	12	15	123	19	21	164	25	28	205	30	38			

B.3.6 Ground Structure 6

Table B.18: Nodal coordinates [m] of the ground structure GS_{10}.

i	x	y	i	x	y
1	0.000	0.000	23	12.000	0.600
2	1.155	-2.000	24	13.085	0.546
3	1.155	0.058	25	13.085	-2.000
4	2.239	-2.000	26	14.169	0.492
5	2.239	0.112	27	14.169	-2.000
6	3.324	-2.000	28	15.254	0.437
7	3.324	0.166	29	15.254	-2.000
8	4.408	-2.000	30	16.338	0.383
9	4.408	0.220	31	16.338	-2.000
10	5.493	-2.000	32	17.423	0.329
11	5.493	0.275	33	17.423	-2.000
12	6.577	-2.000	34	18.507	0.275
13	6.577	0.329	35	18.507	-2.000
14	7.662	-2.000	36	19.592	0.220
15	7.662	0.383	37	19.592	-2.000
16	8.746	-2.000	38	20.676	0.166
17	8.746	0.437	39	20.676	-2.000
18	9.831	-2.000	40	21.761	0.112
19	9.831	0.492	41	21.761	-2.000
20	10.915	-2.000	42	22.845	0.058
21	10.915	0.546	43	22.845	-2.000
22	12.000	-2.000	44	24.000	0.000

Table B.19: Element connectivity table of the ground structure GS_{10}.

e	1	2	e	1	2	e	1	2	e	1	2	e	1	2	e	1	2
1	1	2	53	7	9	105	13	16	157	22	25	209	28	32	261	34	39
2	1	3	54	7	10	106	13	17	158	22	26	210	28	33	262	34	40
3	1	4	55	7	11	107	13	18	159	22	27	211	28	34	263	34	41
4	1	5	56	7	12	108	13	19	160	22	28	212	28	35	264	34	42
5	1	6	57	7	13	109	13	21	161	22	29	213	28	36	265	34	44
6	1	7	58	7	15	110	13	23	162	22	31	214	28	38	266	35	36
7	1	9	59	7	17	111	14	15	163	22	33	215	29	30	267	35	37
8	1	11	60	8	9	112	14	16	164	23	24	216	29	31	268	35	38
9	2	3	61	8	10	113	14	17	165	23	25	217	29	32	269	35	39
10	2	4	62	8	11	114	14	18	166	23	26	218	29	33	270	35	40
11	2	5	63	8	12	115	14	19	167	23	27	219	29	34	271	35	41
12	2	6	64	8	13	116	14	20	168	23	28	220	29	35	272	35	43
13	2	7	65	8	14	117	14	21	169	23	29	221	29	37	273	36	37
14	2	8	66	8	15	118	14	22	170	23	30	222	29	39	274	36	38
15	2	9	67	8	16	119	15	16	171	23	32	223	30	31	275	36	39
16	2	10	68	8	18	120	15	17	172	24	25	224	30	32	276	36	40
17	2	12	69	9	10	121	15	18	173	24	26	225	30	33	277	36	41
18	3	4	70	9	11	122	15	19	174	24	27	226	30	34	278	36	42
19	3	5	71	9	12	123	15	20	175	24	28	227	30	35	279	36	43
20	3	6	72	9	13	124	15	21	176	24	29	228	30	36	280	36	44
21	3	7	73	9	14	125	15	23	177	24	30	229	30	37	281	37	38
22	3	8	74	9	15	126	16	17	178	24	31	230	30	38	282	37	39
23	3	9	75	9	17	127	16	18	179	24	32	231	30	40	283	37	40
24	3	11	76	9	19	128	16	19	180	24	34	232	31	32	284	37	41
25	3	13	77	10	11	129	16	20	181	25	26	233	31	33	285	37	42
26	4	5	78	10	12	130	16	21	182	25	27	234	31	34	286	37	43
27	4	6	79	10	13	131	16	22	183	25	28	235	31	35	287	38	39
28	4	7	80	10	14	132	16	23	184	25	29	236	31	36	288	38	40
29	4	8	81	10	15	133	17	18	185	25	30	237	31	37	289	38	41
30	4	9	82	10	16	134	17	19	186	25	31	238	31	39	290	38	42
31	4	10	83	10	17	135	17	20	187	25	33	239	31	41	291	38	43
32	4	11	84	10	18	136	17	21	188	25	35	240	32	33	292	38	44
33	4	12	85	10	20	137	17	22	189	26	27	241	32	34	293	39	40
34	4	14	86	11	12	138	17	23	190	26	28	242	32	35	294	39	41
35	5	6	87	11	13	139	18	19	191	26	29	243	32	36	295	39	42
36	5	7	88	11	14	140	18	20	192	26	30	244	32	37	296	39	43
37	5	8	89	11	15	141	18	21	193	26	31	245	32	38	297	39	44
38	5	9	90	11	16	142	18	22	194	26	32	246	32	39	298	40	41
39	5	10	91	11	17	143	18	23	195	26	33	247	32	40	299	40	42
40	5	11	92	11	19	144	18	27	196	26	34	248	32	42	300	40	43
41	5	13	93	11	21	145	19	20	197	26	36	249	33	34	301	40	44
42	5	15	94	12	13	146	19	21	198	27	28	250	33	35	302	41	42
43	6	7	95	12	14	147	19	22	199	27	29	251	33	36	303	41	43
44	6	8	96	12	15	148	19	23	200	27	30	252	33	37	304	41	44
45	6	9	97	12	16	149	20	21	201	27	31	253	33	38	305	42	43
46	6	10	98	12	17	150	20	22	202	27	32	254	33	39	306	42	44
47	6	11	99	12	18	151	20	23	203	27	33	255	33	41	307	43	44
48	6	12	100	12	19	152	20	25	204	27	35	256	33	43			
49	6	13	101	12	20	153	21	22	205	27	37	257	34	35			
50	6	14	102	12	22	154	21	23	206	28	29	258	34	36			
51	6	16	103	13	14	155	22	23	207	28	30	259	34	37			
52	7	8	104	13	15	156	22	24	208	28	31	260	34	38			

References

Achterberg, T., Koch, T. & Martin, A. (2005), 'Branching rules revisited', *Optimization Research Letters* **33**, 42–54.

Achtziger, W. (1999*a*), 'Local stability of trusses in the context of topology optimization part I: Exact modelling', *Structural Optimization* **17**, 235 – 246.

Achtziger, W. (1999*b*), 'Local stability of trusses in the context of topology optimization part II: A numerical approach', *Structural Optimization* **17**, 247 – 258.

Adeli, H. & Sarma, K. C. (2006), *Cost Optimization of Structures*, John Wiley & Sons.

Alves, M. & Clímaco, J. (2007), 'A review of interactive methods for multiobjective integer and mixed-integer programming', *European Journal of Operation Research* **180**, 99–115.

Arora, J. (2002), Methods for discrete variable structural optimization, *in* S. A. Burns, ed., 'Recent Advances in Optimal Structural Design', ASCE, pp. 1–40.

Arora, J., Huang, M.-W. & Hsieh, G. (1994), 'Methods for optimization of nonlinear problems with discrete variables: a review', *Structural optimization* **8**, 69–85.

Arora, J. & Wang, Q. (2005), 'Review of formulations for structural and mechanical system optimization', *Structural and Multidisciplinary Optimization* **30**, 251–272.

Balling, R. J., Briggs, R. R. & Gillman, K. (2006), 'Multiple optimum size/shape/topology designs for skeletal structures using a genetic algorithm', *Journal of Structural Engineering* **132**, 1158–1165.

Barta, J. (1957), 'On the minimum weight of certain redundant structures', *Acta Technica Academiae Scientiarum Hungaricae* **18**, 67–76.

Beale, E. & Forrest, J. (1976), 'Global optimization using special ordered sets', *Mathematical Programming* **10**, 52–69.

Beale, E. & Tomlin, J. (1970), Special facilities in a general mathematical programming system for non-convex problems using ordered sets of variables, *in* J. Lawrence, ed., 'Proceedings of the fifth international conference on operational research', Tavistock Publications, pp. 447–454.

Ben-Tal, A. & Nemirovski, A. (1997), 'Robust truss topology design via semidefinite programming', *SIAM Journal on Optimization* **7**(4), 991–1016.

Bendsøe, M. P. & Sigmund, O. (2003), *Topology Optimization: Theory, Methods and Applications*, Springer Verlag.

Bixby, R. (2012), 'A brief history of linear and mixed-integer programming computation', *Documenta Mathematica* **Extra Volume: Optimization Stories**, 107–121.

Bixby, R. & Rothberg, E. (2007), 'Progress in computational mixed in programming – a look back from the other side of the tipping point', *Mathematical Programming* **149**, 37–41.

Bollapragada, S., Ghattas, O. & Hooker, J. (2001), 'Optimal design of truss structures by logic-based branch and cut', *Operations research* **49**, 42–51.

Bonami, P., Cornuéjols, G., Dash, S., Fischetti, M. & Lodi, A. (2008), 'Projected chvátal-gomory cuts for mixedinteger linear programs', *Mathematical Programming* **113**, 241–257.

Bruns, T. (2006), 'Zero density lower bounds in topology optimization', *Computer Methods in Applied Mechanical Engineering* **196**, 566 – 578.

Cheng, G. & Guo, X. (1997), 'ϵ-relaxed approach in structural topology optimization', *Structural Optimization* **13**, 258 – 266.

Cheng, G. & Jiang, Z. (1992), 'Study on topology optimization with stress constraints', *Engineering Optimization* **20**, 129 – 148.

Codato, G. & Fischetti, M. (2006), 'Combinatorial benders' cuts for mixed-integer linear programming', *Operations Research* **54**, 756–766.

Cornuéjols, G. (2008), 'Valid inequalities for mixed integer linear programs', *Mathematical Programming* **112**, 3–44.

Deb, K. (2002), *Multi-Objective Optimization using Evolutionary Algorithms*, John Wiley & Sons.

Dominguez, A., Stiharu, I. & Sedaghati, R. (2006), 'Practical design optimization of truss structures using the genetic algorithms', *Research in Engineering Design* **17**, 73–84.

Dorn, W., Gomory, R. & Greenberg, M. (1964), 'Automatic design of optimal structures', *Journal de Mecanique* **3**, 25–52.

EC 3 NA (2005), *National Annex to Standard Eurocode 3: Design of Steel Structures. Part 1-1: General rules and rules for buildings*, Ministry of Environment, Finland.

EN 15978 (2011), *Sustainability of construction works – Assessment of environmental performance of buildings – Calculation method*, CEN.

EN 1993–1–1 (2005), *Eurocode 3: Design of Steel Structures. Part 1-1: General rules and rules for buildings*, CEN.

EN 1993–1–8 (2005), *Eurocode 3: Design of Steel Structures. Part 1-8: Design of joints*, CEN.

Erbatur, F., Hasançebi, O., Tütüncü, İ. & Kılıç, H. (2000), 'Optimal design of planar and space structures with genetic algorithms', *Computers & Structures* **75**, 209–224.

Eschenauer, H. A. & Olhoff, N. (2001), 'Topology optimization of continuum structures: A review', *Applied Mechanics Reviews* **54**, 331–390.

Eschenauer, H., Koski, J. & Osyczka, A. (1990), *Multicriteria Design Optimization, Procedures and Applications*, Springer-Verlag.

Farkas, J. & Jármai, K. (1997), *Analysis and Optimum Design of Metal Structures*, A.A. Balkema.

Farkas, J. & Jármai, K. (2003), *Economic Design of Metal Structures*, Millpress Rotterdam.

Farkas, J. & Jármai, K. (2008), *Design and Optimization of Metal Structures*, Horwood Publishing.

Faustino, A., Júdice, J., Ribeiro, I. & Neves, A. (2006), 'An integer programming model for truss topology optimization', *Investigação Operacional* **26**, 111–127.

Fleron, P. (1964), 'The minimum weight trusses', *Bygningsstatiske Meddelelser* **35**, 81–96.

Floudas, C. (1995), *Nonlinear and Mixed-Integer Optimization, Fundamentals and Applications*, Oxford University Press.

Galante, M. (1996), 'Genetic algorithms as an approach to optimize real-world trusses', *International Journal of Numerical Methods in Engineering* **39**, 361—-382.

Ghattas, O. & Grossmann, I. E. (1991), MINLP and MILP strategies for discrete sizing structural optimization problems, *in* O. Ural & T. L. Wang, eds, 'Proceedings of the 10th conference on electronic computation', ASCE, pp. 197–204.

Grossmann, I. E., Voudouris, V. T. & Ghattas, O. (1992), Mixed-integer linear programming reformulations for some nonlinear discrete design optimization problems, *in* C. A. Floudas & P. M. Pardalos, eds, 'Recent advances in global optimization', Princeton University Press, pp. 478–512.

Guo, X., Cheng, G. & Olhoff, N. (2005), 'Optimum design of truss topology under buckling constraints', *Structural and Multidisciplinary Optimization* **30**, 169–180.

Guo, X., Cheng, G. & Yamazaki, K. (2001), 'A new approach for the solution of singular optima in truss topology optimization with stress and local buckling constraints', *Structural and Multidisciplinary Optimization* **22**, 364–372.

Gurobi Optimization, Inc. (2012), 'Gurobi optimizer reference manual', `http://www.gurobi.com`.

Haapio, J. (2012), Feature-Based Costing Method for Skeletal Steel Structures Based on the Process Approach, PhD thesis, Tampere University of Technology.

Jalkanen, J. (2007), Tubular Truss Optimization Using Heuristic Algorithms, PhD thesis, Tampere University of Technology.

Jármai, K. & Farkas, J. (1999), 'Cost calculation and optimisation of welded steel structures', *Journal of Constructional Steel Research* **50**, 115–135.

Kanno, Y. & Guo, X. (2010), 'A mixed integer programming for robust truss topology optimization with stress constraints', *International Journal for Numerical Methods in Engineering* **83**(13), 1675–1699.

Kirsch, U. (1989), 'Optimal topologies of structures', *Applied Mechanics Review* **42**(2), 223–239.

Kirsch, U. (1990), 'On singular topologies in optimum structural design', *Structural Optimization* **2**, 133–142.

Kirsch, U. (1993), *Structural Optimization*, Springer Verlag.

Koski, J. (1994), Multicriterion structural optimization, *in* H. Adeli, ed., 'Advances in design optimization', Chapman & Hall, pp. 194–224.

Koski, J. & Silvennoinen, R. (1987), 'Norm methods and partial weighting in multicriterion optimization of structures', *International Journal for Numerical Methods in Engineering* **24**, 1101–1121.

Kravanja, S., Kravanja, Z. & Bedenik, B. (1998), 'The MINLP optimization approach to structural synthesis. part I: A general view on simultaneous topology and parameter optimization', *International Journal for Numerical Methods in Engineering* **43**, 263–292.

Land, A. & Doig, A. (1960), 'An automatic method of solving discrete programming problems', *Econometrica* **28**, 497–520.

Marchand, H., Martin, A., Weismantel, R. & Wolsey, L. (2002), 'Cutting planes in integer and mixed integer programming', *Discrete Applied Mathematics* **123**, 397–446.

Marler, R. & Arora, J. (2004), 'Survey of multi-objective optimization methods for engineering', *Structural and Multidisciplinary Optimization* **26**, 369–395.

Miettinen, K. (1999), *Nonlinear Multiobjective Optimization*, Kluwer Academic Publishers.

Nemhauser, G. & Wolsey, L. (1999), *Integer and Combinatorial Optimization*, John Wiley & Sons.

Ohsaki, M. & Katoh, N. (2005), 'Topology optimization of trusses with stress and local constraints on nodal stability and member intersection', *Structural and Multidisciplinary Optimization* **29**, 190–197.

Osyczka, A. (2002), *Evolutionary Algorithms for Single and Multicriteria Design Optimization*, Physica-Verlag.

Pareto, V. (1896), *Cours d'Economie Politique*, F. Rouge.

Pavlovčič, L., Krajnc, A. & Beg, D. (2004), 'Cost function analysis in the structural optimization of steel frames', *Structural and Multidisciplinary Optimization* **28**, 286–295.

Pedersen, N. & Nielsen, A. (2003), 'Optimization of practical trusses with constraints on eigenfrequencies, displacements, stresses, and buckling', *Structural and Multidisciplinary Optimization* **25**, 436–445.

Rasmussen, M. & Stolpe, M. (2008), 'Global optimization of discrete truss topology design problems using a parallel cut-and-branch method', *Computers and Structures* **86**, 1527–1538.

Rozvany, G. (1992), 'Optimal layout theory: Analytical solutions for elastic structures with several deflection constraints and load conditions', *Structural Optimization* **4**, 247–249.

Rozvany, G. (1996), 'Difficulties in truss topology optimization with stress, local buckling and system stability constraints', *Structural Optimization* **11**, 213 – 217.

Rozvany, G. (2001), 'On design-dependent constraints and singular topologies', *Structural and Multidisciplinary Optimization* **21**, 164–172.

Rozvany, G., Bendsøe, M. & Kirsch, U. (1995), 'Layout optimization of structures', *Applied Mechanics Review* **48**(2), 41–119.

Ruukki (2011), *Steel sections. Hollow sections.* Dimensions and cross-sectional properties.

Sankaranarayanan, S., Haftka, R. & Kapania, R. (1994), 'Truss topology optimization with simultaneous analysis and design', *AIAA Journal* **32**(2), 420–424.

Sarma, K. C. & Adeli, H. (2000*a*), 'Cost optimization of steel structures', *Engineering Optimization* **32**, 777–802.

Sarma, K. C. & Adeli, H. (2000*b*), 'Fuzzy discrete multicriteria cost optimization of steel structures', *Journal of Structural Engineering* **126**, 1339–1347.

Savelsbergh, M. (1994), 'Preprocessing and probing techniques for mixed integer programming problems', *ORSA Journal on Computing* **6**(4), 445–454.

Shea, K. & Smith, I. F. C. (2006), 'Improving full-scale transmission tower design through topology and shape optimization', *Journal of Structural Engineering* **132**, 781–790.

Šilih, S. & Kravanja, S. (2008), Topology, shape and standard sizing optimization of trusses using MINLP optimization approach, *in* K. Jármai & J. Farkas, eds, 'Design, Fabrication and Economy of Welded Structures', Horwood Publishing, pp. 143–150.

Šilih, S., Premrov, M. & Kravanja, S. (2005), 'Optimum design of plane timber trusses considering joint flexibility', *Engineering Structures* **27**, 145–154.

Stolpe, M. (2004), 'Global optimization of minimum weight truss topology problems with stress, displacement, and local buckling constraints using branch-and-bound', *International Journal for Numerical Methods in Engineering* **61**, 1270–1309.

Stolpe, M. & Svanberg, K. (2001), 'On the trajectories of the epsilon-relaxation approach for stress-constrained truss topology optimization', *Structural and Multidisciplinary Optimization* **21**, 140–151.

Sved, G. (1954), 'The minimum weight of certain redundant structures', *Australian Journal of Applied Science* **5**, 1–9.

Sved, G. & Ginos, Z. (1968), 'Structural optimization under multiple loading', *International Journal of Mechanical Sciences* **10**, 803–805.

Thanedar, P. & Vanderplaats, G. (1995), 'Survey of discrete variable optimization for structural design', *Journal of Structural Engineering* **121**, 301–306.

Trahair, N. & Bradford, M. (1988), *The behaviour and design of steel structures*, Chapman and Hall.

Wardenier, J., Packer, J., Zhao, X.-L. & van der Vegte, G. (2010), *Hollow Sections in Structural Applications*, CIDECT.

Wolsey, L. A. (1998), *Integer Programming*, John Wiley & Sons.

Zhou, M. (1996), 'Difficulties in truss topology optimization with stress and local buckling constraints', *Structural Optimization* **11**, 134 – 136.

Tampereen teknillinen yliopisto
PL 527
33101 Tampere

Tampere University of Technology
P.O.B. 527
FI-33101 Tampere, Finland

ISBN 978-952-15-3076-0
ISSN 1459-2045